PROPAGATION OF ELECTROMAGNETIC WAVES ALONG DIELECTRIC INTERFACE

Zahid Hameed Qazi

DEPARTMENT OF ELECTRONICS
QUAID-I-AZAM UNIVERSITY
ISLAMABAD, PAKISTAN
JUNE, 2008

This work is submitted as a thesis in partial fulfilment of the requirement for the degree of

DOCTOR OF PHILOSPHY

IN

ELECTRONICS

DEPARTMENT OF ELECTRONICS
QUAID-I-AZAM UNIVERSITY
ISLAMABAD, PAKISTAN
JUNE, 2008

CERTIFICATE

It is certified that the work contained in this thesis was carried out and completed under my supervision at Quaid-i-Azam university, Islamabad Pakistan.

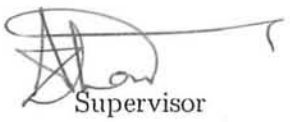

Supervisor

(Prof. Dr. Azhar Abbas Rizvi)

Submitted through:

Prof. Dr. Azhar Abbas Rizvi,
Chairman,
Department of Electronics,
Quaid-i-Azam University,
Islamabad, Pakistan.

To my late parents.

Table of Contents

Table of Contents v

List of Figures vi

Abstract ix

Acknowledgements xii

1 Introduction 1

2 Interfacial Line Source 10
- 2.1 Problem Formulation 10
- 2.2 Asymptotic Solution for Upper Half Space 14
- 2.3 Asymptotic Solution for Lower Half Space 26
- 2.4 Wave Propagation along the Interface 33
- 2.5 Location of Field Nulls or Critical Points 37

3 Two Dimensional Finite Sources 42
- 3.1 Line Source In Upper Half Space 43
- 3.2 Line Source In Lower Half Space 52
- 3.3 Existence of Critical Points 62
- 3.4 Generalization 66

4 Current Sheet Perpendicular to Plane Dielectric Interface 73
- 4.1 Problem Formulation 74
- 4.2 Electric Field In Upper Half Space 80
- 4.3 Electric Field In Lower Half Space 90

5 Conclusion 96

References 101

List of Figures

1.1 Typical oblique incidence case - A text book problem 2

1.2 Propagation along a wedge in the far zone 5

1.3 A line source radiates cylindrical EM waves 6

1.4 Circular phase fronts due to interfacial line source between two dielectric half spaces 9

2.1 Geometry of the problem 11

2.2 Branch cuts drawn to satisfy radiation conditions in E_{z1} 14

2.3 Deformed Path of Integration for Branch cuts for E_{z1} 15

2.4 Mapped complex α plane 17

2.5 Only one pair of branch cuts left in the new α plane. 18

2.6 Branch point at $\alpha = i\cosh\eta$ contributes in evaluation for E_{z1} 19

2.7 Neither of the Branch Cut will Contribute when $\theta = \pi/2$ 20

2.8 Lower Branch Cut will Contribute when $\pi/2 < \theta < \pi$ 21

2.9 No Branch Point Contribution when $\eta_c > \eta_b$ 22

2.10 Original path of integration, Q and the pair of branch cuts for E_{z2} in α-plane 28

2.11 Deformed Path of Integration, Q' and the pair of branch cuts for E_{z2} in α-plane 29

2.12 Branch point contribution is to be taken when $\theta < \cos^{-1}(1/n)$ 31

2.13 Lines of equiphase planes with critical points for E_{z1} and E_{z2}, continuous across the interface 36
2.14 The critical points seem to densely packed in the lower half space while the refractive index, n value is increased 37

3.1 A displaced line source in upper half space 44
3.2 Phase map near the interface with displaced line source in upper half space 53
3.3 A displaced line source in lower half space 54
3.4 Phase map continuity preserved when displace line source is below the interface 62
3.5 Two line sources placed arbitrarily in the upper half space 68
3.6 A displaced arbitrary source in upper half space 69
3.7 A displaced arbitrary source in lower half Space 70
3.8 Phase map near the interface due to arbitrary shaped electric source in the upper half space 71
3.9 Critical points move away as refractive index decreases in lower half space 72

4.1 Two half current sheets present in the yz plane 75
4.2 Current sheet present in the yz plane 81
4.3 The corresponding path of integration in complex α plane of I_{1U} 83
4.4 Integration path and two branch cuts with poles in the k_x plane of I_{2U} . 86
4.5 Integration path in the mapped s plane of I_{2U} 88
4.6 Critical points in the region, $y > 0$ due to a current sheet across the interface while no such points in $y < 0$ 95

5.1 Poynting vector and the phase map in the rarer medium 98
5.2 Flow lines due to finite extent sources in the rarer medium 99
5.3 Flow lines due to current sheet in the rarer medium 100

5.4 Close view of phase map structures with horizontal displacement of the lower pair 100

Abstract

Investigation of electromagnetic waves propagating along plane dielectric interface poses a very interesting and challenging problem. It is known that the phase velocities of the electromagnetic waves in dielectric media depend on the constitutive parameters of the media. Although phase velocities of electromagnetic waves in different dielectric media are different the tangential electric and magnetic fields across the interface must be continuous to satisfy the boundary conditions. The studies carried out so far in the field of propagation along dielectric interface show discontinuous tangential field components across the interface thereby violating boundary conditions. The discontinuity exists in the phase and hence in the phase velocity of the field components whereas the magnitude is continuous across the interface. It is desired to find such a solution for which phase as well as magnitude of field components, $\vec{E}$ and $\vec{H}$ are continuous across the interface thereby satisfying Maxwell's equations.

To study the propagation behavior along the interface two classes of problems have been considered. In the first class of problems current sources of finite extent have been considered and in the second class the source considered is an infinite current sheet. In the first class of problems electric field due to electric currents source parallel to the interface was investigated. The first order asymptotic evaluation of field components shows a null of the electric field at the interface. This solution satisfies the continuity of electric field while the magnetic field component is discontinuous. Higher order asymptotic evaluations have been employed to get further insight into this propagation problem. The results show that the wavefronts need not be discontinuous. In the second

class of problems a current sheet was assumed to be present across the interface to see the behavior of plane wave near the dielectric interface due to an infinite source.

Among various source configurations considered in this work the continuity of the phase fronts is found to be preserved with the help of interesting and stable structures of phase fronts. These structures are formed by two types of critical points in the phase map known as saddle points and center points. The phase map plots show that these points exist near the interface in both half spaces when finite extent sources are present. While the infinite extent source was responsible for creation of these points in the upper half space only . These points are located periodically along the interface while their position above or below the interface depends upon the refractive index of the denser medium of the two dielectric half spaces. It was found that the refractive index also effects the periodicity of these points along the interface.

Don't just say "it is impossible" without putting in a sincere effort. Observe the word "Impossible" carefully. You can see "I'm possible". What really matters is your attitude and your perception.

Anonymous

Acknowledgements

A few people have helped me in the progression of my research in writing this thesis and any merit in it is in large dimension due to them.

First and foremost, I sincerely and truthfully express recognition of my debt to Prof. Dr. Syed Azhar Abbas Rizvi for his guidance, encouragement, insight and support throughout this research journey in the wilderness of Electromagnetics. He always felt me welcome in his office, no matter how busy he was, or how silly my questions were. He let me experience the freedom and excitement of personal discovery alongside the dense smoke of his cigarettes (which always caused headache in the end) . Without his professional advice and trust in me this thesis would not has been possible.

I am grateful to Dr. J. A. Mirza, who initiated me into this research work and kindly allowed me to take leave from office. My thanks are due to Mr. Khalid Mehmood, head of my division at my workplace, for his considerate, thoughtful and optimistic attitude towards my research capabilities which always kept me at my toes in this research work. I am indebted to Dr. M. Aslam, who constantly enquired and pushed me throughout my PhD work. I appreciate the help of Mr. Khaliq Dad Khan who showed great generosity during the last leg of my research work for taking leaves from office. My lots of thanks for Mr. Tahir Majeed Butt, my senior colleague, who encouraged me in my research work throughout all these years.

My sincere gratitude and thankfulness are for Prof. Dr. Hongo, who has been so corporative on a number of times for discussing and clearing some key difficult points of my research work. I must not foreget to mention, my friend, Tafazal Hussain who has

been very kind and helpful in providing me access to various scientific databases on the internet during early years of my research work.

Finally, I wish to thank the following: Arshad Ali and Asif Nadeem for their friendship and support during difficult times of my work; Syed Khalid Badar for his encouragement and push, both at a time; Shahid Aslam for his 'go and get it' advice; Saeed Ahmed and Chaudary Akbar for sharing my worries; my sisters for giving me tips of seeking help form Almighty Allah; my wife for showing all the patience and unlocking our home's main door for me at midnight after I got back from university; *and* my younger brother-in-law because he asked me to.

Last but not the least, I want to thank my elder brother who kept asking all these years: "Have you finished your thesis yet?". Silencing that question is an extra benefit of this work.

Quaid-e-Azam University, Islamabad Zahid Hameed Qazi

Chapter 1

Introduction

It is well known that plane waves are fundamental solutions of Maxwell's equations. Plane wave is generated by an infinite sheet of electric current. It is physically impossible to have sources of infinite dimensions. The finite sources radiate divergent waves but these waves can be considered locally as plane waves in the far zone of the source. In various two dimensional radiation and scattering problems of electromagnetic waves, the waves have to travel parallel to interface in the far zone. An example is of radio wave propagation parallel to earth's surface with source at or near the surface. Another example can be given of a normal incidence of electromagnetic wave on a dielectric wedge. In the far zone near the interface of this wedge, direction of propagation of the wave would become parallel to interface.

The phase velocity of electromagnetic waves in a medium depend upon the constitutive parameters of the medium. When the electromagnetic waves have to propagate parallel to an interface of dielectric media the difference in phase velocity in different media poses some interesting questions at and near the interface. For example, how the phase velocity will change over from one value to the other value across the interface in a continuous manner? Extensive work has been done in radiation and scattering of electromagnetic waves in the presence of dielectric interfaces but the interest has generally

been in calculating fields away from interface or in the far zone.

The most basic interface problem is, of course, the problem of reflection and refraction of a plane electromagnetic wave by a plane interface, which was solved by Fresnel and presented to the French Academy in 1823. The propagation of waves is not parallel to interface in this particular case. Consider Fig. 1.1, a plane wave strikes a dielectric

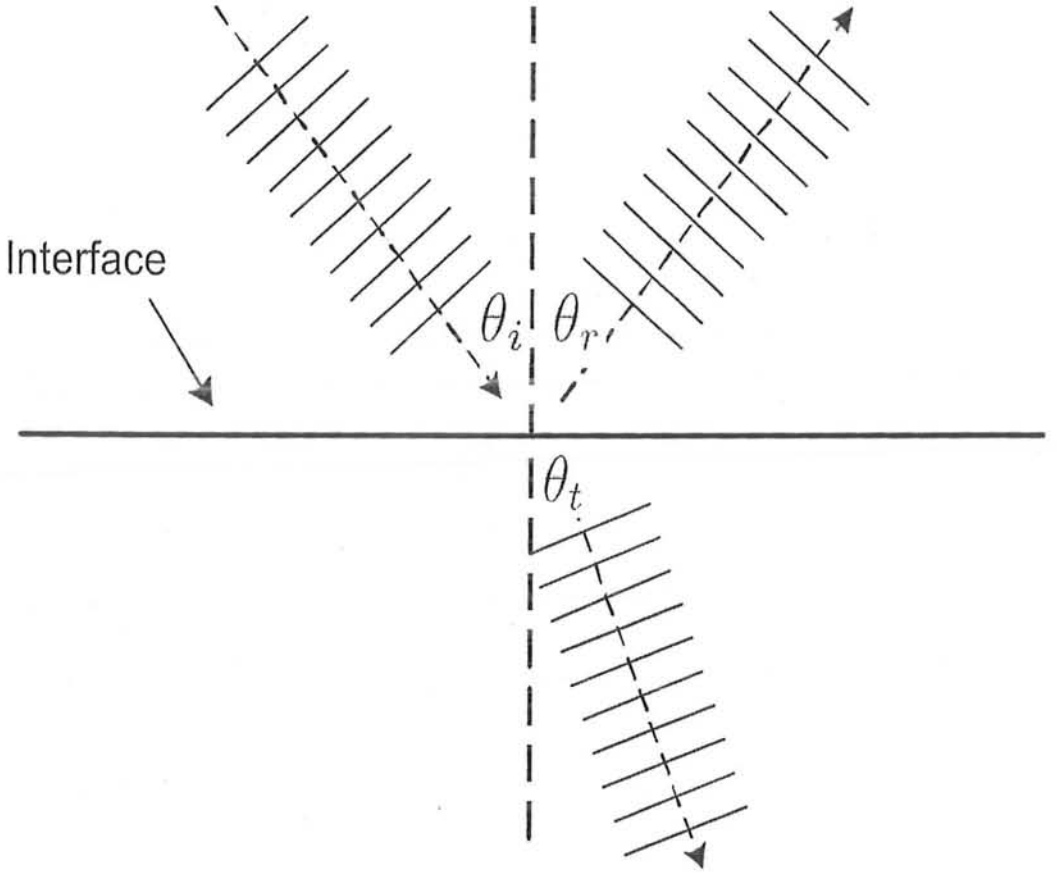

Figure 1.1: Typical oblique incidence case - A text book problem

interface at an incidence angle, θ_i and is reflected at an angle, θ_r. The wave penetrates in the second medium at an angle, θ_t. The field in the upper medium is sum of incident and reflected plane waves, or $E^i + E^r$. The transmitted field is E^t. These fields are related

through reflection and transmission co-efficients by Snell's law. To obtain propagation parallel to the interface the angle of incidence, θ_i must approach $\pi/2$. As a result the reflection and transmission co-efficients tend to become zero and only the incident field remains. The aim of obtaining propagation parallel to the dielectric interface cannot be achieved by this simplistic model. The failure of this model is due to its idealized nature because an infinite source and and an infinite dielectric interface are required by this model. Therefore one has to look elsewhere to study wave propagation parallel to a dielectric interface.

Parviz Parhami et. al. [1] derived fields due to current elements radiating over a lossy ground. They numerically evaluated Sommerfeld integrals present in the expressions for vector potentials. These vector potentials are valid only above the ground, so the resulting field gives no information about the fields at or below the surface. Similarly Parhami and Mittra [2] worked on problem of an arbitrarily shaped thin wire antenna radiating over a lossy half space. They employed method of moments to solve the integral equation arising from center-fed vertical dipole and center-fed inverted V-dipole. Their results show that the far field radiation pattern of the electric field component parallel to the interface is zero along the interface. Kin-Lu [3] studied interference effects of a Gaussian electromagnetic pulse incident on an air-dielectric interface for a micro strip circuit. The numerically obtained results show that the power absorption by the dielectric surface drops to zero as the incidence angle approaches $\pi/2$. Engheta and Papas [4] had analytically solved the problem of an interfacial line source on a dielectric-dielectric interface. Their results also show zero electric field along the interface. They had observed sub-surface peaking of the field pattern in the denser medium at critical angle.

Geometrical theory of diffraction(GTD) and Expansion Wave Concept have been

employed by Volski and Vandenbosch [5] to find radiation pattern of an electric line source present on a semi-infinite dielectric slab. They have used GTD to investigate the diffraction effects of the truncation while expansion wave concepts were employed to find out field at the edges of the slab. The field patterns of their results also show a null of electric field at the interface of the dielectric slab.

Scattering and diffraction problems due to wedge shaped objects also present the same kind of situation on the interface far from the edge of the wedge. Such problems have been treated extensively in the literature and several solutions for the scattered far field have been presented. Complicated field distributions exist near the edge of the wedge due to presence of diffracted and scattered fields as shown in Fig. 1.2. But far from the edge of the wedge near the interface the phase velocity continuity again becomes questionable. For example, Maliuzhinets [6] has given a rigorous solution based on approximate boundary conditions referred to as impedance boundary conditions. His solutions are valid only if the magnitude of refractive index of the wedge is large compared to unity. Kraut and Lehman [7] investigated the problem of diffraction of a plane-polarized electromagnetic wave incident on a right-angled dielectric wedge. They examined the electric field amplitude at the tip of the wedge. Their results are not valid to investigate the field behavior along the interface far away from the tip, as shown in Fig. 1.2. Zuffada [8] had also solved a dielectric wedge problem. Her results are not valid at the wedge interface.

It can be seen that some solutions are invalid at the interface and provide no clue to the interfacial wave propagation problem. While in the solutions that are valid on the interface either there is discontinuity of fields at the interface or field is zero at the interface. The discontinuous field along the interface does not satisfy the Maxwell's equations and the zero field on the interface does not satisfy boundary condition that

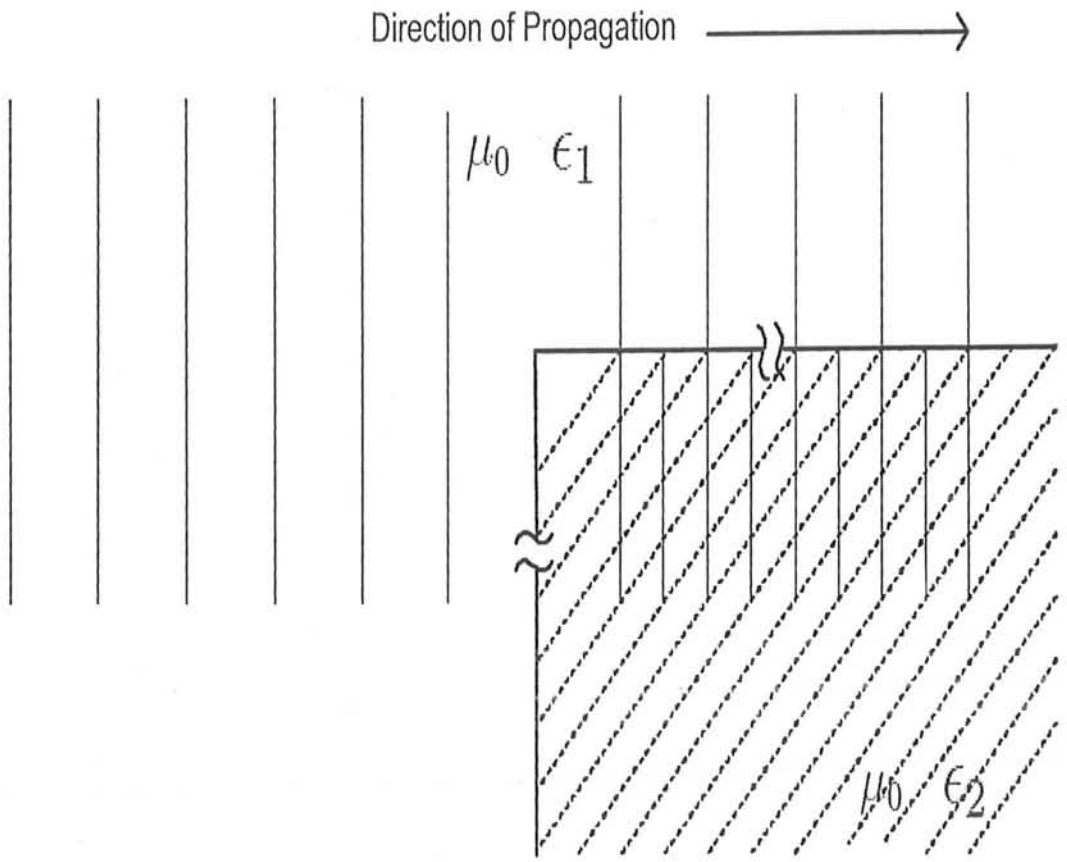

Figure 1.2: Propagation along a wedge in the far zone

magnetic field must be continuous on the interface. The solutions which give a field null on the interface are in fact approximations.This means that actual field will have additional higher order terms. The zero field on the interface is an unstable condition. Any small perturbation will change the location of zero away from the interface. This can be best understood by considering a simple polynomial, $y = x^3$. This polynomial has three roots at the origin. Addition of a small term, αx will give two complex roots $(\pm i\sqrt{\alpha})$ along with a root at origin thereby changing the nature of roots in the original polynomial $y = x^3$. Similarly subtraction of the same term will give two real roots

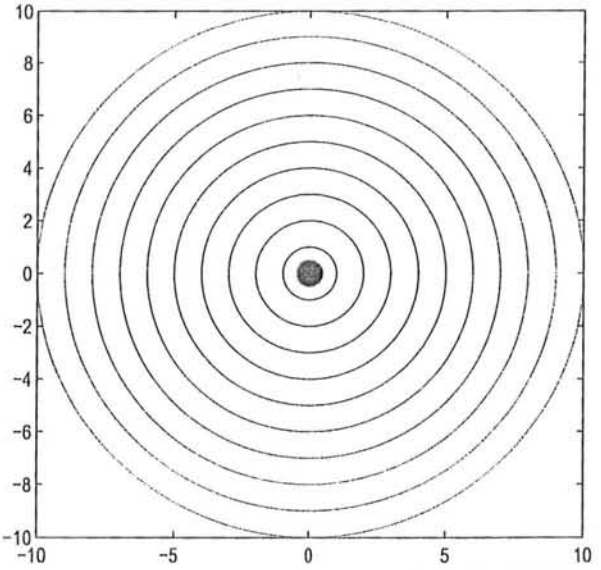

Figure 1.3: A line source radiates cylindrical EM waves

$(\pm\sqrt{\alpha})$ along with a root at origin.

In two dimensional electromagnetic propagation problems the Poynting vector of an electric field $E_z\hat{e}_z = A(x,y)e^{i\phi(x,y)}\hat{e}_z$ is given by [9],

$$\vec{S}(x,y) = \frac{1}{2\omega\mu}A^2\nabla\phi(x,y).$$

The amplitude function $A(x,y)$ is continuous and differentiable. Associated with this electric field is the phase velocity of the wave given by,

$$\vec{v} = \frac{\omega}{|\nabla\phi|^2}\nabla\phi(x,y)$$

It is observed that the phase velocity is parallel to the Poynting vector and both of them are normal to the surfaces of constant phase. The behavior of phase velocity can

be observed by looking at the surfaces of constant phase. For example a line source of electric current placed in a homogenous dielectric radiates a field whose surfaces of constant phase are circular cylinder as shown in Fig. 1.3. The phase velocity is completely radial in this case. The situation changes when the line source is at the interface of two different media. Away from the interface in both media the surfaces of constant phase will be nearly semi cylindrical but the density of constant phase surfaces will be different due to different dielectric constants as seen in Fig. 1.4. Since field is continuous along the interface the interesting question is how these surfaces connect in a continuous manner without going through a structurally unstable null field condition. The phase velocity map near the interface cannot be clearly shown as in Fig. 1.4. Therefore the continuous transition of the phase velocity across the interface needs further investigation. This is the question that will be addressed in this thesis.

Wave propagation along the interface depends on the source of excitation. The simplest source is an interfacial line source. Although this problem has been solved by Engetha and Papas [4] but a more detailed analysis is required along the interface and this will be done in chapter 2. Interfacial propagation is not limited to interfacial source. In Chapter 3 arbitrary sources are placed in the half space above the interface and below the interface. The nature of the field near the interface due to these sources has been investigated in this chapter. Later a generalized finite source of radiation is assumed to be located arbitrarily in the two media. The resulting fields near the interface are found asymptotically in the far zone.

Interfacial propagation may also happen due to infinite extent sources. In Chapter 4 a current sheet is placed across the dielectric half space interface. Electric field in the vicinity of the interface is found asymptotically. The behaviour of phase velocity in this case is also determined. In the fifth and the final chapter a discussion on results of

various cases considered in this thesis is carried out. An effort has been made to explain the true nature of the phase velocity near the interface in this work.

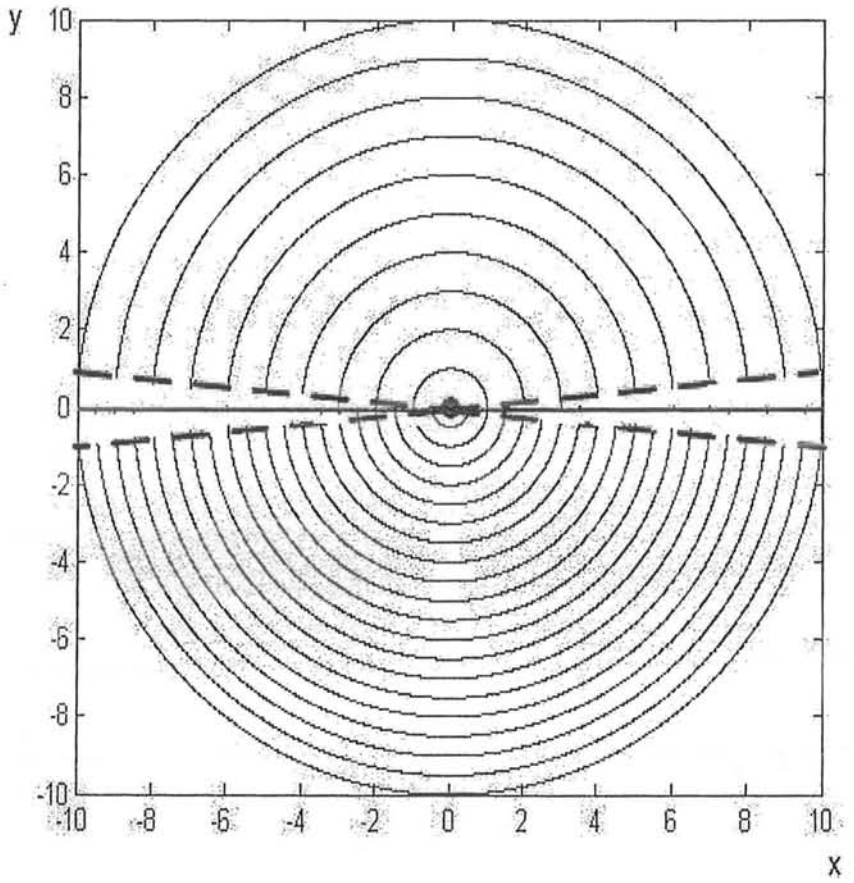

Figure 1.4: Circular phase fronts due to interfacial line source between two dielectric half spaces

Chapter 2

Interfacial Line Source

It is desired to formulate a problem where EM waves will propagate parallel to the dielectric interface. The simplest geometrical configuration possible is the current carrying line source present at the interface of two dielectric media. Engheta and Papas [4] has solved this problem. First order asymptotic solution has been obtained by him which describes power radiated in the two half spaces. The limitations present in the solution are that they do not describe the conditions existing at the interface. According to his results the electric field, E_z which is zero at the boundary is continuous but the magnetic field H_x is discontinuous. Further a zero field indicates a zero phase velocity $\vec{v}$ which is structurally an unstable condition. In this chapter the work carried out in [4] is extended in such a way that the above raised objections are removed and an structurally stable configuration of surfaces of constant phase is determined.

2.1 Problem Formulation

Consider Fig. 2.1 in which a dielectric with permittivity ϵ_1 fills the region $y > 0$ and another dielectric with permittivity ϵ_2 fills the region $y < 0$. As materials are non-magnetic in nature generally the permeability of free space, μ_0 is assumed for both half

spaces. A linear source of electric current is placed coincident with the z-axis on the interface of the dielectric media. The current distribution associated with this source is given as,

$$\mathbf{J} = I\delta(x)\delta(y)e^{-i\omega t}\hat{a_z},$$

where $\delta(\cdot)$ is Dirac delta function, I is the current whose magnitude is given in Amperes, and $\hat{a_z}$ is unit vector along z-axis. The time harmonic dependence term is take as $e^{-i\omega t}$

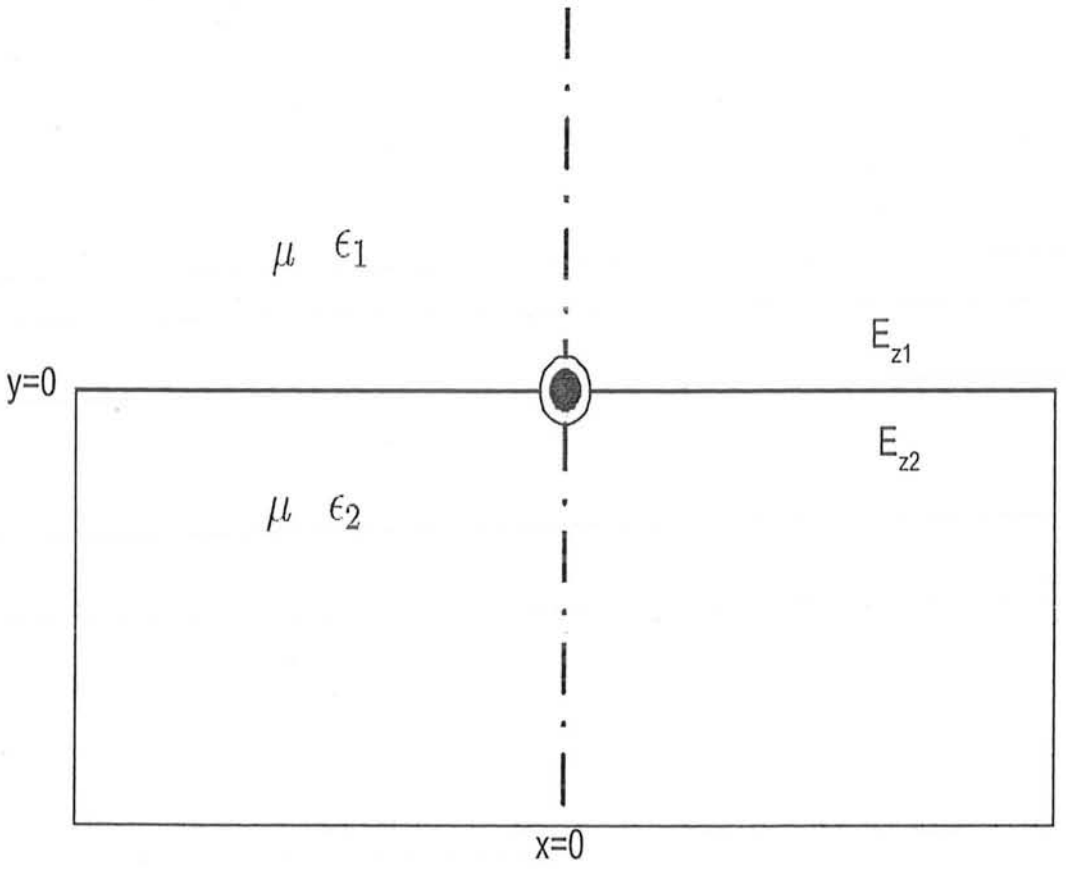

Figure 2.1: Geometry of the problem

and it will be suppressed in further calculations. Due to the geometry of the problem,

only the z-component of the electric field, $E_z\hat{a_z}$ will be present. Maxwell's equations reduce the problem to the solution of Helmohltz's equation for the electric field $E_z(x,y)$ given as,

$$\nabla^2 E_z + k^2 E_z = -i\omega\mu I\delta(x)\delta(y), \tag{2.1}$$

where $k = \omega\sqrt{\mu_0\varepsilon}$ is commonly known as wavenumber. The wavenumber is k_1 for $y > 0$ and it is k_2 for $y < 0$. The refractive index in region $y < 0$ is $n = \sqrt{\epsilon_2/\epsilon_1} > 1$.

Solution for E_z in (2.1) is called Green's function. The solution given below follows that of Engheta and Papas [4]. This solution is given in terms of spectrum of plane waves. Homogenous solution to the Helmohltz's equation is a plane wave,

$$E_z = \begin{cases} e^{i\sqrt{k_1^2 - k_x^2}y} e^{ik_x x} = e^{ik_{1y}y} e^{ik_x x} & y > 0; \\ \\ e^{-i\sqrt{k_2^2 - k_x^2}y} e^{ik_x x} = e^{-ik_{2y}y} e^{ik_x x} & y < 0; \end{cases}$$

where k_x is arbitrary and

$$k_{1y} = \sqrt{k_1^2 - k_x^2}, \qquad k_{2y} = \sqrt{k_2^2 - k_x^2}.$$

The coordinate chosen for k_{1y} and k_{2y} is such that the radiation condition is satisfied. A linear combination of all such solutions for all values of k_x will also represent a solution to the Helmohltz's equation. This statement can be mathematically written as,

$$E_z = \int_{-\infty}^{\infty} A(k_x) e^{ik_x x} e^{ik_{1y}y} dk_x \qquad y \geq 0, \tag{2.2}$$

$$E_z = \int_{-\infty}^{\infty} A(k_x) e^{ik_x x} e^{-ik_{2y}y} dk_x \qquad y \leq 0. \tag{2.3}$$

The complex amplitude function $A(k_x)$ is same for both the regions to satisfy the boundary condition that tangential component of electric field, E_z is continuous across the interface at $y = 0$.

The proposed solutions are used in the wave equation using the fact that,

$$\delta(x) = \frac{1}{2\pi}\int_{-\infty}^{\infty} e^{ik_x x}dk_x,$$

and that $e^{ik_x x}$ form an orthogonal set of functions. The magnetic field component tangential to the interface is $H_x = -(i/\omega\mu)\partial E_Z/\partial y$ and it must be continuous at the interface $y = 0$. This boundary condition when applied to (2.2) and (2.3) yields

$$\frac{i}{\omega\mu}\Big\{\int_{-\infty}^{\infty} ik_{1y}A(k_x)e^{ik_x x}dk_x + \int_{-\infty}^{\infty} ik_{2y}e^{ik_x x}dk_x\Big\} = -I\delta(x) \tag{2.4}$$

The above can be written as

$$\int_{-\infty}^{\infty}\Big\{k_{1y}A + k_{2y}A - \frac{\omega\mu I}{2\pi}\Big\}e^{ik_x x}dk_x = 0 \tag{2.5}$$

The above condition gives the complex amplitude coefficient,

$$A(k_x) = -\frac{\omega\mu I}{2\pi\Big\{\sqrt{k_1^2 - k_x^2} + \sqrt{k_2^2 - k_x^2}\Big\}} = -\frac{\omega\mu I}{2\pi(k_{1y} + k_{2y})}. \tag{2.6}$$

Therefore the plane wave representation of E_z, for the two regions is,

$$E_{z1} = -\frac{\omega\mu I}{2\pi}\int_{-\infty}^{\infty}\frac{e^{i(k_x x + k_{1y}y)}}{(k_{1y} + k_{2y})}dk_x \qquad y > 0, \tag{2.7}$$

$$E_{z2} = -\frac{\omega\mu I}{2\pi}\int_{-\infty}^{\infty}\frac{e^{i(k_x x - k_{2y}y)}}{(k_{1y} + k_{2y})}dk_x \qquad y < 0. \tag{2.8}$$

The solutions of equations (2.7) and (2.8) at $y = 0$ is given as,

$$E_z = E_{z1} = E_{z2} = \frac{\omega\mu I}{2(n^2 - 1)k_1}\left\{\frac{1}{|x|}H_1^{(1)}(k_1|x|) - \frac{n}{|x|}H_1^{(1)}(nk_1|x|)\right\}. \tag{2.9}$$

The asymptotic evaluation of (2.7) and (2.8) will be carried out for the two half spaces separately.

2.2 Asymptotic Solution for Upper Half Space

In the expression (2.7) the path of integration runs on real axis of complex k_x plane from $k_x = -\infty$ to $k_x = +\infty$. There are branch point singularities present in (2.7). These singularities are present at $k_x = \pm k_1$ and $k_x = \pm k_2$. The path of integration, P and the branch points are shown in Fig. 2.2. The branch cuts present at $k_x = -k_n$ where

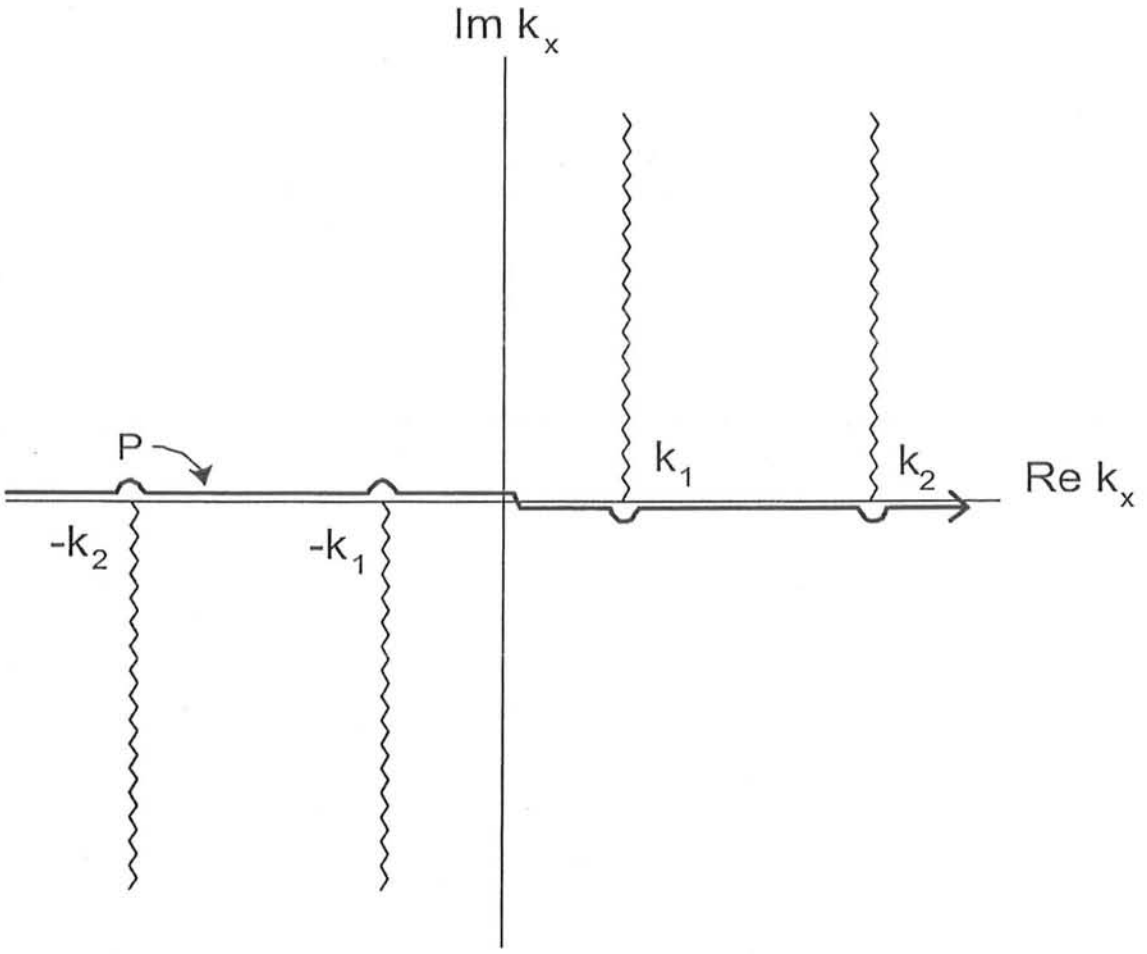

Figure 2.2: Branch cuts drawn to satisfy radiation conditions in E_{z1}

$n = 1, 2$ are made to run arbitrarily in in the plane $\Im k_x < 0$ to satisfy the radiation

conditions. Similarly to satisfy the radiation conditions the branch cuts originating from $k_x = k_1$ and $k_x = k_2$ are extended in $\Im k_x > 0$ plane. The path of integration P is to be closed at infinity to evaluate the integrals. The path P will be deformed to avoid the branch cuts. This deformed path is shown as P' in Fig. 2.3.

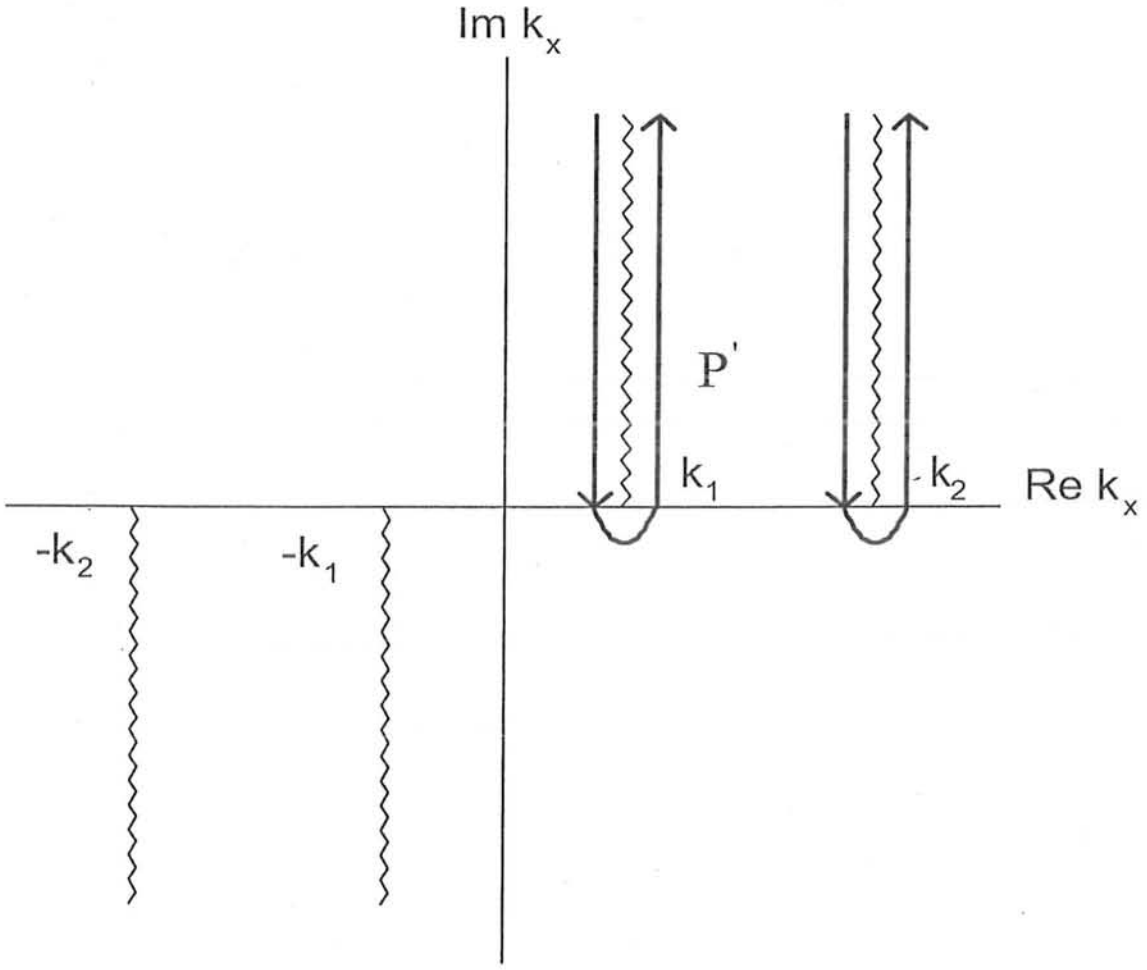

Figure 2.3: Deformed Path of Integration for Branch cuts for E_{z1}

For the convenience in the subsequent evaluation of integral (2.7) the mapping from the complex k_x plane to the complex α plane is carried out. The relationship which

governs this mapping is,

$$k_x = k_1 \cos\alpha = k_1 \cos(\eta + i\zeta). \tag{2.10}$$

Under this transformation $k_{1y} = k_1 \sin\alpha$ and

$$k_{2y} = \sqrt{k_2^2 - k_1^2 \cos^2\alpha}.$$

The transcendental function $\cos(\alpha)$ is single-valued in the above relationship. From its periodicity property $\cos(\alpha + 2n\pi) = \cos(\alpha)$where $n = \pm 1, \pm 2, ...$, it is evident that a multiplicity of α values corresponds to the same value of k_x. Thus the entire k_x plane can be mapped into various adjacent sections of width π in the α plane. To investigate in detail the properties of the mapping from the k_x to the α plane (2.10) is separated into its real and imaginary parts, assuming k_1 to be real,

$$k_r = k_1 \cos\eta \cosh\zeta, \qquad k_i = -k_1 \sin\eta \sinh\zeta, \tag{2.11}$$

where,

$$k_x = k_r + ik_i.$$

The four quadrants in the k_x plane are mapped in the α plane into corresponding regions identified according to equation (2.10) as shown in Fig. 2.4. These can also be identified by the encircled numbers in the same Fig. 2.4. The repetitious nature of the regions in the α plane can be noted as η changes by multiples of 2π. So this mapping is seen not to be $1-1$, rather $1-$ many. The path of integration P in the original k_x plane is now shown as Q in the new α plane. The transformation also results in the removal of one branch point pair at $\pm k_1$. The remaining two branch cuts also run arbitrarily as shown in Fig. 2.5.

To put the integral (2.7) in a simplified form, cartesian coordinates x and y are converted to polar coordinates r and θ. The relationship used relating these two coordinates

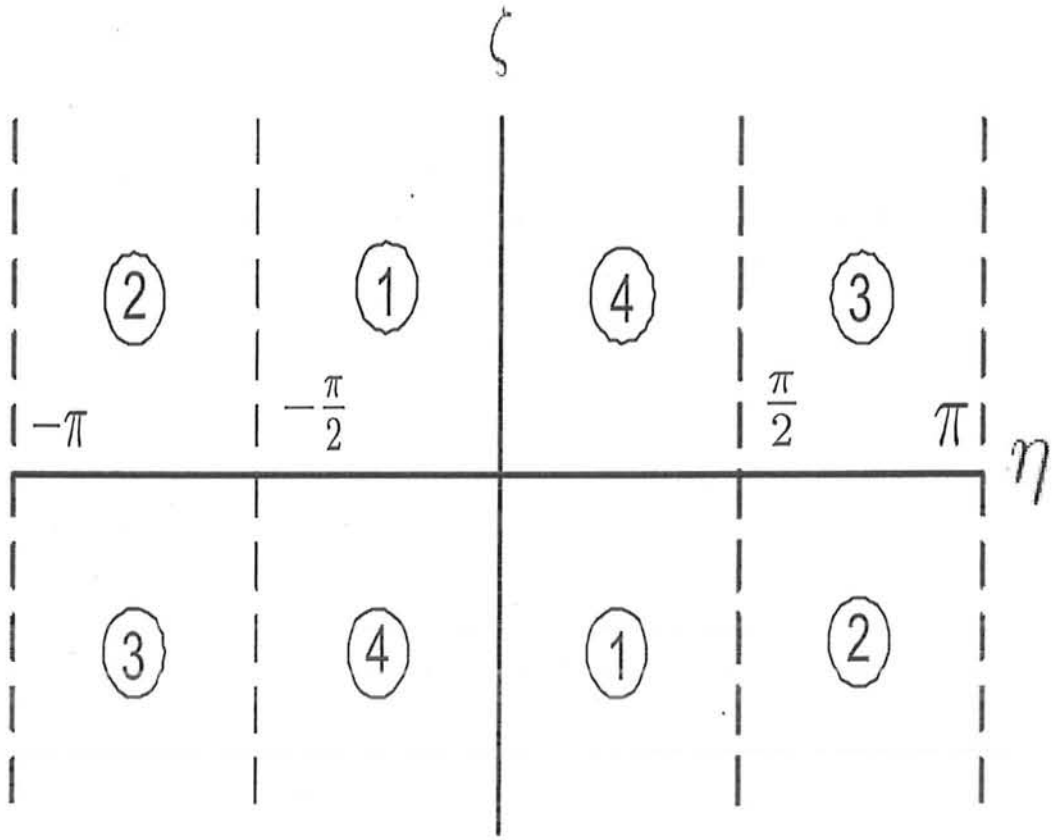

Figure 2.4: Mapped complex α plane

is,

$$x = r\cos\theta, \qquad y = r\sin\theta.$$

The field represented in the upper half space by (2.7) is now represented by,

$$E_{z1} = \frac{\omega\mu I}{2\pi}\int_Q F(\alpha)e^{k_1 r f(\alpha)}d\alpha, \tag{2.12}$$

where,

$$F(\alpha) = \frac{\sin\alpha}{(\sin\alpha + \sqrt{n^2 - \cos^2\alpha})},$$

and,

$$f(\alpha) = i\cos(\alpha - \theta).$$

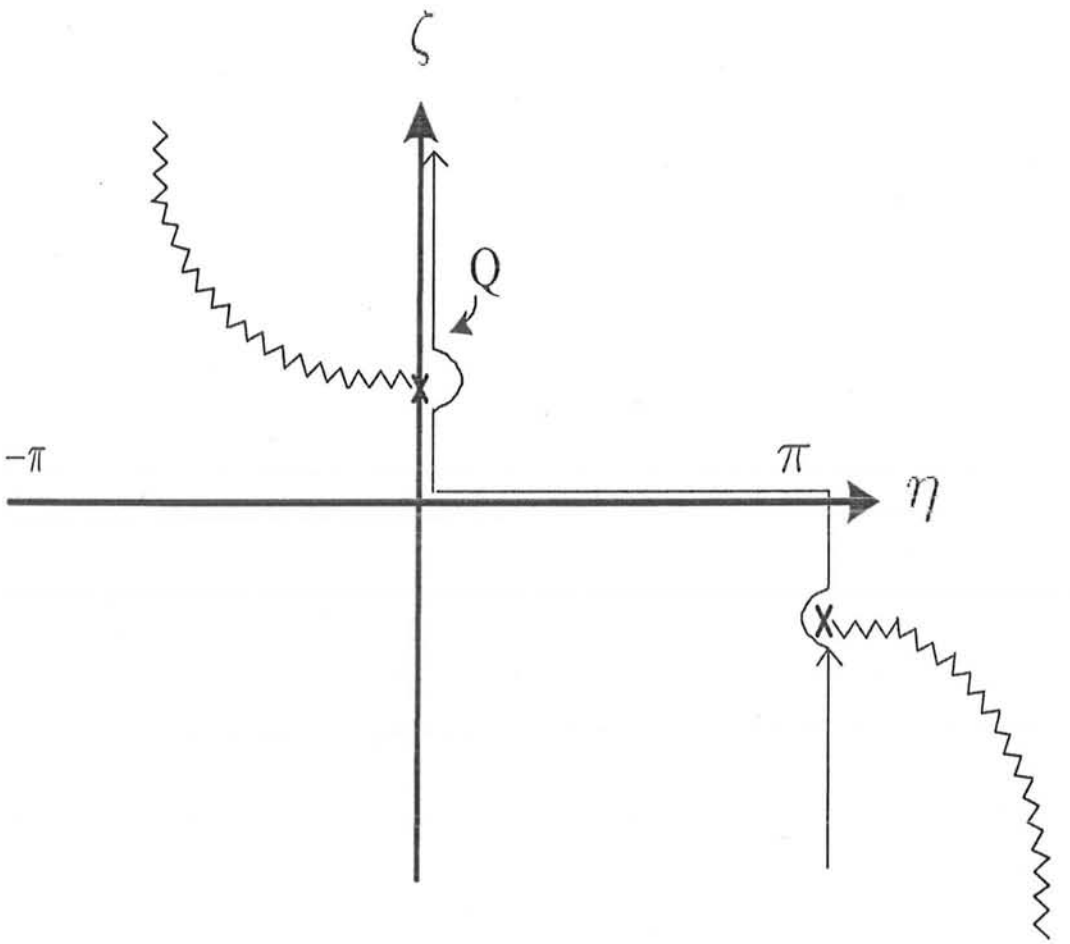

Figure 2.5: Only one pair of branch cuts left in the new α plane.

The integral in (2.12) is of Laplace type. The observation point is in the far zone thus $k_1 r$ is a large parameter which appears in the exponential term. It is the large value of $k_1 r$ which permits to observe the field behavior near the interface for small values of θ. There are only two branch points present at $\alpha = i\cosh^{-1}(n)$ and $\alpha = \pi - i\cosh^{-1}(n)$ in

(2.12). The amplitude function $F(\alpha)$ varies slowly in comparison with the exponential function. The method of steepest descent is the most convenient to evaluate (2.12).

$\eta = \theta$

$\zeta = \zeta_c$ An examination of $f(\alpha)$ shows that there is a saddle point at $\alpha = \theta$. The path of integration will be now changed so as to run on path of constant phase while passing through the saddle point. This deformed path of integration is shown as Q' in Fig. 2.6. The endpoints of deformed path of integration are joined with the original

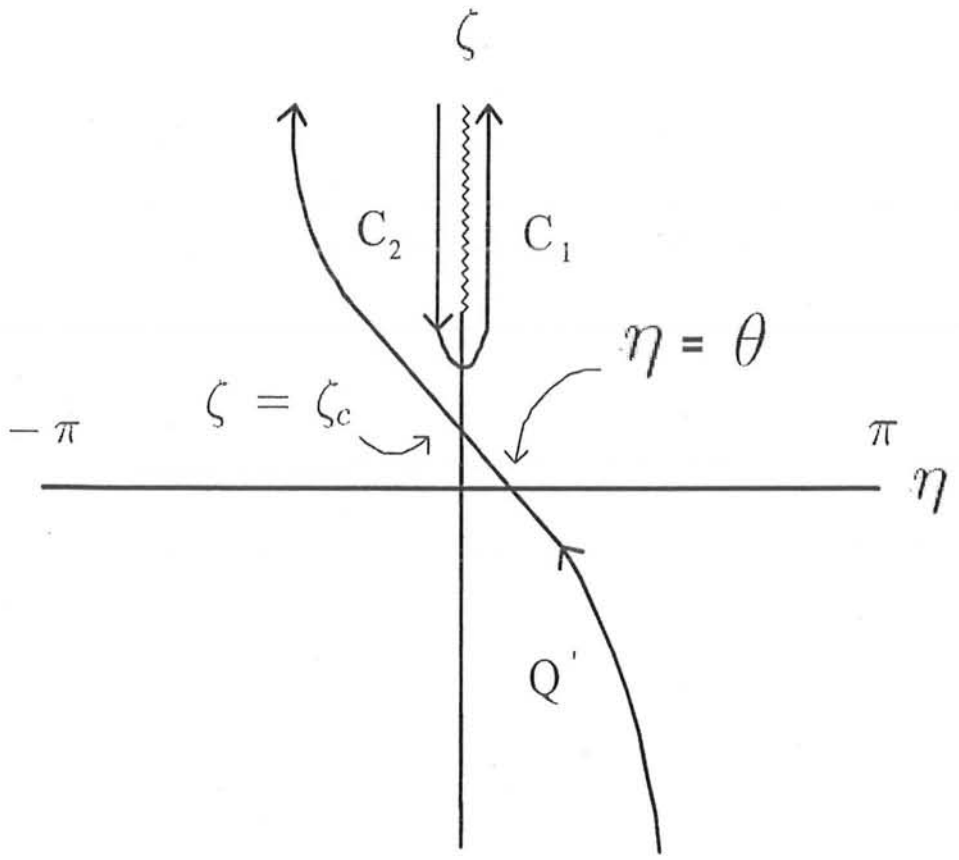

Figure 2.6: Branch point at $\alpha = i\cosh\eta$ contributes in evaluation for E_{z1}

path of integration, Q at infinity. The enclosed region between Q and Q' should not

contain any singularities. The contribution of branch point singularity at $\alpha = i\cosh^{-1}\eta$ will be summed with the saddle point contribution when $0 \leq \theta \leq \cos^{-1}(1/n)$, as shown in Fig. 2.6. When the condition $0 \leq \theta \leq \cos^{-1}(1/n)$ is met, the path of integration will be deformed with its segments shown as $C1$ and $C2$ in this figure. Similarly when $\pi/2 \leq \theta \leq \pi$ the contribution from the second branch point at $\alpha = \pi - i\cosh^{-1}\eta$ will be included in the evaluation of integral (2.12). It can be seen from Fig. 2.7 that neither of the branch point contributes when the observation angle is $\pi/2$.

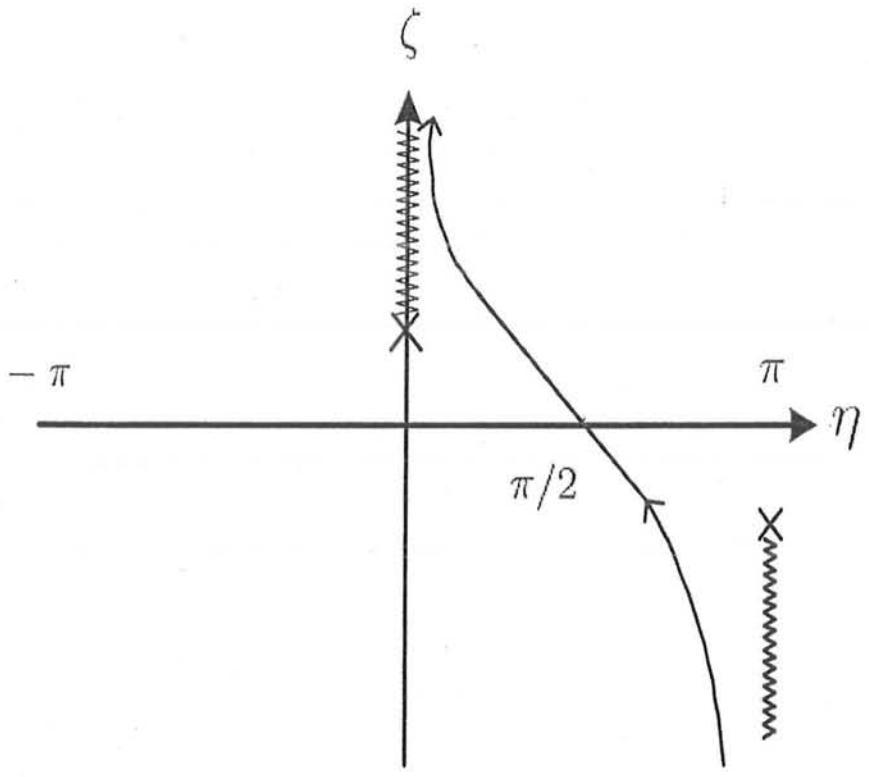

Figure 2.7: Neither of the Branch Cut will Contribute when $\theta = \pi/2$

For a further facilitation in the evaluation of (2.12) the phase function $f(\alpha)$ is replaced by the simplest polynomial having the same local behavior as $f(\alpha)$ near the saddle point.

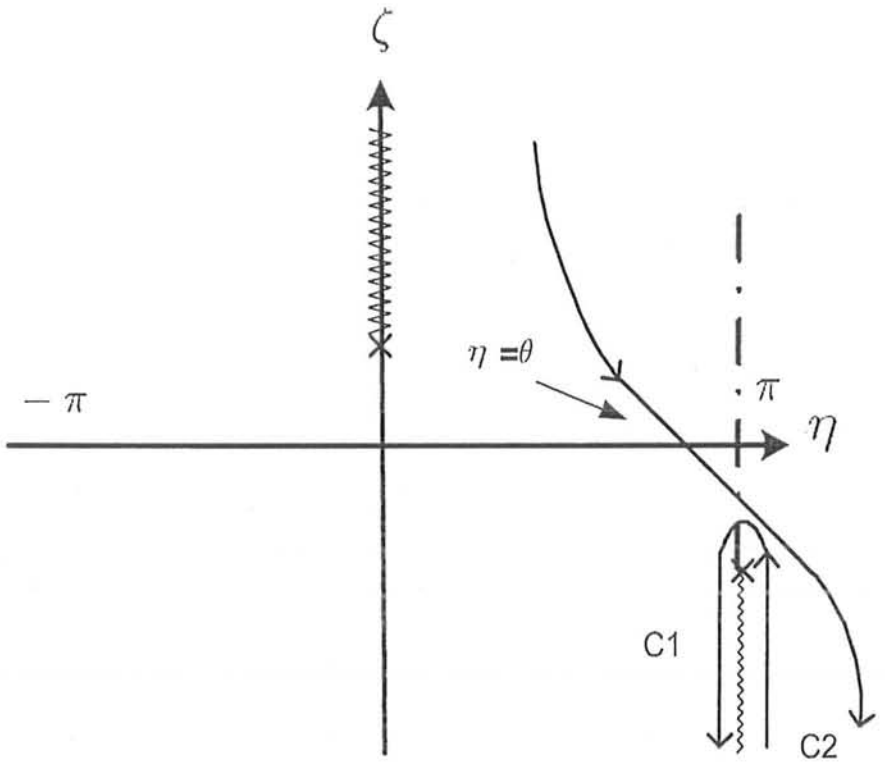

Figure 2.8: Lower Branch Cut will Contribute when $\pi/2 < \theta < \pi$

The transformation is carried out according to [10],

$$f(\alpha) = f(\alpha_s) - s^2. \tag{2.13}$$

The steepest descent path in the s plane, along which $\Im\tau(s)$=constant, has shifted along real s-axis. The integral in (2.12) becomes,

$$E_{z1} = \frac{\omega\mu I e^{ik_1 r}}{2\pi}\int_{-\infty}^{\infty} G(s)e^{-k_1 r s^2}ds, \tag{2.14}$$

where,

$$G(s) = F(\alpha_s)\frac{d\alpha}{ds}.$$

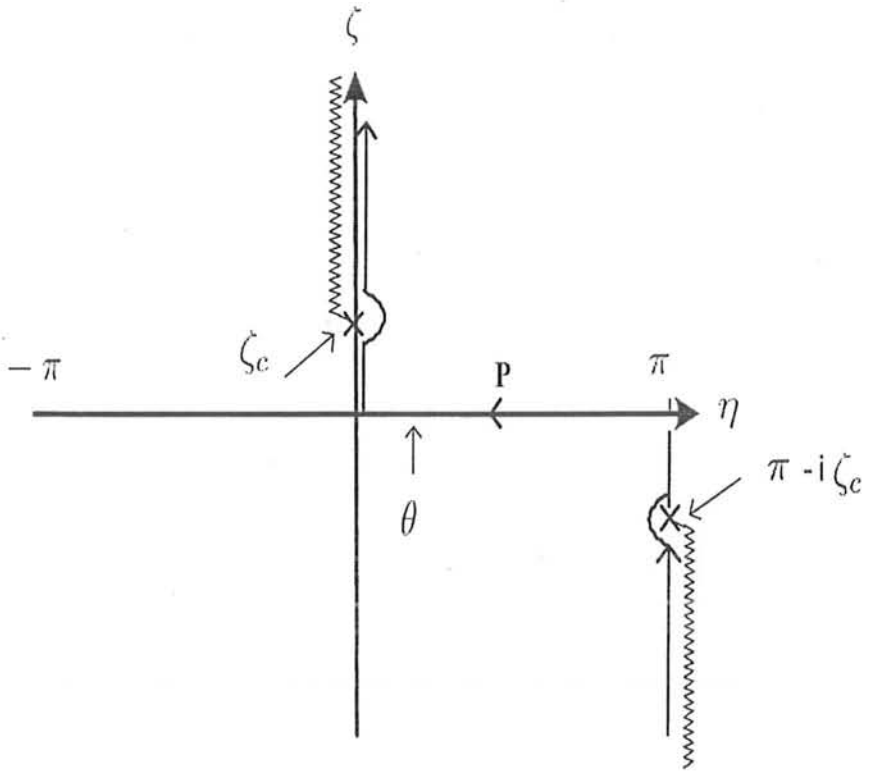

Figure 2.9: No Branch Point Contribution when $\eta_c > \eta_b$

The saddle point is now shifted to the origin of new s plane. The power series expansion of $G(s)$ about $s = 0$ is given as,

$$G(s) = G(0) + G'(0)s + G''(0)\frac{s^2}{2!} + ... + G^{(n)}(0)\frac{s^n}{n!}.$$

Only first and third terms of expansion will be taken for the evaluation of (2.12). The second term makes the integrand in (2.12) as an odd function of s and the symmetrical integration interval around $s = 0$ will result into a zero for this second term. The term

by term integration results into the following expression representing the saddle point contribution,

$$E_{z1-\text{sad}} = \frac{\omega\mu I e^{ik_1 r}}{2\pi\sqrt{k_1 r}} \sum_{n=0}^{\infty} \frac{G^{(2n)}(0)}{(2n)!} \frac{\Gamma(n+\frac{1}{2})}{(k_1 r)^n}. \tag{2.15}$$

The first term in power series expansion of $G(s)$ will be,

$$G(0) = F(\alpha_s) \left.\frac{d\alpha}{ds}\right|_{s=0},$$

where,

$$\left.\frac{d\alpha}{ds}\right|_{s=0} = \sqrt{\frac{-2}{f''(\alpha_S)}} = \sqrt{2}e^{-i\pi/4},$$

and

$$F(\alpha_s) = \frac{\sin\theta}{(\sin\theta + \sqrt{n^2 - \cos^2\theta})}.$$

Similarly the second term is given as,

$$G^{(2)}(0) = \{F^{(2)}(\alpha_s)[\phi(0)]^3 + 3F'(\alpha_s)\phi(0)\phi'(0) + F(\alpha_s)\phi^{(2)}(0)\},$$

where,

$$\begin{aligned} [\phi(0)]^3 &= 2\sqrt{2}e^{-i3\pi/4}, \\ \phi^{(2)}(0) &= \frac{e^{-i3\pi/4}}{\sqrt{2}}, \\ \phi'(0) &= 0, \end{aligned}$$

and,

$$F^{(2)}(\alpha_s) = \frac{\{2\cos^4\theta + n^2\sin\theta(\sin\theta - \sqrt{n^2 - \cos^2\theta}) - 2\cos^2\theta(n^2 - \sqrt{n^2 - \cos^2\theta})\}}{(n^2 - \cos^2\theta)^{3/2}(\sin\theta + \sqrt{n^2 - \cos^2\theta})}.$$

Substitution of the above relationships in (2.14) results into the expression for the saddle point contribution in the upper half space,

$$E_{z1-\text{sad}} = -\frac{\omega\mu I e^{ik_1 r}}{\sqrt{2\pi k_1 r}} \left\{ F_1(\theta)e^{-i\pi/4} + \frac{F_2(\theta)e^{-i3\pi/4}}{2k_1 r} \right\}, \tag{2.16}$$

where,

$$F_1(\theta) = \frac{\sin\theta}{(\sin\theta + \sqrt{n^2 - \cos^2\theta})},$$

and,

$$\begin{aligned} F_2(\theta) &= \frac{1}{(\sin\theta + \sqrt{n^2 - \cos^2\theta})} \times \\ &\left[\frac{\{2\cos^4\theta + n^2\sin\theta(\sin\theta - \sqrt{n^2 - \cos^2\theta}) - 2\cos^2\theta(n^2 - \sin\theta\sqrt{n^2 - \cos^2\theta})\}}{(n^2 - \cos^2\theta)^{3/2}}\right. \\ &\left. + \frac{\sin\theta}{4}\right]. \end{aligned} \tag{2.17}$$

It can be seen that the dominant term which decays as $(k_1 r)^{-1/2}$ vanishes at the interface. This is in accordance with the results of [4]. But it is not true for the next higher order term which decays as $(k_1 r)^{-3/2}$. The zero electric field conditions which existed in the results of Engheta and Papas no longer hold true if higher order terms in the asymptotic evaluations are taken. As it has been already pointed out that (2.12) contains an isolated saddle point at $\alpha = \theta$ along with a pair of branch points at $\alpha = i\cosh\eta$ and $\alpha = \pi - i\cosh\eta$. The point of observation in the far field is assumed to be located in the region $x > 0$ due to the symmetry of the problem geometry. It means the observation angle will lie in the range of $0 < \theta < \pi/2$.

The branch cut originating from branch point present at $\alpha = i\cosh\eta$ is made to follow a steepest descent path Q' thereby facilitating the evaluation of the integral, as shown in Fig. 2.6. The same kind of polynomial transformation is carried out as was done to find out the saddle point contribution,

$$f(\alpha) = f(\alpha_b) - s^2, \tag{2.18}$$

where,

$$f(\alpha_b) = \cos(\alpha_b - \theta) = (n\cos\theta + i\sqrt{(n^2 - 1)}\sin\theta).$$

The above substitution transforms (2.11) into the following form,

$$E_{z1} = e^{ik_1 r\cos(\alpha_b-\theta)}\int_{-\infty}^{\infty} G(s)e^{-k_1 r s^2}ds, \tag{2.19}$$

where,

$$G(s) = F(s)\frac{d\alpha}{ds},$$

and,

$$F(s) = \frac{\sin\alpha}{(\sin\alpha + \sqrt{n^2-\cos^2\alpha})}.$$

From the relationship (2.18) of plane transformation,

$$\frac{d\alpha}{ds} = -\frac{i2s}{\sin(\alpha-\theta)} = -\frac{i2s}{\sqrt{1-[\cos(\alpha_b-\theta)+is^2]^2}} \tag{2.20}$$

The above can be approximated near $s = 0$ as,

$$\frac{d\alpha}{ds} \approx \frac{2se^{-i\pi/2}}{\sin(\alpha_b-\theta)}. \tag{2.21}$$

The power series expansion of $F(s)$ around $\alpha = \alpha_b$ is,

$$F(s) \approx 1 - \frac{\sqrt{2n}(1-n^2)^{1/4}\sqrt{\alpha-\alpha_b}}{(1-n^2)^{1/2}}. \tag{2.22}$$

The factor $\sqrt{\alpha-\alpha_b}$ is obtained by expansion of $\cos(\alpha-\alpha_b)$ around $\alpha = \alpha_b$ resulting in the following form,

$$\sqrt{\alpha-\alpha_b} = \frac{s}{\sqrt{i\sin(\alpha_b-\theta)}\ i}.$$

The resultant form of $F(s)$ is,

$$F(s) = 1 - \frac{\sqrt{2n}se^{-i5\pi/4}}{(1-n^2)^{1/4}\sqrt{\sin(\alpha_b-\theta)}}.$$

The even term of s^2 in the final form of $G(s)$ will integrate out to give results while the odd term containing the factor of s will integrate out to zero.

$$\begin{aligned} G(s) &= -\frac{\sqrt{2n}se^{-i5\pi/4}}{(1-n^2)^{1/4}\sqrt{\sin(\alpha_b-\theta)}} \times \frac{2se^{-i\pi/2}}{\sin(\alpha_b-\theta)} \\ &= -\frac{2\sqrt{2n}s^2}{(n^2-1)^{1/4}\{\sin(\alpha_b-\theta)\}^{3/2}} \end{aligned} \tag{2.23}$$

The following result is obtained, involving powers of s^2 according to (2.23),

$$E_{z1-br} \approx -\frac{\omega\mu I\sqrt{n}e^{i(k_2 r\cos\theta)-k_1 r\sqrt{n^2-1}\sin\theta}}{\sqrt{2\pi}(n^2-1)^{1/4}(k_1 r)^{3/2}(\sin(\alpha_b-\theta))^{3/2}}. \tag{2.24}$$

As,

$$\sin(\alpha_b-\theta) = i\sqrt{n^2-1}\cos\theta - n\sin\theta,$$

the branch point contribution given in (2.24) result into the following form,

$$E_{z1-br} \approx -\frac{\omega\mu I\sqrt{n}e^{i(k_2 r\cos\theta-3\pi/4)-k_1 r\sqrt{n^2-1}\sin\theta}}{\sqrt{2\pi}(n^2-1)^{1/4}(k_1 r)^{3/2}(\sqrt{n^2-1}\cos\theta+in\sin\theta)^{3/2}}. \tag{2.25}$$

It can be seen from the expression that the branch cut contribution is in the form of a lateral wave, [11], which decays fast perpendicular to the interface and propagates along the interface. The total field in the upper half space near the interface is given as,

$$\begin{aligned} E_{z1} &= -\frac{\omega\mu I e^{ik_1 r}}{\sqrt{2\pi k_1 r}}\left\{F_1(\theta)e^{-i\pi/4}+\frac{F_2(\theta)e^{-i3\pi/4}}{2k_1 r}\right\} \\ &- \frac{\omega\mu I\sqrt{n}e^{i(k_2 r\cos\theta+ik_1 r\sqrt{n^2-1}\sin\theta)}e^{-i3\pi/4}}{\sqrt{2\pi}(n^2-1)^{1/4}(k_1 r)^{3/2}(\sqrt{n^2-1}\cos\theta+in\sin\theta)^{3/2}}u(\cdot). \end{aligned} \tag{2.26}$$

The first two terms of the above field expression contains the leading term and the next higher order term from saddle point contribution in the field expression for the upper half space. The third term is the branch point contribution present in the electric field expression for the upper half space.

2.3 Asymptotic Solution for Lower Half Space

The expression in (2.8) which is integral representation of electric field E_{z2} for lower half space has also two pairs of branch points at $k_x = \pm k_2$ and $k_x = \pm k_1$. The path of integration in (2.8) also runs on real k_x-axis from $k_x = -\infty$ to $k_x = \infty$ as in (2.7) which represents electric field for upper half space. The path deformation and extensions of

branch cuts in the k_x plane are according to Fig. 2.2. The k_x plane is mapped to α-plane according to the following relationship to facilitate the evaluation.

$$k_x = k_2 \cos\alpha, \qquad k_{2y} = k_2 \sin\alpha, \qquad k_{1y} = \sqrt{1/n^2 - \cos^2\alpha}.$$

Cartesian coordinates x and y are changed to polar coordinates r and θ to convert the integral in a more simplified form. Electric field E_{z2} for the lower half space is now represented in new α-plane as,

$$E_{z2} = \frac{\omega\mu I}{2\pi}\int_Q F(\alpha)e^{k_2 r f(\alpha)}d\alpha, \tag{2.27}$$

where,

$$F(\alpha) = \frac{\sin\alpha}{(\sin\alpha + \sqrt{1/n^2 - \cos^2\alpha})},$$

and,

$$f(\alpha) = i\cos(\alpha + \theta).$$

According to (2.27) it is clear that one pair of branch points at $k_x = \pm k_2$ has been converted to a saddle point at $\alpha = -\theta$. The other pair of branch points at $k_x = \pm k_1$ in the original k_x plane has now shifted on the real axis of α-plane at $\alpha_1 = \cos^{-1}(1/n)$ and $\alpha_2 = \pi - \cos^{-1}(1/n)$. This is shown in Fig. 2.10 along with the path of integration, Q.

The observation point is in the far zone so $k_2 r$ is a large parameter present in the exponential term in (2.27). Due to this reason it is pertinent to use steepest descent method for its evaluation. The path of integration Q will be deformed to run along a constant phase path Q' shown in Fig. 2.11. It can be seen in this figure that while joining endpoints of Q' with the original path Q at infinity the branch cut will be enclosed while $\theta < \cos^{-1}(1/n)$. Path Q' will be deformed to follow path P_b path as shown in Fig. 2.12 to avoid crossing the branch cut. It will be required to sum the saddle point contribution as well as branch point contribution in this particular case. On the contrary when

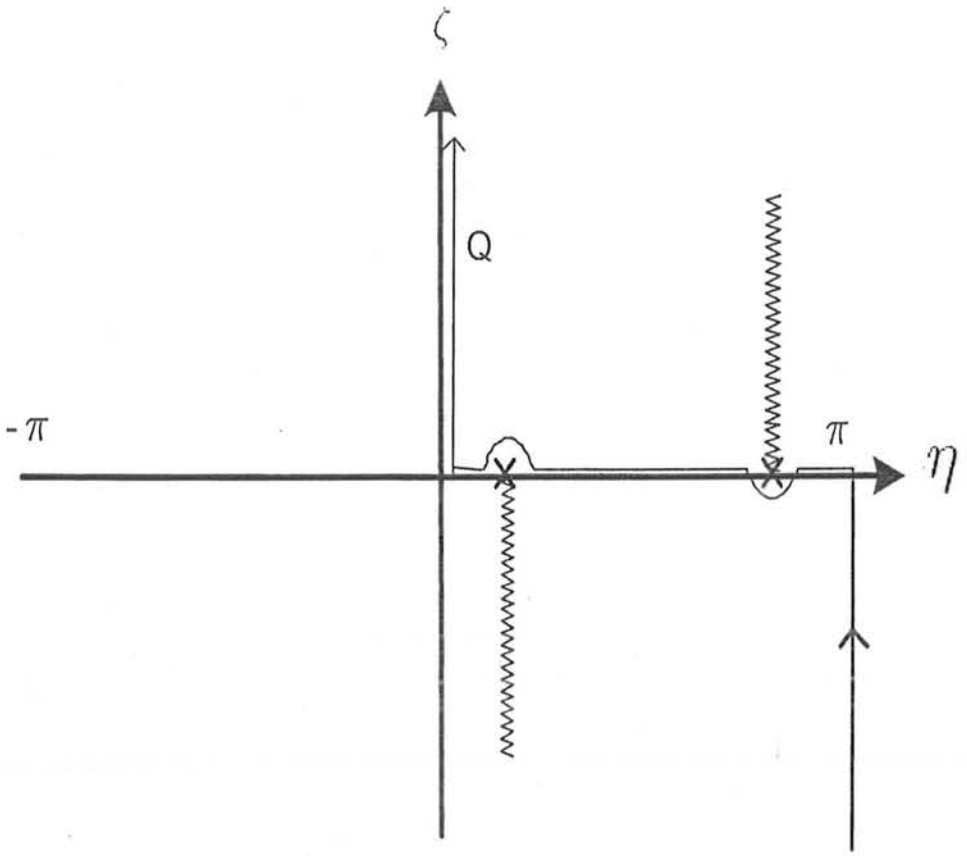

Figure 2.10: Original path of integration, Q and the pair of branch cuts for E_{z2} in α-plane

$\theta > \cos^{-1}(1/n)$ only the saddle point contribution will represent the electric field in the lower half space. The steepest descent path for the evaluation of the saddle point contribution follows the equation,

$$\cos(\zeta + \theta)\cosh\eta = 1.$$

A transformation of α-plane to s-plane is carried out similar to equation (2.13). The

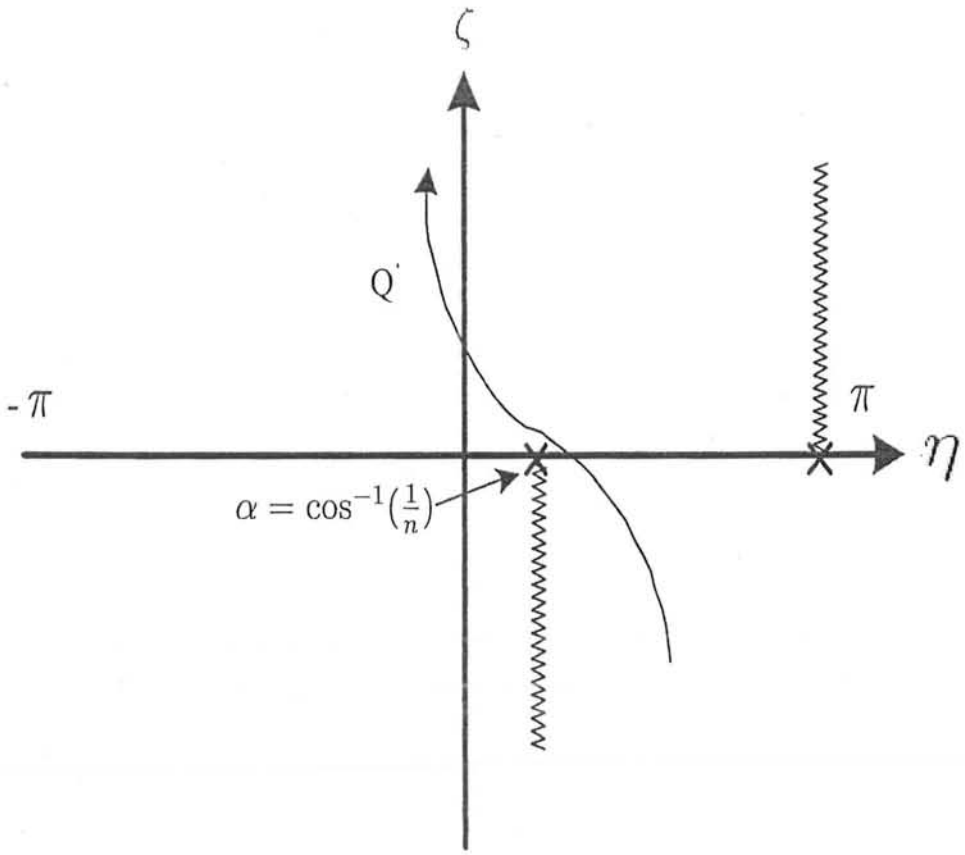

Figure 2.11: Deformed Path of Integration, Q' and the pair of branch cuts for E_{z2} in α-plane

resulting integral becomes,

$$E_{z2} = \frac{\omega\mu I e^{k_2 r f(\alpha_s)}}{2\pi(n^2-1)} \int G(s) e^{-k_2 r s^2} ds, \tag{2.28}$$

with,

$$G(s) = F(s)\frac{d\alpha}{ds}.$$

Taking the power series expansion of $G(s)$ at $s = 0$ only the first two even powered terms of s will be used. The terms involving odd powers of s integrate out to zero due

to the interval of integration being identical on both sides of $s = 0$. The saddle point contribution comes out to be,

$$E_{z2-sad} = -\frac{\omega\mu I e^{ik_2 r}}{\sqrt{2\pi k_2 r}}\left\{F_3(\theta)e^{-i\pi/4} + \frac{F_4(\theta)e^{-i3\pi/4}}{2(k_2 r)}\right\}, \tag{2.29}$$

where,

$$F_3(\theta) = \frac{\sin\theta}{(\sin\theta + \sqrt{1/n^2 - \cos^2\theta})},$$

and,

$$\begin{aligned} F_4(\theta) = & \frac{1}{(\sin\theta + \sqrt{1/n^2 - \cos^2\theta})(1/n^2 - \cos^2\theta)^{3/2}} \times \\ & \left\{2\cos^4\theta + \frac{1}{n^2}\sin\theta(\sin\theta - \sqrt{1/n^2 - \cos^2\theta}) - \right. \\ & \left. 2\cos^2\theta(1/n^2 - \sin\theta\sqrt{1/n^2 - \cos^2\theta}) + \frac{\sin\theta(1/n^2 - \cos^2\theta)^{3/2}}{4}\right\}. \end{aligned} \tag{2.30}$$

The dominant term which decays with $(k_2 r)^{-1/2}$ vanishes at the interface. In this case also the next higher order term results into non-zero electric field at the interface which is an extension of Engheta and Papas results.

As discussed in the last section due to the symmetry of the problem geometry the far zone electric field is being analyzed only for $x > 0$ region near the interface. Before application of the steepest descent method to evaluate the integral a transformation is made according to (2.18) in the last section which is,

$$f(\alpha) = f(\alpha_b) - s^2,$$

where,

$$f(\alpha) = i\cos(\alpha + \theta), \qquad f(\alpha_b) = i\cos(\alpha_b + \theta).$$

With the fact that $\alpha_b = \cos^{-1}(1/n)$ the following relationship is obtained,

$$f(\alpha_b) = i\cos(\alpha_b + \theta) = \frac{i}{n}\{\cos\theta - \sqrt{n^2 - 1}\sin\theta\}$$

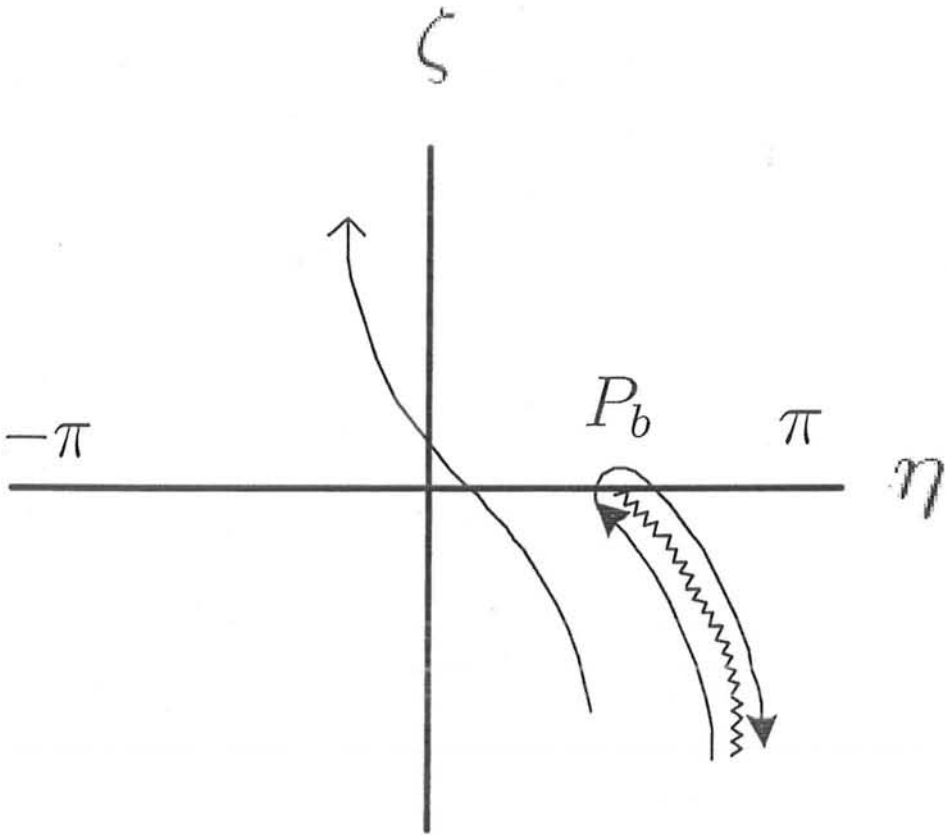

Figure 2.12: Branch point contribution is to be taken when $\theta < \cos^{-1}(1/n)$

The above substitutions result into the following form of electric field below the interface,

$$E_{z2} = -\frac{\omega\mu I e^{ik_1 r(\cos\theta - \sqrt{n^2-1}\sin\theta)}}{2\pi(n^2-1)} \int_{-\infty}^{\infty} G(s) e^{-k_2 r s^2} ds. \tag{2.31}$$

In the above expression,

$$G(s) = F(\alpha)\frac{d\alpha}{ds},$$

while,

$$F(\alpha) = n\sin\alpha(n\sin\alpha - i\sqrt{n^2\cos^2\alpha - 1}).$$

The power series expansion of $F(\alpha)$, around $\alpha = \alpha_b$, is,

$$F(\alpha) = \frac{\sin\alpha}{\sin\alpha + \sqrt{1/n^2 - \cos^2\alpha}} \approx 1 - \frac{\sqrt{2/n}(1-1/n^2)^{1/4}\sqrt{\alpha-\alpha_b}}{\sqrt{1-1/n^2}}, \tag{2.32}$$

while,

$$\frac{d\alpha}{ds} \approx \frac{2se^{-i\pi/2}}{\sin(\alpha_b+\theta)},$$

near $s = 0$.

It is known previously from last section that,

$$\sqrt{\alpha-\alpha_b} = \frac{se^{-i5\pi/4}}{\sqrt{\sin(\alpha_b+\theta)}}.$$

This gives,

$$F(s) = 1 - \frac{\sqrt{2}se^{-i5\pi/4}}{(n^2-1)^{1/4}\sqrt{\sin(\alpha_b+\theta)}}. \tag{2.33}$$

The last two relationships combine to give,

$$\begin{aligned} G(s) &= -\frac{\sqrt{2}se^{-i5\pi/4}}{(n^2-1)^{1/4}\sqrt{\sin(\alpha_b+\theta)}}\frac{2se^{-i\pi/2}}{\sin(\alpha_b+\theta)} \\ &= \frac{2\sqrt{2}s^2e^{-i3\pi/4}}{(n^2-1)^{1/4}\sin(\alpha_b+\theta)^{3/2}}. \end{aligned} \tag{2.34}$$

Carrying out the integration of (2.31) with $G(s)$ given by (2.34),

$$E_{z2-br} \approx -\frac{\omega\mu I e^{ik_1r(\cos\theta-\sqrt{n^2-1}\sin\theta)}e^{-i3\pi/4}}{\sqrt{2\pi}(n^2-1)^{1/4}(k_1r)^{3/2}\{\sqrt{n^2-1}\cos\theta+\sin\theta\}^{3/2}}. \tag{2.35}$$

Total field below the interface comes out to be by addition of (2.29) and (2.35),

$$\begin{aligned} E_{z2} &\simeq -\frac{\omega\mu I e^{ik_2r}}{\sqrt{2\pi k_2 r}}\left\{F_3(\theta)e^{-i\pi/4} + \frac{F_4(\theta)e^{-i3\pi/4}}{2(k_2r)}\right\} \\ &- \frac{\omega\mu I e^{ik_1r(\cos\theta-\sqrt{n^2-1}\sin\theta)}e^{-i3\pi/4}}{\sqrt{2\pi}(n^2-1)^{1/4}(k_1r)^{3/2}\{\sqrt{n^2-1}\cos\theta+\sin\theta\}^{3/2}}u(n\cos\theta-1). \end{aligned} \tag{2.36}$$

The first two terms of the above field expression are due to the saddle point in the expression for E_{z2} and the leading term from the branch point is represented by the third

term in the above field expression. The leading term due to saddle point is according to Engheta and Papas results which vanish at the interface but the next higher order term does not vanish at the interface. The branch point term also does not vanish at the interface.

2.4 Wave Propagation along the Interface

The expressions for the electric field have been obtained after the asymptotic evaluation of the field integrals (2.7) and (2.8). The solutions obtained satisfy the Helmohltz's equation as well as the boundary conditions at the interface. These solutions are given in (2.26) and (2.36). The contributions of different terms in the overall field expression present in these two equations will be discussed.

A very close mathematical symmetry is found to exist in (2.26) and (2.36). A close resemblance is found to exist between $F_1(\theta)$ and $F_3(\theta)$ which differ by reciprocal of refractive index, n. The same is also true for $F_2(\theta)$ and $F_4(\theta)$. Therefore it is evident that the branch point contribution for E_{z1} equals the saddle point contribution for E_{z2} at $y = 0$. The same is true for saddle point contribution in E_{z1} and branch point contribution in E_{z2} at $y = 0$. The branch point in E_{z1} is responsible for lateral wave which travels according to the velocity of the slower medium ($y < 0$) in a fast medium ($y > 0$) but decays exponentially across the interface. This slow wave in upper medium is supported by the normal slow wave in the lower medium due to the saddle point contribution in E_{z2}. Similarly the fast wave in the upper medium supports a similar wave in the lower medium to preserve the continuity of the phase fronts. The wave due to branch point contribution in E_{z2} also bends towards the interface normal in the lower half space.

The results obtained are for the cases of isolated saddle points and branch points in both the media. This is because the interest was to investigate the electric field behavior near the interface. As the observation angle is increased from the interface in the far zone the saddle point approached the branch point. The field contribution coming from branch point integral decays as $(kr)^{-3/4}$ when the transition from the point of observation, $\theta \neq$ branch point towards $\theta =$ branch point occurs. The field then decays as $(kr)^{-3/4}$ and can be expressed as parabolic cylinder functions [10].

The wave propagation phenomena near the dielectric interface can also be studied now with the help of (2.26) and (2.36). The focus in this study will be on the phase velocity and direction of propagation of the wave.

It has been mentioned earlier that phase velocity, $\vec{v}$ and Poynting vector field, $\vec{S}$ are parallel and proportional to each other. It means that the continuous phase velocity field will give the continuous Poynting vector field. This necessitates the continuity of $\vec{E}$ and $\vec{H}$ fields across the interface. It was observed earlier in the solution of Engheta and Papas [4] that the electric field was continuous across the interface but the magnetic field component was discontinuous. But the results in (2.26) and (2.36) show that E_z and H_θ are continuous upto the term which decays as $(k\rho)^{-3/2}$ across the interface. This can be easily verified by using Maxwell's equations. The continuity of electric field across the interface employs that the phase fronts must be continuous across the interface. Therefore in the following discussion careful attention will be paid to the phase of the electric field derived in the previous section to investigate the field behavior near the interface.

The phase velocity of an electromagnetic wave may be defined as

$$\vec{v} = \frac{\omega}{|\nabla\phi|^2}\nabla\phi$$

in analogy with plane waves. The equiphase contours of electric field will be called phase

maps. Due to the symmetry of the problem the phase maps for $x > 0$ will be shown and discussed only. The lines of phase velocity will be orthogonal to these phase maps. The phase map of the field in the close vicinity of the interface is shown in Fig. 2.13. A close observation of the phase map in this figure shows two types of points occurring periodically in both half spaces near the interface. The phase deform around these points to form interesting structures.

The lines of phase velocity near these points of this structure form closed curves and waves seem to circulate around these points. These points are called center type critical points [12]. Above each center type of critical point is another type of critical point where equiphase contours intersect each other. The lines of phase velocity near these points form hyperbolic curves. This is a point of stagnation and waves seem to avoid flowing through these points. At these points the electric and magnetic fields are in time quadrature. Hence Poynting vector field is zero at these points. Such points on phase maps are called saddle type critical points [12].

It is obvious from Fig. 2.13 that two adjacent arms of the saddle type of critical point enclose the center type of critical point. The overall effect of the structure formed by the pair of these critical points is to slow down the wave as it enters in the second medium. It can also be seen in Fig. 2.14 that these two types of critical points occur with a different arrangement in the denser medium. For each pair of the two types of critical point in the rarer medium there are two such pairs in the denser medium.

The field decays as $(k_1 r)^{-1}$ due to the leading terms of saddle points in both half spaces. The next higher order terms cause more rapid decay of field along the interface, recognized by $(k_1 r)^{-3/2}$ factor. The leading term contribution due to branch points in both half spaces can be distinguished by $(k_1 r)^{-3/2}$ factor.

It has been observed from Fig. 2.14 that the locations of critical points are dependent

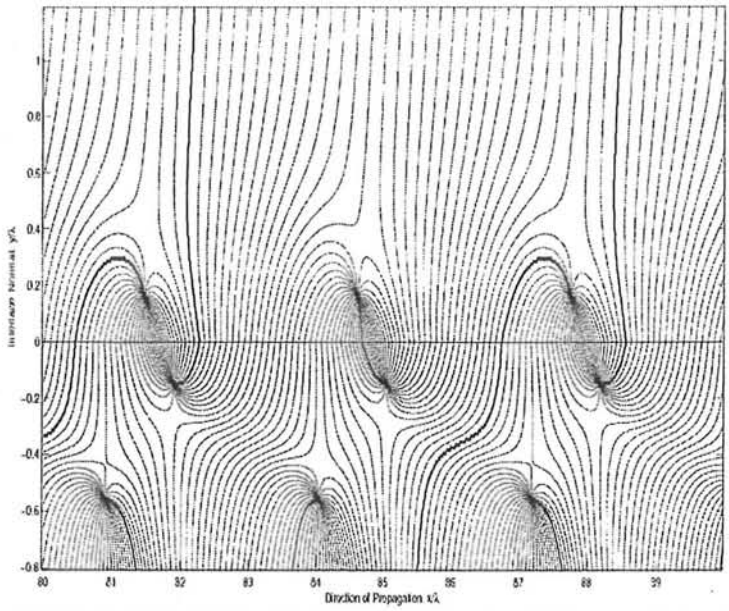

Figure 2.13: Lines of equiphase planes with critical points for E_{z1} and E_{z2}, continuous across the interface

on the refractive index, n. As the medium 2 is made more denser by increasing its permittivity, critical points in the region for $y > 0$ move closer to the interface. The increase in the value of n also brings closer the pair of critical points in the lower half space for $y < 0$. These points will try to merge together when refractive index is still increased further, [9]. This effect of refractive index on the critical points is shown in Fig. 2.14. These points are interesting because they redirect the energy and the Poynting vector, $\vec{S}$, is zero at these points [9].

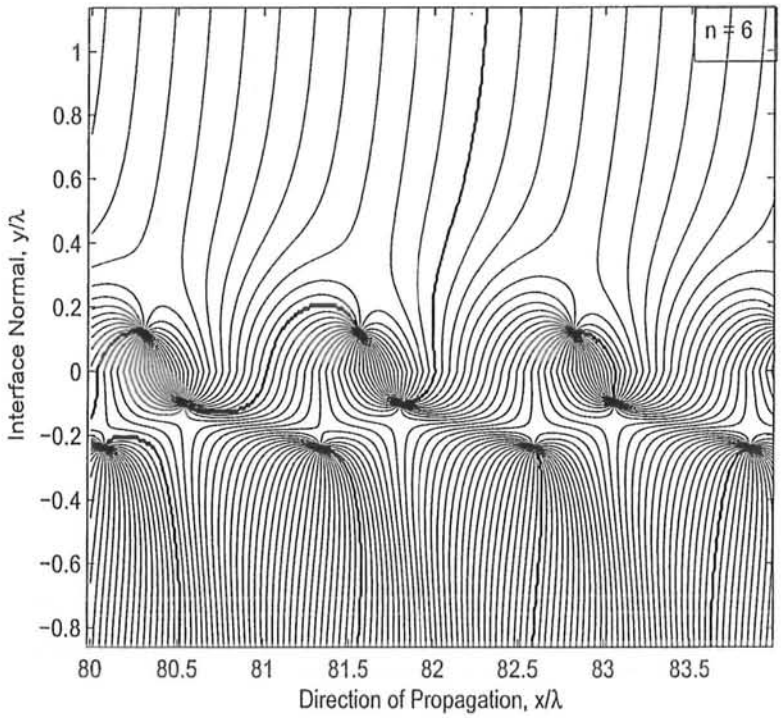

Figure 2.14: The critical points seem to densely packed in the lower half space while the refractive index, n value is increased

2.5 Location of Field Nulls or Critical Points

It is known that the phase and the phase velocity of an electromagnetic wave become ambiguous at the points where the electric field is zero. These points known as critical points have been discussed in the last section. Therefore the location of the field nulls or of critical points will be determined. An observation of (2.26) and (2.36) shows that electric field due to the leading terms of the saddle point contributions become zero at the interface, $\theta = 0$. The next higher order term of the saddle point contributions which decays as $kr^{-3/2}$ is not zero at the interface. The branch point contributions in

both half space electric field expressions are also non-zero at the interface boundary of the two dielectric half spaces. The location(s) where the electric field E_z is zero will be determined now. Considering the case of upper half space first, one has to find roots of the following relationship involving (2.26),

$$E_{z1} = 0$$

The field expression above the interface can be written as,

$$E_{z1} = A\frac{e^{ik_1 r}}{\sqrt{k_1 r}}\left\{F_1(\theta) + \frac{F_2(\theta)}{k_1 r} + \frac{F_3(\theta)}{k_1 r}e^{-k_1 r \sin\theta\sqrt{n^2-1}}e^{i\{k_1 r(n\cos\theta - 1)-\psi\}}\right\} \tag{2.37}$$

The various variables in the above expression are,

$$A = -\frac{\omega\mu I}{\sqrt{2\pi}}e^{-i3\pi/4},$$

$$F_1(\theta) = \frac{i\sin\theta}{\sin\theta + \sqrt{n^2 - \cos^2\theta}},$$

$$\begin{aligned} F_2(\theta) \;=\; & \frac{1}{\sin\theta + \sqrt{n^2 - \cos^2\theta}} \times \\ & \left[\frac{\{2\cos^4\theta + n^2\sin\theta(\sin\theta - \sqrt{n^2-\cos^2\theta}) - 2\cos^2\theta(n^2 - \sqrt{n^2-\cos^2\theta}\sin\theta)\}}{2(n^2-\cos^2\theta)^{3/2}}\right. \\ & \left. + \frac{\sin\theta}{8}\right], \end{aligned} \tag{2.38}$$

$$F_3(\theta) = \left(\frac{n^2}{n^2-1}\right)^{1/4}\frac{1}{(n^2-\cos^2\theta)^{3/4}},$$

and,

$$\psi(\theta) = \frac{3}{2}\tan^{-1}\left(\frac{n\tan\theta}{\sqrt{n^2-1}}\right).$$

As field is being investigated near the interface, so Taylor series of the above four functions of θ is taken near $\theta = 0$. This makes the above functions as,

$$F_1(\theta) \approx \frac{i\theta}{\sqrt{n^2-1}}, \quad F_2(\theta) \approx -\frac{1}{n^2-1}, \quad \psi(\theta) = \frac{3n}{2\sqrt{n^2-1}}\theta, \quad F_3(\theta) \approx \frac{\sqrt{n}}{n^2-1}.$$

With the assumption that $k_1 r = R$ and $R(n\cos\theta - 1) - \psi \approx R(n\cos\theta - 1)$ when $R \gg 1$, following simplified electric field representation is obtained,

$$E_{z1} = A\frac{e^{iR}}{\sqrt{R}}\Big[\frac{i\theta}{\sqrt{n^2-1}} - \frac{1}{(n^2-1)R} + \frac{\sqrt{n}}{(n^2-1)R}e^{-R\theta\sqrt{n^2-1}}e^{iR(n-1)}\Big] \tag{2.39}$$

The above equation is a non-linear equation whose solution is difficult to obtain so Taylor series of its terms around $\theta = 0$ is taken.

Taking the first terms of the Taylor series expansion and equating the real and imaginary parts of these terms, respectively, the following simultaneous equations are obtained,

$$\cos\{R(n-1)\} = \frac{1}{\sqrt{n}}e^{R\theta\sqrt{n^2-1}} \doteq \frac{e^u}{\sqrt{n}}, \tag{2.40}$$

and,

$$\sin\{R(n-1)\} = -\frac{R\theta\sqrt{n^2-1}}{\sqrt{n}}e^{R\theta\sqrt{n^2-1}} = -\frac{u}{\sqrt{n}}e^u. \tag{2.41}$$

where,

$$u = R\theta\sqrt{n^2-1}$$

Equations (2.40) and (2.41) are squared and added to get rid of R. The result is a transcendental equation of the following form,

$$1 + u^2 = ne^{-2u}.$$

This transcendental equation can be solved using the fixed point iterations of the following form,

$$u_{k+1} = -\frac{1}{2}\ln\left(\frac{1+u_k^2}{n}\right)$$

where k is the iterations index. For a given value of n the right hand sides of equations (2.40) and (2.41) are fixed. Thus there are many values of R and θ, which satisfy these

simultaneous equations. Hence the locations of center points is given as,

$$\begin{aligned} R_m &= \frac{2m\pi - \sin^{-1}(\frac{u}{\sqrt{1+u^2}})}{n-1}, \\ \theta_m &= \frac{u}{R_m\sqrt{n^2-1}}, \end{aligned} \tag{2.42}$$

where m is a positive integer. In the cartesian coordinates the field nulls are located at x_m and y_m which are given as,

$$\begin{aligned} x_m &= \frac{2m\pi - \sin^{-1}(\frac{u}{\sqrt{1+u^2}})}{k_1(n-1)}, \\ y_m &= \frac{u}{k_1\sqrt{n^2-1}}, \end{aligned} \tag{2.43}$$

It is observed that the field nulls are located periodically at a constant height above the interface and the distance between them is given as,

$$\frac{\lambda}{n-1}.$$

This is also evident from the Fig. 2.14 that the periodic nulls occur along x–axis.

The points where electric field is null in the lower half space will be determined now. These points can be located for $y < 0$ region by setting $E_{z2} = 0$ and finding solution for this equation. The first terms of factors of (2.36) representing E_{z2} in their Taylor series expansion are,

$$E_{z2} = \frac{1}{\sqrt{1-1/n^2}}\left\{\delta\theta + \frac{1}{n\sqrt{1-1/n^2}R} - \frac{e^{-iR(n-1)}}{n\sqrt{n}\sqrt{1-1/n^2}}\right\} = 0 \tag{2.44}$$

Equating the real and imaginary parts of the above relationship equal to zero following simultaneous equations are obtained,

$$\frac{\delta\theta}{\sqrt{1-1/n^2}} + \frac{1}{n(1-1/n^2)R} - \frac{\sqrt{n}\cos R(n-1)}{R(n^2-1)} = 0,$$

and,

$$\frac{\sqrt{n}\sin R(n-1)}{R(n^2-1)} = 0.$$

From the above relationship,

$$R(n-1) = \pm m\pi,$$

$$\delta\theta = \frac{\sqrt{1-1/n^2}}{R}\left\{\frac{\sqrt{n}}{n^2-1}(\pm 1)^m - \frac{1}{n(1-1/n^2)}\right\},$$

$$R\delta\theta = \frac{(\pm 1)^m}{\sqrt{n}\sqrt{n^2-1}} - \frac{1}{\sqrt{n^2-1}} = \frac{1}{\sqrt{n^2-1}}\left\{\frac{(\pm 1)^m}{\sqrt{n}} - 1\right\}.$$

From the above expression it is clear that for a given constant height from the interface critical points exist in a the form of a pair. Their location is also dependent on the refractive index, n of the medium. This observation is evident from Fig. 2.13.

Chapter 3

Two Dimensional Finite Sources

In the last chapter asymptotic expressions of electric field were found due to a line source placed at the interface of two dielectric half spaces. The leading terms in the solution were observed to be in accordance with the solution of Engheta and Papas. But their solution gave null of electric field at the interface. Investigating further into this propagation problem it was found that addition of next higher order term perturbed zero field condition at the interface. This perturbation resulted in the generation of critical points which were responsible for generation of extra phase lines near the interface. These extra phase lines preserved the continuity of electric field phase map across the interface.

The next question to consider is whether the behavior of phase velocity remains qualitatively unchanged when the source moves away from the dielectric interface. Green's functions have been found due to sources present near dielectric interfaces in various works for example in [13]. The field represented by the Green's functions is either in integral representation or if field is asymptotically evaluated in these integrals then only the first term which decays as $(k\rho)^{-1/2}$ is given. The results presented in such papers as [13] provide no answer to the preservation of phase map of waves near the interface.

In this chapter the problem of wave propagation near the interface will be investigated

with different source configurations present in the two dielectric half spaces. As a first step among these source configurations, a line source will be placed above and below the interface one by one. Electric field due to the line source will be calculated. Then the line source will be replaced by an arbitrary current distribution confined to either of the dielectric half space. The electric field behavior near the interface will be examined in both cases. Finally generalized current distribution which may be distributed in both half spaces will be assumed and electric field near the dielectric interface will be examined.

3.1 Line Source In Upper Half Space

Consider Fig. 3.1 of two dielectric half spaces with a line source of electric current located at θ', r' in the upper half space. The constitutive parameters of upper half space are assumed as ε_0 and μ_0 while for lower half space as ε_1 and μ_0. The permeability μ_0 of free space is assumed for both half spaces as most of dielectric materials are non-magnetic in nature. A line source carrying electric current, IA/m is placed at (x', y'). The current density $\vec{J}$ is represented as,

$$\vec{J} = I\delta(x - x')\delta(y - y')\hat{a_z},$$

where $\delta(\cdot)$ is Dirac delta function. The objective is to find the electric field due to the above source distribution in both half spaces near the interface. The formulation of the problem is carried out identically to the one given for interfacial line source in the previous chapter. Various notations used for the electric field representations in the following evaluations should be taken as, a 'U' in the superscript stands for Upper half space while a 'L' in the superscript for Lower half space. Similarly a '+' in the subscript stands for positive (+) y-axis while a '-' in the subscript stands for negative (-) y-axis.

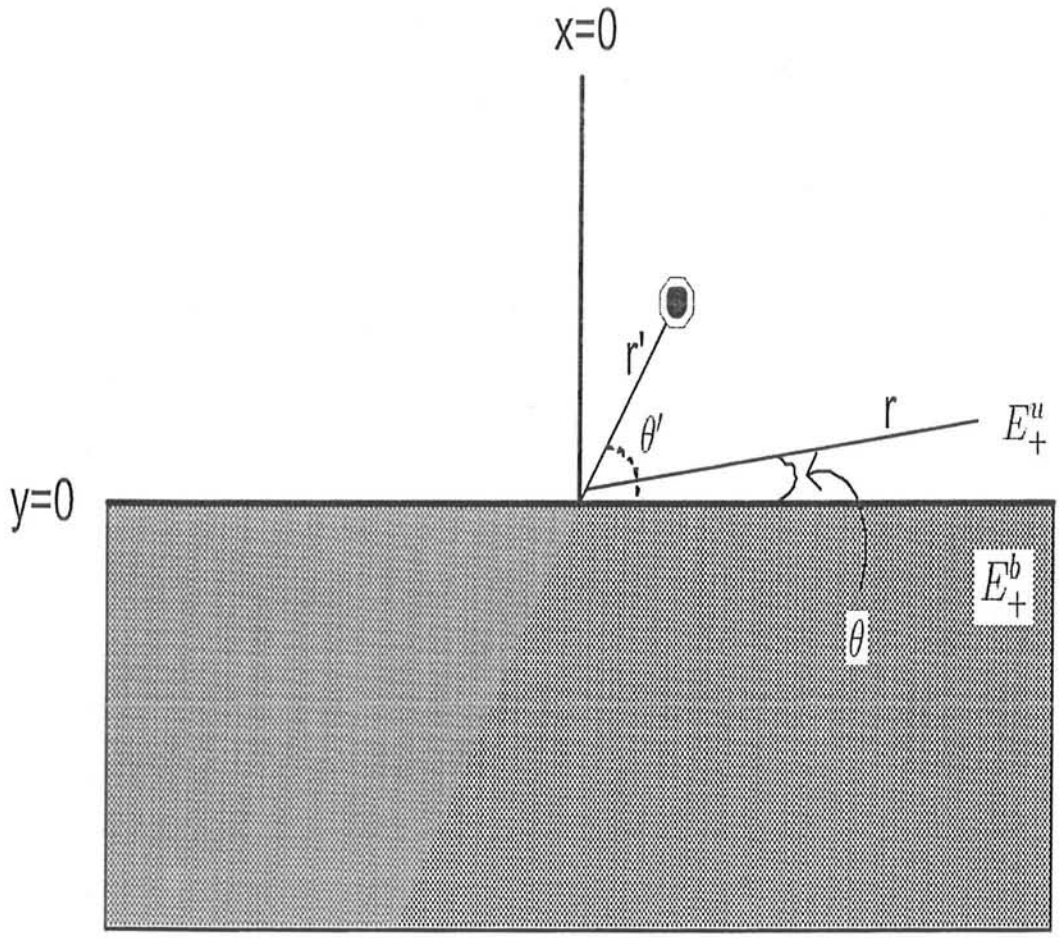

Figure 3.1: A displaced line source in upper half space

'sd' stands for saddle point while 'br' stands for branch point. According to [13] the electric field in the upper half space is given as,

$$E_+^{\mathrm{U}} = \frac{\omega\mu I}{4\pi}\int_{-\infty}^{\infty}\frac{(k_{2y}-k_{1y})}{k_{1y}(k_{2y}+k_{1y})}e^{ik_x(x-x')+ik_{1y}(y-y')}dk_x$$
$$-\frac{\omega\mu I}{4\pi}\int_{-\infty}^{\infty}\frac{1}{k_{1y}}e^{ik_x(x-x')+ik_{1y}|y-y'|}dk_x = \Big\{I_1 - I_2\Big\}. \tag{3.1}$$

The first integral, i.e., I_1 represents the reflected field from the interface. It possesses branch point singularities at $k_x = \pm k_1$ and $k_x = \pm k_2$. The second integral, i.e., I_2

on the right hand side of (3.1) is proportional to the integral representation of the Hankel function. It represents the field due to the source in an unbounded medium with propagation constant k_1. This integral has a pair of branch point singularities at $k_x = \pm k_1$. The path of integration for both the integrals runs on real axis of complex k_x plane. The branch cuts are extended in the k_x plane according to Fig. 2.2 so as to give decaying field when the path of integration is closed at infinity. Evaluation of the two integrals will be carried out separately.

The integral I_1 is considered first. To facilitate the evaluation, a transformation from k_x plane to α plane is carried out according to,

$$k_x = k_1 \cos\alpha, \quad k_{1y} = k_1 \sin\alpha, \quad k_{2y} = k_1\sqrt{n^2 - \cos^2\alpha}.$$

A further transformation from cartesian to polar coordinates is also carried out for the spacial coordinates according to,

$$x = r\cos\theta, \qquad y = r\sin\theta, \qquad x' = r'\cos\theta', \qquad y' = r'\sin\theta'.$$

Due to the above transformation I_1 is given as,

$$I_1 = \frac{\omega\mu I}{4\pi(n^2-1)}\int_P F(\alpha, r')e^{k_1 r f(\alpha)}d\alpha, \tag{3.2}$$

where,

$$F(\alpha, r') = \{\sqrt{n^2 - \cos^2\alpha} - \sin\alpha\}^2 e^{-ik_1 r'\cos(\alpha-\theta')},$$

and,

$$f(\alpha) = i\cos(\alpha - \theta).$$

The path of integration is identical to the path P in the Fig. 2.2. There is a saddle point at $\alpha = \theta$ and a pair of branch points are located at $\alpha = i\cosh^{-1}\zeta$ and $\alpha = \pi - i\cosh^{-1}\zeta$. The contribution of the saddle point denoted as $E^U_{+\mathrm{sd}}$ will be determined first. The saddle

point is present at $\alpha = \theta$ in (3.2) at which $f'(\alpha) = 0$. A transformation from α plane to s plane is carried out according to (2.13). The transformed integral is given as,

$$I_1 = e^{k_1 r f(\alpha_s)} \int_{-\infty}^{\infty} G(s) e^{-k_1 r s^2} ds,$$

where,

$$G(s) = F_1(\theta, r') \frac{d\alpha}{ds},$$

and,

$$f(\alpha_s) = i.$$

Whereas,

$$F_1(\theta, r') = \{\sqrt{n^2 - \cos^2\theta} - \sin\theta\}^2 e^{-ik_1 r' \cos(\theta - \theta')},$$

and,

$$\frac{d\alpha}{ds} = \sqrt{\frac{-2}{f''(\alpha_S)}}.$$

The saddle point has shifted to the origin of new s plane. Hence a power series expansion of $G(s)$ at $s = 0$ will be taken. The second order derivative of the function $F_1(\theta, r')$ required in this power series expansion is given as,

$$\begin{aligned} F_1^{(2)}(\theta, r') \;=\; & \frac{F_1(\theta, r')}{(n^2 - \cos^2\theta)^{3/2}} \times \\ & \Big[4\cos^2\theta \sqrt{n^2 - \cos^2\theta} + k_1 r' (n^2 - \cos^2\theta)^{3/2} \Big\{ i\cos(\theta' - \theta) \\ & - k_1 r' \sin^2(\theta' - \theta) \Big\} + i4 k_1 r' \cos\theta \sin(\theta' - \theta)(n^2 - \cos^2\theta) \\ & + 2n^2 \sin\theta \Big]. \end{aligned} \tag{3.3}$$

The evaluation of the integral I_1 yields the saddle point contribution which is given as,

$$I_{1\mathrm{sd}} = \frac{\omega\mu I}{4\pi(n^2 - 1)} \frac{e^{ik_1 r}}{\sqrt{k_1 r}} \sum_{n=0}^{\infty} \frac{G^{(2n)}(0)}{(2n)!} \frac{\Gamma(n + \frac{1}{2})}{(k_1 r)^n}. \tag{3.4}$$

Only the first two terms involving even powers of s will be retained in the above series. The odd powers of s integrate out to zero due to the identical interval of integration on both sides of $s = 0$. The truncated form of the result will be given as under,

$$I_{1\text{sd}} = -\frac{\omega\mu I e^{ik_1 r}}{4\sqrt{\pi}(n^2-1)\sqrt{k_1 r}}\left\{\sqrt{2}F_1(\theta,r')e^{-i\pi/4} + \left\{\frac{F_1^{(2)}(\theta,r')}{\sqrt{2}} + \frac{F_1(\theta,r')}{4\sqrt{2}}\right\}\frac{e^{-i3\pi/4}}{k_1 r}\right\} \quad (3.5)$$

The contribution of branch point present in I_1 will be determined now. The complex k_x plane is transformed to complex s plane according to (2.13) to facilitate the evaluation which shifts one of the branch point to the origin of new plane. The new form of integral, I_1, is,

$$I_1 = e^{ik_1 r\cos(\alpha_b-\theta)}\int_P F(s)e^{-k_1 r s^2}ds = e^{ik_1 r\{n\cos\theta + i\sqrt{n^2-1}\sin\theta\}}\int_P F(s)e^{-k_1 r s^2}ds \quad (3.6)$$

The same procedure is followed as was followed in case of (2.19) to give the following result for branch point contribution of the integral, I_1

$$I_{1\text{br}} = -\frac{\omega\mu I}{\sqrt{2\pi}}F_{(U+b)}(\theta,r')\frac{e^{ik_1 r\{n\cos\theta + i\sqrt{n^2-1}\sin\theta\}}}{(n^2-1)^{1/4}(k_1 r)^{3/2}} \quad (3.7)$$

where,

$$F_{(U+b)}(\theta,r') = \frac{\sqrt{n}e^{-ik_1 r'\{n\cos\theta' + i\sqrt{n^2-1}\sin\theta'\}}}{\{i\sqrt{n^2-1}\cos\theta - n\sin\theta\}^{3/2}}.$$

The asymptotic evaluation of the second integral, I_2 will now be carried out. The same transformation is applied to this integral as was applied to I_1. The resulting shape of the integral is,

$$I_2 = -\frac{\omega\mu I}{4\pi}\int_P F_2(\alpha,r')e^{k_1 r f_2(\alpha)}d\alpha \quad (3.8)$$

where,

$$F_2(\alpha,r') = e^{-ik_1 r'\cos(\alpha-\theta')},$$

and,

$$f_2(\alpha) = ik_1 r\cos(\alpha-\theta).$$

The original path of integration Q of this integral is the same as given in Fig. 2.10. This integral has no branch points. The path of integration is deformed to pass through the saddle point at $\alpha = \theta$. The deformed path of integration is the same as shown Q' in Fig. 2.11. The contribution of this saddle point is evaluated similarly as for I_1, with the unknowns in the power series expansion being,

$$F_2(\theta, r') = e^{-i\{k_1 r' \cos(\theta - \theta')\}},$$

$$F_2^{(2)}(\theta, r') = -k_1 r' F_2(\theta, r') \Big\{ i\cos(\theta - \theta') - (k_1 r') \sin^2(\theta - \theta') \Big\}.$$

This results into,

$$I_{2\text{sd}} = -\frac{\omega\mu I e^{ik_1 r}}{4\sqrt{\pi k_1 r}} \left[\sqrt{2} F_2(\theta, r') e^{-i\pi/4} + \frac{e^{-i3\pi/4}}{\sqrt{2} k_1 r} \Big\{ \frac{F_2(\theta, r')}{4} - F_2^{(2)}(\theta, r') \Big\} \right] \tag{3.9}$$

Hence the total saddle point contribution,

$$\begin{aligned} E^{\text{U}}_{+\text{sd}} = \frac{\omega\mu I e^{ik_1 r}}{4\sqrt{\pi}(n^2-1)\sqrt{k_1 r}} \Bigg[& \sqrt{2} e^{-i\pi/4} \{ F_1(\theta, r') + (n^2-1) F_2(\theta, r') \} \\ & + \frac{e^{-i3\pi/4}}{\sqrt{2} k_1 r} \Big\{ F_1^{(2)}(\theta, r') - (n^2-1) F_2^{(2)}(\theta, r') + \frac{1}{4} \{ 1 + (n^2-1) F_2(\theta, r') \} \Big\} \Bigg] \end{aligned} \tag{3.10}$$

The combined field expression involving the saddle point and branch points contribution is given below,

$$\begin{aligned} E^{\text{U}}_{+} = \frac{\omega\mu I e^{ik_1 r}}{4\sqrt{\pi}(n^2-1)\sqrt{k_1 r}} \Bigg[& \sqrt{2} e^{-i\pi/4} \{ F_1(\theta, r') + (n^2-1) F_2(\theta, r') \} \\ & + \frac{e^{-i3\pi/4}}{\sqrt{2} k_1 r} \Big\{ F_1^{(2)}(\theta, r') - (n^2-1) F_2^{(2)}(\theta, r') + \frac{1}{4} \{ 1 + (n^2-1) F_2(\theta, r') \} \Big\} \Bigg] \\ & + \frac{\omega\mu I}{2\pi} F_{(U+b)}(r', \theta) \frac{e^{ik_1 r \{ n\cos\theta + i\sqrt{n^2-1}\sin\theta \}}}{(n^2-1)^{1/4} (k_1 r)^{3/2}} \end{aligned} \tag{3.11}$$

Now the electric field transmitted in the lower half space will be evaluated. This field is given as [13],

$$E_{+}^{\mathrm{L}} = -\frac{\omega\mu I}{2\pi}\int_{-\infty}^{\infty}\frac{e^{-i(k_x x' + k_{1y} y')}e^{i(k_x x - k_{2y} y)}}{(k_{1y} + k_{2y})}dk_x \tag{3.12}$$

The above representation is seen to possess branch point singularities at $k_x = \pm k_1$ and at $k_x = \pm k_2$. A transformation from k_x to α plane is carried out according to,

$$k_x = k_2\cos\alpha, \quad k_{2y} = k_2\sin\alpha, \quad k_{1y} = k_2\sqrt{\frac{1}{n^2} - \cos^2\alpha}$$

whereas the rectangular spatial coordinates, x', y' and x, y are also converted to polar coordinates, r', θ' and r, θ respectively using the following relationships,

$$x' = r'\cos\theta', \quad y' = r'\sin\theta', \quad x = r\cos\theta, \quad y = r\sin\theta.$$

The above substitutions result into,

$$E_{+}^{\mathrm{L}} = \frac{\omega\mu I}{2\pi}\int_{P} F_3(\alpha, r')e^{k_2 r f(\alpha)}d\alpha, \tag{3.13}$$

where,

$$F_3(\alpha;\theta', r') = \frac{\sin\alpha e^{-ik_2 r'(\sqrt{\frac{1}{n^2}-\cos^2\alpha}\,\sin\theta' + \cos\alpha\cos\theta')}}{(\sin\alpha + \sqrt{\frac{1}{n^2} - \cos^2\alpha})},$$

and,

$$f(\alpha) = i\cos(\alpha + \theta).$$

The above field expression is seen to possess a saddle point at $\alpha = \theta$ and a pair of branch points at $\alpha = \cos^{-1}(1/n)$ and $\alpha = \pi - \cos^{-1}(1/n)$. Due to symmetry of problem the electric field being investigated near the interface is for $x > 0$ region so the branch point present at $\alpha = \cos^{-1}(1/n)$ will have to be included in the evaluation if $\theta < \cos^{-1}(1/n)$. This evaluation will again be carried by running the branch cut along a steepest descent path. The path on each side of the branch cut gives similar contribution which is added to give total contribution of the branch cut.

The contribution of the saddle point will be evaluated first of all. A transformation is carried out for convenience, as in the case of field for upper half space, into another $s-$plane according to (2.19). This transformation converts the integral into the following form,

$$E_{+}^{\mathrm{L}} = \frac{\omega\mu I e^{k_2 r f(\alpha_s)}}{2\pi}\int_P G(s)e^{-k_2 r s^2}ds.$$

The power series expansion of $G(s)$ around $s = 0$ is taken. First two terms containing even powers of s are considered for their saddle point contribution. $F_3(\theta, r')$ and its derivative are required for this purpose. The value of $F_3(\alpha, r')$ at $\alpha = \theta$ and its second derivative are,

$$F_3(\theta, r') = \frac{\sin\theta e^{-ik_2 r'(\sqrt{\frac{1}{n^2}-\cos^2\theta}\,\sin\theta'+\cos\theta\cos\theta')}}{(\sin\theta+\sqrt{\frac{1}{n^2}-\cos^2\theta})},$$

and,

$$\begin{aligned}
F_3^{(2)}(\theta, r') \;=\; & \frac{F_3(\theta, r')}{\sin\theta\sqrt{\frac{1}{n^2}-\cos^2\theta}(n^2\cos^2\theta-1)} \times \\
& -n^2\cos^4\theta(2+i3k_2r'\sin\theta'\sin\theta) \\
& +in^2k_2r'\cos\theta'\cos^3\theta\sin\theta(3\sqrt{\frac{1}{n^2}-\cos^\theta}-2\sin\theta-i2k_2r'\sin\theta'\sin^2\theta) \\
& +\sin\theta\{\sqrt{\frac{1}{n^2}-\cos^2\theta}-\sin\theta \\
& -ik_2r'\sin^2\theta(ik_2r'\cos^2\theta'\sqrt{\frac{1}{n^2}-\cos^2\theta}+\sin\theta')\} \\
& +\cos^2\theta\Big\{2-\sin\theta(2n^2\sqrt{\frac{1}{n^2}-\cos^2\theta}-i3k_2r'\sin\theta') \\
& -i2n^2k_2r'\sqrt{\frac{1}{n^2}-\cos^2\theta}\sin\theta'\sin^2\theta \\
& -n^2(k_2r')^2\cos 2\theta'\sin^2\theta\sqrt{\frac{1}{n^2}-\frac{1}{2}(1+\cos 2\theta)} \\
& +ik_2r'\cos\theta\sin\theta\Big(ik_2r'\sin 2\theta'\sin^2\theta-\cos\theta'(3\sqrt{\frac{1}{n^2}-\cos^2\theta}+2\sin\theta)\Big)\Big\}
\end{aligned} \tag{3.14}$$

The resultant expression for saddle point contribution below the interface would be,

$$E^{\mathrm{L}}_{+\mathrm{sd}} = \frac{\omega\mu I}{2\pi}\frac{e^{ik_2r}}{\sqrt{k_2r}}\left[\sqrt{2\pi}F_3(\theta,r')e^{-i\pi/4} + \frac{\sqrt{\pi}e^{-i3\pi/4}}{4k_2r}\left\{\frac{F_3(\theta,r')}{\sqrt{2}} + 2\sqrt{2}F_3^{(2)}(\theta,r')\right\}\right] \tag{3.15}$$

The complex k_x plane is transformed to complex α plane. The branch points in the complex α plane have moved to $\alpha_b = \cos^{-1}(1/n)$ and $\alpha_{\mathrm{b1}} = \pi - \cos^{-1}(1/n)$ on the real axis of the plane. The branch cut originating from the branch point is made to run along a constant phase path. Under these conditions the method of steepest descent is most convenient to evaluate asymptotically the integral, E^L_+. The transformation results into,

$$E^L_{+\mathrm{br}} = \frac{\omega\mu I}{2\pi}e^{k_2rf(\alpha_s)}\int_{-\infty}^{\infty}G(s)e^{-k_2rs^2}ds, \tag{3.16}$$

where,

$$G(s) = F(\alpha)\frac{d\alpha}{ds} = \frac{\sin\alpha e^{-ik_2r'\left(\sqrt{\frac{1}{n^2}-\cos^2\alpha}\sin\theta'+\cos\alpha\cos\theta'\right)}}{\sin\alpha + \sqrt{\frac{1}{n^2}-\cos^2\alpha}}\frac{d\alpha}{ds},$$

$$\frac{d\alpha}{ds} \simeq \frac{2se^{-i\pi/2}}{\sin\alpha_b + \theta}.$$

Expanding $G(s)$ in the Power series at $s = 0$ or $\alpha = \alpha_{\mathrm{b}}$ and retaining only the s^2 term of the expansion results into the following form of the branch point contribution,

$$E^{\mathrm{L}}_{+\mathrm{br}} = \frac{\omega\mu I F_{(\mathrm{L+b})}(r',\theta)}{\sqrt{2\pi}(n^2-1)^{1/4}(k_1r)^{3/2}}e^{ik_1r\{\cos\theta-\sqrt{n^2-1}\sin\theta\}-i3\pi/4}, \tag{3.17}$$

where,

$$F_{(\mathrm{L+b})}(r',\theta) = \frac{e^{-ik_1r'\cos\theta'}(1+i\sqrt{n^2-1}k_1r'\sin\theta')}{\{\sqrt{n^2-1}\cos\theta+\sin\theta\}^{3/2}}. \tag{3.18}$$

The addition of the saddle point and branch point contributions in (3.15) and (3.17) respectively gives the total field below the interface due to the presence of source above

the interface,

$$E_+^{\mathrm{L}} = \frac{\omega\mu I}{2\pi}\frac{e^{ik_2r}}{\sqrt{k_2r}}\left[\sqrt{2\pi}F_3(\theta,r')e^{-i\pi/4} + \frac{\sqrt{\pi}e^{-i3\pi/4}}{4k_2r}\left\{\frac{F_3(\theta,r')}{\sqrt{2}} + 2\sqrt{2}F_3^{(2)}(\theta,r')\right\}\right]$$
$$+ \frac{\omega\mu I F_{(\mathrm{B+b})}(r',\theta)}{\sqrt{2\pi}(n^2-1)^{1/4}(k_1r)^{3/2}}e^{ik_1r\{\cos\theta-\sqrt{n^2-1}\sin\theta\}-i3\pi/4} \qquad (3.19)$$

The expression of the electric field below the interface has been obtained asymptotically. The leading terms of the (3.19) decay as $(k_2r)^{-1/2}$. The next higher order term come from the saddle point and branch point contributions near the interface while only the saddle point contribution is included in the solution when the observation angle if away from the interface beyond the critical angle. The term from the saddle point can be identified by the factor of $(k_2r)^{-3/2}$ while the factor of $(k_1r)^{-3/2}$ distinguishes the branch point contribution.

Phase maps of equations (3.11) and (3.19) combined are shown in Fig. 3.2. Interestingly enough the same structures of phase map can be seen in this figure as were seen in Fig. 2.13 and Fig. 2.14 in the last chapter. The continuity of phase lines of the electric field across the interface is preserved in Fig. 3.2.

3.2 Line Source In Lower Half Space

Consider Fig. 3.3 in which a displaced line source placed in the lower dielectric half space for $y < 0$ has been shown. The constitutive parameters of this half space are μ_0 and ε_1 being its permeability and permittivity respectively. The source is located at (x'', y''). The electric field due to this line source will be investigated near the interface in both dielectric half spaces.

First of all electric field in the upper half space will be examined. With this source

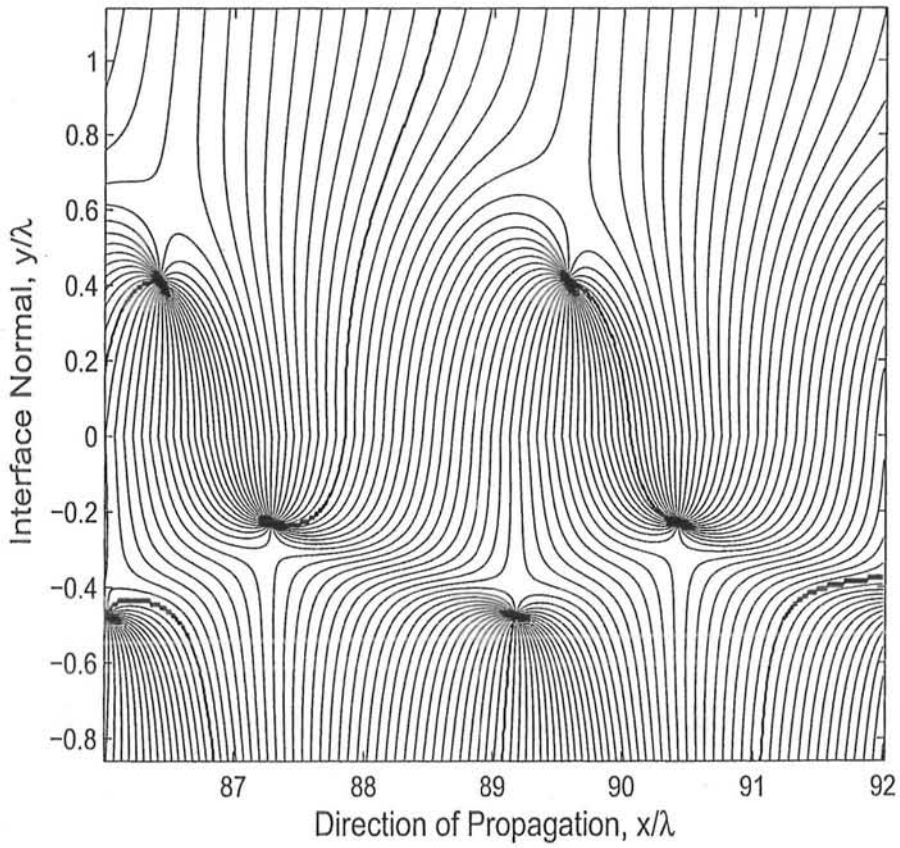

Figure 3.2: Phase map near the interface with displaced line source in upper half space

configuration electric field above the interface is represented as spectrum of plane waves,

$$E_{-}^{\mathrm{U}} = -\frac{\omega\mu I}{2\pi}\int_{-\infty}^{\infty}\frac{e^{-ik_{2y}y''}e^{-ik_x x''}e^{ik_{1y}y}e^{ik_x x}}{k_{2y}+k_{1y}}dk_x. \tag{3.20}$$

The path of integration runs along the real axis of the complex k_x plane. There are two pairs of branch points which exist at $k_x = \pm k_2$ and $k_x = \pm k_1$ in the integral given in (3.20). These branch points are to be avoided on the path of integration while the path is closed at ∞ as shown in Fig. 2.2 in the previous chapter. A transformation will be

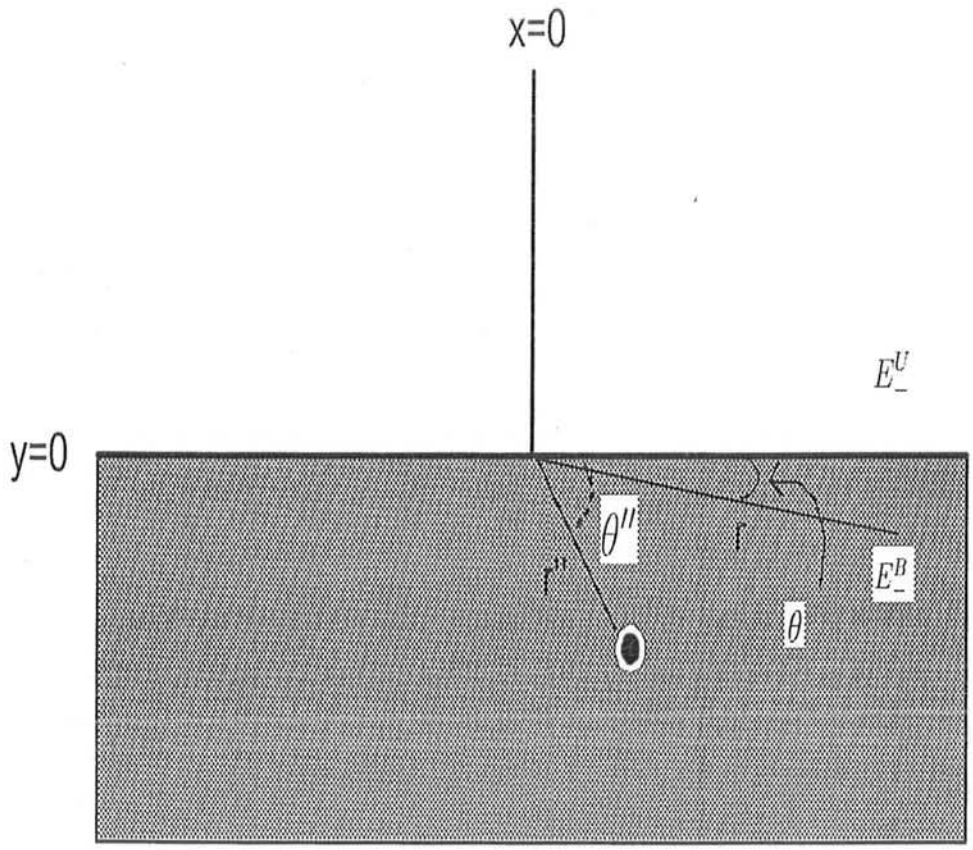

Figure 3.3: A displaced line source in lower half space

made again from k_x to the α-plane and spatial cartesian coordinates x and y will be transformed to polar coordinates r and θ for convenience in the asymptotic evaluation of this integral. These transformations are carried out using the relationships,

$$k_x = k_1 \cos\alpha, \quad k_{1y} = k_1 \sin\alpha, \quad k_{2y} = \sqrt{k_2^2 - k_1^2 \cos^2\alpha},$$

while the cartesian coordinates transformation is carried out using,

$$x = r\cos\theta, \quad y = r\sin\theta, \quad x'' = r''\cos\theta'', \quad y'' = -r''\sin\theta''.$$

After carrying out these substitutions the resulting form of (3.20) becomes,

$$E_{-}^{U} = \frac{\omega\mu I}{2\pi}\int_{P} F(\alpha, r'')e^{k_1 r f(\alpha)}d\alpha, \tag{3.21}$$

where,

$$F(\alpha, r'') = \frac{\sin\alpha e^{-ik_1 r''(\sqrt{n^2-\cos^2\alpha}\sin\theta''-\cos\alpha\cos\theta'')}}{\sin\alpha+\sqrt{n^2-\cos^2\alpha}},$$

and

$$f(\alpha) = i\cos(\alpha-\theta).$$

It can be seen that a saddle point exists at $\alpha = \theta$ due to the choice of $k_x = k_1\cos\alpha$ and the corresponding branch point pair at $k_x = \pm k_1$ has disappeared. The remaining branch points now are located on the imaginary axis at $\alpha = \cosh^{-1}\zeta_b$ and $\alpha = \pi - i\cosh^{-1}\zeta_b$. The path of integration is deformed to run along a constant phase path. This path deformation permits to use the most convenient method, steepest descent method for asymptotic evaluation of this integral given in (3.21).

Carrying out the transformation from α plane to a new complex, s-plane using the following relationship,

$$f(\alpha) = f(\alpha_s) - s^2$$

the resulting form of the relationship comes out to be,

$$E_{-}^{U} = \frac{\omega\mu I e^{k_1 r f(\alpha_s)}}{2\pi}\int_{P} G(s)e^{-k_1 r s^2}ds, \tag{3.22}$$

where,

$$f(\alpha_s) = i,$$

and,

$$G(s) = F(s)\frac{d\alpha}{ds}.$$

In the above relationship,

$$\frac{d\alpha}{ds} = \frac{2s}{i\sin(\alpha-\theta)}.$$

The saddle point contribution at $\alpha = \theta$ is given as,

$$E^{U}_{\text{-sd}} = \frac{\omega\mu I e^{ik_1 r}}{2\pi\sqrt{k_1 r}}\left[\frac{G(0)}{0!}\Gamma(1/2) + \frac{G^{(2)}(0)}{2!}\frac{\Gamma(3/2)}{k_1 r}\right]. \tag{3.23}$$

The functions $F(\alpha_s, r'')$ and its second derivative at the saddle point is required in $G(0)$ and $G^{(2)}(0)$ respectively. These are found to be,

$$F(\alpha_s, r'') = \frac{\sin\theta e^{-ik_1 r''(\sqrt{n^2-\cos^2\theta}\sin\theta'' - \cos\theta\cos\theta'')}}{(\sin\theta + \sqrt{n^2-\cos^2\theta})},$$

and,

$$\begin{aligned}
F^{(2)}(\alpha_s, r'') \;=\; & -\frac{F(\theta, r'')}{\sin\theta(n^2-\cos^2\theta)^{3/2}} \times \\
& -\cos^4\theta(2 + i3k_1 r''\sin\theta''\sin\theta) \\
& +in^2 k_1 r''\cos\theta''\cos\theta\sin\theta(3\sqrt{n^2-\cos^2\theta} - 2\sin\theta - i2k_1 r''\sin\theta''\sin^2\theta) \\
& -n^2\sin\theta\Big\{\sin\theta - \sqrt{n^2-\cos^2\theta} + ik_1 r''\sin^2\theta \times \\
& (ik_1 r''\cos^2\theta''\sqrt{n^2-\cos^2\theta} + \sin\theta'')\Big\} + \cos^2\theta\Big\{2n^2 + \sin\theta \times \\
& (i3n^2 k_1 r''\sin\theta'' - 2\sqrt{n^2-\cos^2\theta}) - i2k_1 r''\sin\theta''\sin^2\theta\sqrt{n^2-\cos^2\theta} \\
& -(k_1 r'')^2\cos(2\theta'')\sin^3\theta\sqrt{n^2 - \frac{1}{2}(1+\cos(2\theta))}\Big\} \\
& +ik_1 r''\cos^3\theta\sin\theta\Big\{ik_1 r''\sin 2\theta''\sin^2\theta \\
& +\cos\theta''(2\sin\theta - 3\sqrt{n^2-\cos^2\theta})\Big\}
\end{aligned} \tag{3.24}$$

Finally the saddle point contribution comes out to be,

$$E^{\text{U}}_{\text{-sd}} = \frac{\omega\mu I}{2\pi\sqrt{k_1 r}}e^{ik_1 r}\left[\sqrt{2\pi}F(\theta, r'')e^{-i\pi/4} + \frac{\sqrt{\pi}e^{-i3\pi/4}}{4k_1 r}\left\{\frac{F(\theta, r'')}{\sqrt{2}} + 2\sqrt{2}F^{(2)}(\theta, r'')\right\}\right] \tag{3.25}$$

The branch point contribution will be evaluated now. It has already been mentioned that the branch points are present on the imaginary axis of α plane in (3.22). The branch cut at $\alpha = i\cosh\eta$ will contribute only when saddle point is less than the critical

angle. The transformation from α plane to s plane is once again carried out,

$$f(\alpha) = f(\alpha_b) - s^2,$$

where,

$$f(\alpha) = i\cos(\alpha - \theta),$$

and,

$$f(\alpha_b) = i\cos(\alpha_b - \theta) = i(n\cos\theta + i\sqrt{n^2-1}\sin\theta).$$

Integral given in (3.22) is now represented in s-plane as,

$$E_{-}^{\mathrm{U}} = \frac{\omega\mu I e^{ik_1 r\{n\cos\theta + i\sqrt{n^2-1}\sin\theta\}}}{2\pi}\int_{-\infty}^{\infty} G(s)e^{-k_1 r s^2}ds, \tag{3.26}$$

where,

$$G(s) = \frac{\sin\alpha e^{-ik_1 r''(\sqrt{n^2-\cos^2\alpha}\sin\theta'' - \cos\alpha\cos\theta'')}}{(\sin\alpha + \sqrt{n^2-\cos^2\alpha})}\frac{d\alpha}{ds}.$$

Power series expansion of $G(s)$, is taken at $s = 0$ or $\alpha = \alpha_b$. The even terms containing factor of s^2 are retained to give the contribution of the branch point while the terms of odd powers of s integrate out to zero. The integration is carried out while running the branch cut along a steepest descent path to give the following result,

$$E_{\text{-br}}^{\mathrm{U}} = \frac{\omega\mu I}{\sqrt{2\pi}}\frac{\sqrt{n}F_{(U-b)}(r'',\theta)}{(n^2-1)^{1/4}\{k_1 r\}^{3/2}}e^{ik_1 r\{n\cos\theta + i\sqrt{n^2-1}\sin\theta - 3\pi/4\}}, \tag{3.27}$$

where,

$$F_{(U-b)}(r'',\theta) = \frac{e^{ik_2 x''}(1 - \sqrt{n^2-1}k_1 y'')}{(\sqrt{n^2-1}\cos\theta - n\sin\theta)^{3/2}}.$$

By adding (3.25) and (3.27) the total field above the interface due to this source below the interface comes out to be,

$$\begin{aligned} E_{-}^{\mathrm{U}} &= \frac{\omega\mu I}{2\pi\sqrt{k_1 r}}e^{ik_1 r}\left[\sqrt{2\pi}F(\theta,r'')e^{-i\pi/4} + \frac{\sqrt{\pi}e^{-i3\pi/4}}{4k_1 r}\left\{\frac{F(\theta,r'')}{\sqrt{2}} + 2\sqrt{2}F^{(2)}(\theta,r'')\right\}\right] \\ &+ \frac{\omega\mu I}{\sqrt{2\pi}}\frac{\sqrt{n}F_{(U-b)}(r'',\theta)}{(n^2-1)^{1/4}\{k_1 r\}^{3/2}}e^{ik_1 r\{n\cos\theta + i\sqrt{n^2-1}\sin\theta - 3\pi/4\}}. \end{aligned} \tag{3.28}$$

Now the field below the interface will be evaluated while the source is also in the same region. The field in the region, $y < 0$ consists of two integrals, I_1 and I_2 given below,

$$E_-^{\mathrm{L}} = \frac{\omega\mu I}{4\pi}\int_{-\infty}^{\infty}\frac{(k_{2y}-k_{1y})}{k_{2y}(k_{2y}+k_{1y})}e^{ik_x(x-x'')-ik_{2y}(y+y'')}dk_x$$
$$-\frac{\omega\mu I}{4\pi}\int_{-\infty}^{\infty}\frac{1}{k_{2y}}e^{ik_x(x-x'')+ik_{2y}|y-y''|}dk_x = \frac{\omega\mu I}{4\pi}\{I_1 - I_2\} \qquad (3.29)$$

The path of integration in both integrals I_1 and I_2 run along real k_x axis and branch points are avoided in the process as given in Fig. 2.2. It can be seen in (3.29) that in I_1 two pairs of branch points exist at $k_x = \pm k_2$ and at $k_x = \pm k_1$ while the second integral is in fact the integral representation of Hankel function. I_1 represents the reflected field from the interface while I_2 gives a cylindrical wave in an unbounded media. Transformation from k_x to α plane will be carried out to facilitate the evaluation of the integrals according to

$$k_x = k_2 \cos\alpha.$$

This above transformation results in the removal of branch points at $k_x = \pm k_2$. Similarly the cartesian coordinates x and y are transformed to polar coordinates r and θ using,

$$x = r\cos\theta, \qquad y = r\sin\theta.$$

The integral I_1 results into the following form after the substitution for α plane,

$$I_1 = \frac{\omega\mu I n^2}{4\pi(n^2-1)}\int_P F_1(r'',\alpha)e^{k_2 r f(\alpha)}d\alpha, \qquad (3.30)$$

where,

$$F_1(\alpha, r'') = \left(\sin\alpha - \sqrt{1/n^2 - \cos^2\alpha}\right)^2 e^{-ik_2 r''\cos(\alpha-\theta'')},$$

and,

$$f(\alpha) = i\cos(\alpha-\theta).$$

There is a saddle point at $\alpha = \theta$ and a pair of branch points at $a = \pm\cos^{-1}(1/n)$. The transformation to the s-plane is carried out as in the last section. The resulting expression is of the form,

$$I_1 = \frac{\omega\mu I n^2 e^{k_2 r f(\alpha_s)}}{4\pi(n^2-1)} \int_{-\infty}^{\infty} H(s) e^{-k_2 r s^2} ds. \tag{3.31}$$

The saddle point has now moved to the origin of the new s plane. Power series expansion of the function $H(s)$ will be taken around $s = 0$. Following functions of observation angle θ and the source coordinates will be used in the term by term integration to be carried out after the expansion.

$$F_1(\theta, r'') = (\sqrt{1/n^2 - \cos^2\theta} - \sin\theta)^2 e^{-i\{k_2 r'' \cos(\theta - \theta'')\}}$$

$$\begin{aligned} F_1^{(2)}(\theta, r'') \;=\; & \frac{F_1(\alpha_s, r'')}{(1/n^2 - \cos^2\theta)^{3/2}} \times \\ & \Big\{ 4\cos^2\theta\sqrt{1/n^2 - \cos^2\theta} + k_2 r''(1/n^2 - \cos^2\theta)^{3/2} \Big\{ i\cos(\theta'' - \theta) \\ & - k_2 r'' \sin^2(\theta'' - \theta) \Big\} + i4k_2 r'' \cos\theta \sin(\theta'' - \theta)(1/n^2 - \cos^2\theta) \\ & + 2\sin\theta/n^2 \Big\} \end{aligned} \tag{3.32}$$

After inserting the above functions in the power series expansion of $H(s)$ and carrying out the integration the final form of the integral under consideration becomes,

$$I_{1\mathrm{sd}} = \frac{\omega\mu I n^2 e^{ik_2 r}}{4\sqrt{\pi}(n^2-1)\sqrt{k_2 r}} \left\{ \sqrt{2} F_1(\theta, r'') e^{-i\pi/4} + \frac{e^{-i3\pi/4}}{4k_2 r} \left(\frac{F_1(\theta, r'')}{\sqrt{2}} + 2\sqrt{2} F_1^{(2)}(\theta, r'') \right) \right\} \tag{3.33}$$

Evaluation for the branch point contribution present in the integral in (3.33) will be carried out now. It has already been discussed in the previous section that the branch point contribution is to be included in the overall integral evaluation of I_1 when the observation angle θ is less than $\alpha_b = \cos^{-1}(1/n)$ on the real axis. The same transformation

to s plane is carried out as in the previous section, i-e.,

$$i\cos(\alpha-\theta) = i\cos(\alpha_b-\theta) - s^2.$$

The resulting integral will be,

$$E_{-}^{\mathrm{L}} = \frac{\omega\mu I n^2 e^{ik_2 r\cos(\alpha_b-\theta)}}{4\pi(n^2-1)}\int_{-\infty}^{\infty} K(s)e^{-k_2 r s^2}ds, \tag{3.34}$$

where,

$$K(s) = \left(\sqrt{\frac{1}{n^2}-\cos^2\alpha}-\sin\alpha\right)^2 e^{-ik_2 r''\cos(\alpha-\theta'')}\frac{d\alpha}{ds}.$$

The path of integration runs on real axis of s-plane. The power series expansion of one of the above relationship, $K(s)$ around $s=0$ or $\alpha=\alpha_b$ is carried out. Keeping only s^2 term from the expansion the branch point contribution comes out to be,

$$E_{\text{-br}}^{\mathrm{L}} = \frac{\omega\mu I F_{(\text{L-b})}(r'',\theta)e^{ik_1 r\{\cos\theta+\sqrt{n^2-1}\sin\theta-3\pi/4\}}}{\sqrt{2\pi}(n^2-1)^{1/4}(k_2 r)^{3/2}} \tag{3.35}$$

while,

$$F_{(L-b)}(r'',\theta) = \frac{e^{-ik_2 r''\cos(\theta''-\alpha_b)}}{\{\sin(\alpha_b-\theta)\}^{3/2}} = \frac{n^{3/2}e^{-ik_1 r''(\cos\theta''-\sqrt{n^2-1}\sin\theta'')}}{\{\sqrt{n^2-1}\cos\theta-\sin\theta\}^{3/2}}$$

It can be seen that when the second integral I_2 is transformed to α plane only a saddle point is present in the transformed integral. The saddle point contribution from the second integral is evaluated by following the same procedure as was done in a similar case when the source was present in the upper half space. The result comes out to be,

$$I_{2\text{-sd}} = -\frac{\omega\mu I}{4\sqrt{\pi}}\frac{e^{ik_2 r}}{\sqrt{k_2 r}}\left\{\sqrt{2}F_2(\theta,r'')e^{-i\pi/4} + F_3(\theta,r'')\frac{e^{-i3\pi/4}}{4k_2 r}\right\}, \tag{3.36}$$

where,

$$F_2(\theta,r'') = e^{-ik_2 r''\cos(\theta-\theta'')},$$

and,

$$F_3(\theta,r'') = F_2(\theta,r'')\left(\frac{1}{\sqrt{2}} - 2\sqrt{2}k_2 r''\left\{i\cos(\theta-\theta'') - (k_2 r'')\sin^2(\theta-\theta'')\right\}\right).$$

The total saddle point contribution is achieved by the difference of (3.33) and (3.36). This result is given as,

$$E^{\mathrm{L}}_{\text{-sd}} = \frac{\omega\mu I e^{ik_2 r}}{4\sqrt{\pi k_2 r}}\Bigg\{\sqrt{2}e^{-i\pi/4}\Big(\frac{n^2F_1(\theta,r'')}{(n^2-1)}+F_2(\theta,r'')\Big)+\frac{e^{-i3\pi/4}}{4k_2r}\times \Big(F_3(\theta,r'')+\frac{F_1(\theta,r'')}{\sqrt{2}}+2\sqrt{2}F_1^{(2)}(\theta,r'')\Big)\Bigg\} \tag{3.37}$$

Hence combining (3.35) and (3.37) will give the total electric field below the interface while the source is also in this half dielectric space,

$$\begin{aligned} E^{\mathrm{L}}_{-} = {} & \frac{\omega\mu I n^2}{4\pi(n^2-1)\sqrt{k_2 r}}e^{ik_2 r}\times \\ & \Bigg\{\sqrt{2\pi}F_1(\theta,r'')e^{-i\pi/4}+\frac{\sqrt{\pi}}{4k_2r}e^{-i3\pi/4}\Big(\frac{F_1(\theta,r'')}{\sqrt{2}}+2\sqrt{2}F^{(2)}(\theta,r'')\Big)\Bigg\} \\ & +\frac{\omega\mu I F_{(\text{L-b})}(r'',\theta)e^{ik_1 r\{\cos\theta+\sqrt{n^2-1}\sin\theta-3\pi/4\}}}{\sqrt{2\pi}(n^2-1)^{1/4}(k_2r)^{3/2}} \end{aligned} \tag{3.38}$$

Equations (3.28) and (3.35) are combined to get the phase map of the electric field near the interface. This phase map has been shown in Fig. (3.4). It can be seen from this figure that phase lines are continuous across the interface due to the continuity of the field across the interface. The same behaviour was observed in case of interfacial line source case where the higher order terms of electric field expressions gave continuous phase lines across the interface.

In this section electric field near the interface has been evaluated using steepest descent method of asymptotic evaluation of integrals. The source configurations used include a line source placed above the interface and field found due to it both above and below the interface. Then the source was moved below the interface and the process of electric field evaluation repeated. The saddle point and branch point contributions were obtained when the observation angle was less than the critical angle. Similarly it was seen that only the saddle point contributes in case the angle of observation was larger

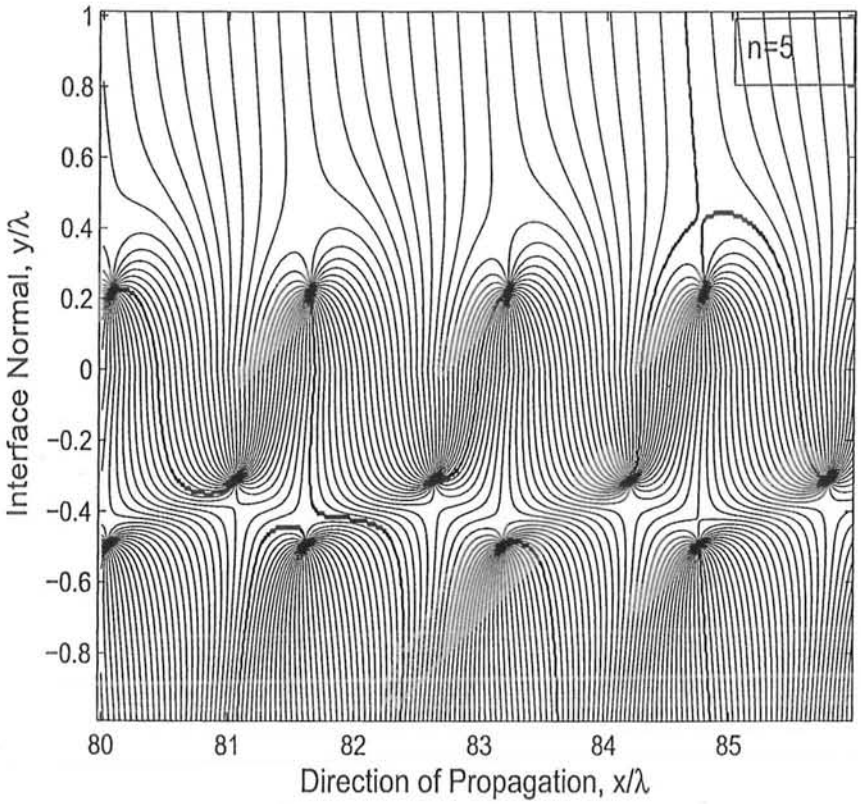

Figure 3.4: Phase map continuity preserved when displace line source is below the interface

than the critical angle. The field due to the branch point decays perpendicular to the interface in the rarer medium while the propagation along the interface of this wave component is with propagation constant of the lower medium.

3.3 Existence of Critical Points

It was proved in the last chapter that critical points existed in both half spaces near the interface when a line source was placed at the interface of the two half spaces. In this

chapter two cases have been considered as far as the electric current line source location is concerned. In the first case the line source was placed in the upper half space and field due to it was evaluated in both half spaces near the interface. In the second case the line source was placed in the lower half space and field was found in both half spaces near the interface. The presence of critical points was observed near the interface in these two cases. The obvious question which now arises is that is it also true in general for any type of source configuration? If the answer is in affirmative then $E_+^{U,L} = 0$, must have a solution. This solution will help to located the center type of critical points near the interface. Corresponding to each center type of critical point will be a saddle type of critical point nearby to conserve the index of rotation of Poynting vector field [9].

An examination of (3.11) reveals various complicated amplitude functions of θ, r' and θ'. To simplify matters (3.11) is written in a simplified form as follows,

$$E_+^U = \frac{e^{ik_1 r}}{(k_1 r)^{3/2}} \left[\left\{ k_1 r \sin\theta C_1(\theta; r', \theta') + C_2(\theta; r', \theta') \right\} + e^{-ik_1 r} e^{ik_1 r \psi(\theta)} C_3(\theta; r', \theta') \right] \quad (3.39)$$

where,

$$\psi(\theta) = (n\cos\theta + i\sqrt{n^2 - 1}\sin\theta)$$

and C_j for $j = 1, 2$ are simplified forms of $F_i^{(n)}$ for $n = 0, 2$ and $i = 1, 2$ as given in (3.11). The first function in the curly braces above vanishes at the interface or at $\theta = 0$. The remaining two functions C_2 and C_3 represent very small terms which are not zero at the interface. These small terms perturb the solution of $E_+^U(r, \theta; r', \theta') = 0$ at $\theta = 0$. The fact that these small terms are being added to the leading term also suggests that the zero of E_+^U has shifted from the line at $\theta = 0$ to some other location near the interface. The source location parameters r' and θ' are constants. It is expedient to expand function C_j for $j = 2, 3$ in a Taylor series about $\theta = 0$. The leading terms of the expansion are constants. It is assumed that $r = x$ and $r\sin\theta = y$ because the point of observation is

in the far zone. The assumption leads to the following simplified form of (3.39),

$$K_1 y + K_2 = e^{ik_1(n-1)x} e^{-k_1\sqrt{n^2-1}y} \tag{3.40}$$

where,

$$K_1 = C_1/C_3 \qquad K_2 = C_2/C_3$$

As K_1 and K_2 are complex numbers the above relationship can be written as,

$$\sqrt{|K_1|^2 y^2 + |K_2|^2} e^{ik\phi} = e^{ik_1(n-1)x} e^{-k_1\sqrt{n^2-1}y} \tag{3.41}$$

where ϕ is the phase of complex number on the left hand side of (3.41).

It can also be seen that the left hand side of (3.41) increases with $y > 0$ in the upper half space. The magnitude of first exponential function on the right hand side varies periodically between -1 and +1 when the observer moves along x-axis. The second exponential function on right hand side is real. Its value decays from one to zero as y increases from 0 to ∞. It leads to the conclusion that product of the right hand side functions periodically equals the left hand side as the value of y is increased from zero in the upper half space. The fact that the solutions of the above relationships repeat periodically results in the creation of critical points in the upper half space near the interface as shown in Fig. 3.2.

The location of the critical points in the lower half space will be ascertained. The total field in the lower half space can be written in the following simplified form,

$$E_-^L = \frac{e^{ik_2 r}}{(k_2 r)^{3/2}} \left[\left\{ \sin\theta C_4(\theta; r'', \theta'') k_2 r + C_5(\theta; r'', \theta'') \right\} + C_6(\theta; r'', \theta'') e^{ik_1 r\chi(\theta)} \right] \tag{3.42}$$

The functions C_n for $n = 4, 5$ and 6 are complicated functions of spatial polar coordinates of the observer as well as the source. It is observed that for small values of angle of observation θ the functions C_4 and C_5 become complex functions. Based on the fact

that the two function become complex a further simplification of the equation (3.42) can be rewritten the following form,

$$E_{-}^{L} = \frac{e^{ik_2 r}}{(k_2 r)^{3/2}} \left[\left\{ C_4(\theta; r'', \theta'') k_2 r + C_5(\theta; r'', \theta'') \right\} + C_6(\theta; r'', \theta'') e^{ik_1 r \chi(\theta)} e^{-ink_1 r} \right] \quad (3.43)$$

The phases of functions $C_4(\theta; r'', \theta'')$ and $C_5(\theta; r'', \theta'')$ can be approximated as constants in the far zone when the angle of observation is increased away from the interface. This assumption leads to the following simplified form of above equation,

$$C_4 k_2 R + C_5 + e^{ik_1 r(\chi(\theta) - n)} = 0 \quad (3.44)$$

The real and imaginary parts of the above equation can be related by the following equations,

$$\cos\{R(\chi(\theta) - n)\} = C_4 nR + C_5,$$

and,

$$\sin\{R(\chi(\theta) - n)\} = 0.$$

This means that,

$$R(\chi(\theta) - n) = \pm m\pi,$$

or,

$$C_4 nR + C_5 = (\pm 1)^m.$$

From the above relationship it can be written that,

$$nR = \frac{(\pm 1)^m - C_5}{C_4}$$

where,

$$R = M - K,$$

and

$$M = \frac{(\pm 1)^m}{nC_4}, \qquad K = \frac{C_5}{nC_4}.$$

From the above equation it can be seen that $M \ll K$ indicating that a pair of critical points will exist in close proximity in the lower region for each value of integer m. Hence for each critical point in the upper half space for a particular value of m a pair of critical points will exist in the lower half space. This is also confirmed by the Fig. 3.4.

It has been seen that the above procedure adopted for simplification of E_+^U and E_-^L can also be followed for E_-^U and E_+^L. As a result of the simplification the form that E_-^U attains resembles that of E_+^U while E_+^L looks similar to E_-^L. From this resemblance of field quantities and observation of phase plots show that the critical points also exist due to E_-^U and E_+^L on both sides of the interface as they exist due to E_+^U and E_-^L respectively.

3.4 Generalization

Electric field expressions have been found near the dielectric interface in the last two sections 3.2 and 3.3. In section 3.2 a line source was placed above the interface. The electric field expressions were found both above and below the interface due to this source. In the next section, 3.3 the line source was moved to the lower half space and field due to it was found in both half spaces. It was observed that the zeros of fields near the interface existed at a fixed height from the interface. The frequency of occurrence of these nulls of field was $(n-1)$ per wavelength. These nulls were also independent of current magnitude of the sources.

Consider now Fig. 3.5 in which two line sources, L and L_1 are shown placed in close proximity to each other in the upper half space. The direct distances of these sources L and L_1 from origin of the geometry are r' and r_1' respectively. As a first step to analyze the field behavior due to these two sources assume presence of only one of the two sources, L only. The periodic nulls of the electric field will be created near the

interface due to this single source as has been proved earlier in this chapter. One of this field null is shown as Z in Fig. 3.5. Now consider the second source, L_1 placed at r_1' while the source L has been removed. The presence of L_1 will also cause field nulls to appear along the interface. One of such field null is shown as Z_1 in this figure. The simultaneous presence of these two sources is now assumed in the geometry of problem as shown in Fig. 3.5. It is known that the electric field is a complex function of two real variables, x and y. The resultant field due to these two sources can be represented by sum of the leading terms of the Taylor series expansion of the individual electric fields of the two sources. The resultant expressions will be linear functions of x and y. Equating real and imaginary parts to zero the resulting two equations can be solved simultaneously for the finding the zeros of the resultant field. In other words it means that simultaneous presence of the two line sources will cause the occurrence of field nulls in the close vicinity of Z and Z_1.

In the next step a source of arbitrary shape and size is obtained by considering a number of line sources in close proximity and integrating them over source coordinates. Field due to this in the upper half space is represented by E_{+ar}^{U} and in the lower half space by E_{+ar}^{L}. This arbitrary source in the upper half space has been shown in Fig. 3.6. Likewise in Fig. 3.7 a similar source in lower half space is assumed with fields due to the source shown in the same figure. Now the simultaneous presence of these sources is considered in this media of two dielectric half spaces. All the field expressions valid for above the interface are summed up to obtain the net effect of fields near the interface in upper half space. In fact this summation is achieved by adding equations (3.11) and (3.28). An integration is carried out over arbitrary volumes v' and v'' in the resulting expression. Later Taylor series expansion of the resulting expression is taken at $\theta = 0$. Retaining only the leading terms of the expansion gives the following form of electric

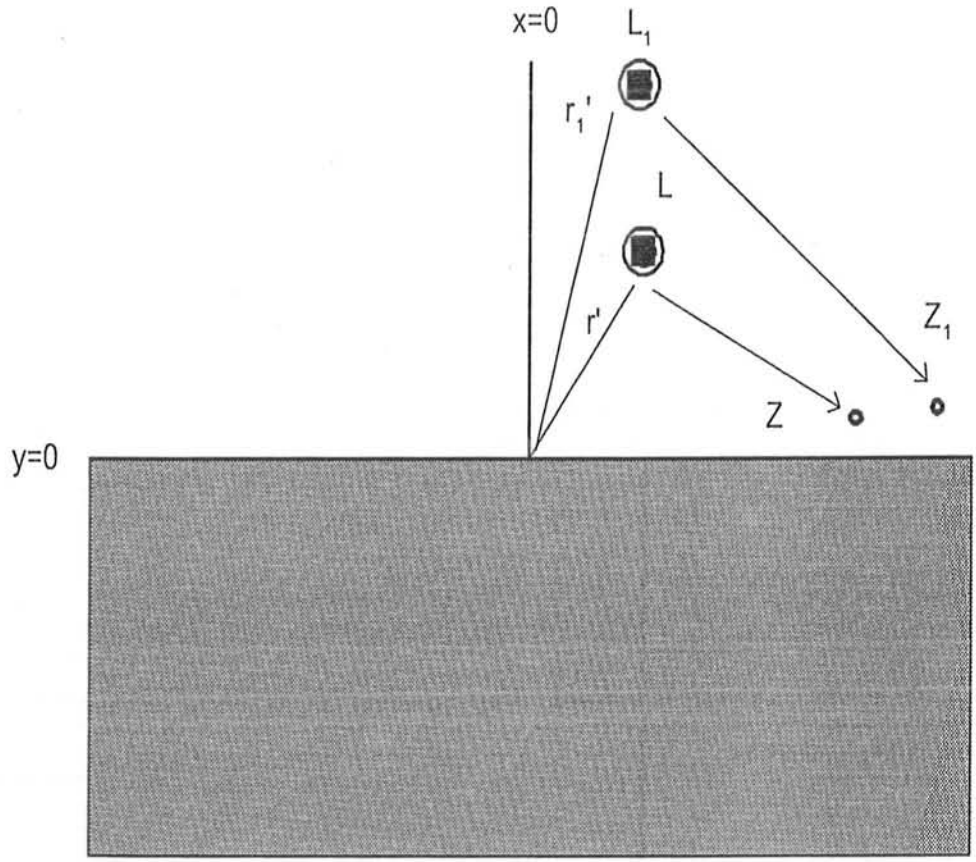

Figure 3.5: Two line sources placed arbitrarily in the upper half space

field expression above the interface,

$$E_{ar}^{U} = \frac{e^{ik_1 r}}{(k_1 r)^{3/2}}\left[\left\{k_1 r \sin\theta E_1(\theta) + J_1(\theta)\right\} + M_3(\theta)e^{ik_1 r\psi(\theta)}\right] \tag{3.45}$$

where,

$$M_3(\theta) = E_3(\theta) + J_3(\theta)$$

It can be observed that (3.45) is similar in shape as (3.40) which shows periodic nulls near the interface. Hence it can be concluded that any number of sources present arbitrarily in the two dielectric half spaces will always lead to a general form of (3.45). This form

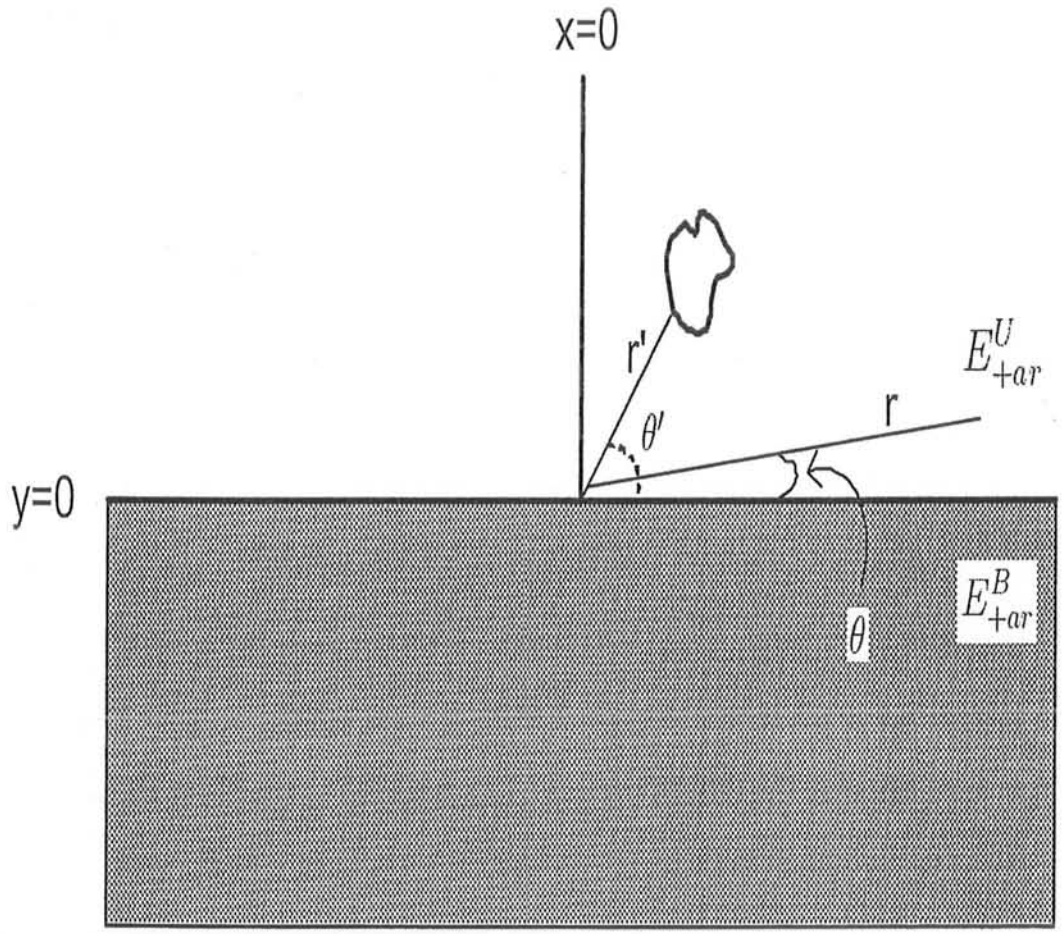

Figure 3.6: A displaced arbitrary source in upper half space

has its solution near and above the interface at periodic points which are responsible for creation of critical points near the interface. Similarly equations (3.19) and (3.38) can also be combined to get electric field expression below the interface while the source's location is arbitrary. Following the same procedure of carrying out integration over the volume parameters v' and v'' the following simplified expression is obtained for the total

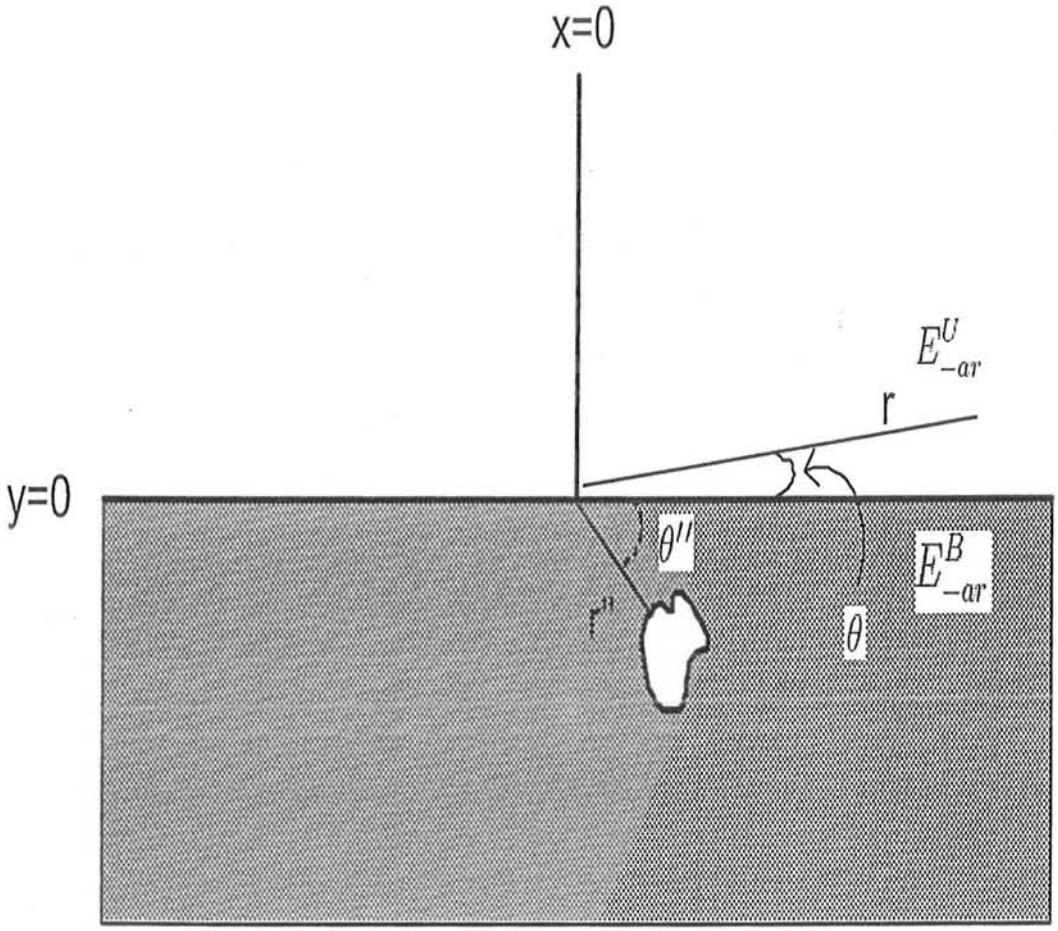

Figure 3.7: A displaced arbitrary source in lower half Space

field below the interface for sources arbitrarily present anywhere in the medium,

$$E^{\mathrm{L}}_{\mathrm{ar}} = \frac{e^{ik_2 r}}{(k_2 r)^{3/2}}\left[\left\{k_2 r \sin\theta E_2(\theta) + J_2(\theta)\right\} + M_4(\theta) e^{ik_1 r \chi(\theta)} e^{-ink_1 r}\right] \tag{3.46}$$

where,

$$M_4(\theta) = E_4(\theta) + J_4(\theta)$$

This expression is similar in form to (3.43). It also has a solution at periodic points valid for lower half space. The phase maps in the due to arbitrary source in the upper half

space is shown in Fig. 3.8. A similar pattern is obtained due to the arbitrary source in the lower half space. Saddle and center type of critical points are generated near the interface which are responsible for the continuity of the phase map of the electromagnetic wave across the interface. The value of refractive index also changes the location of these points on the phase map as shown in Fig. 3.9.

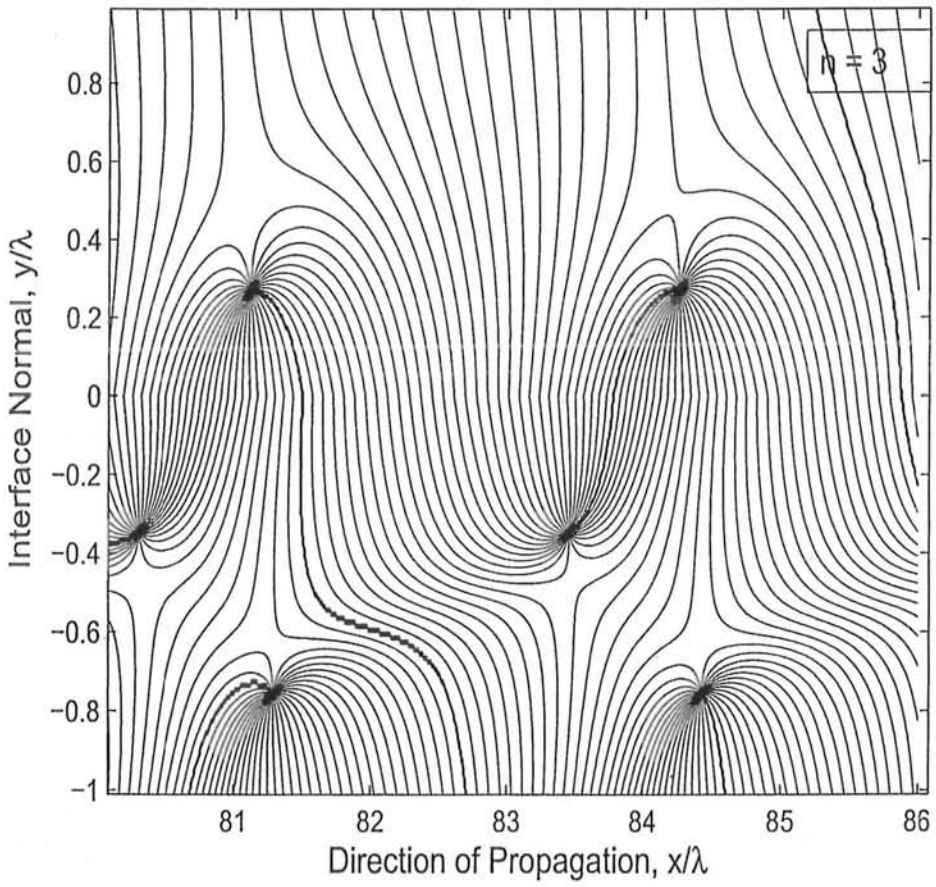

Figure 3.8: Phase map near the interface due to arbitrary shaped electric source in the upper half space

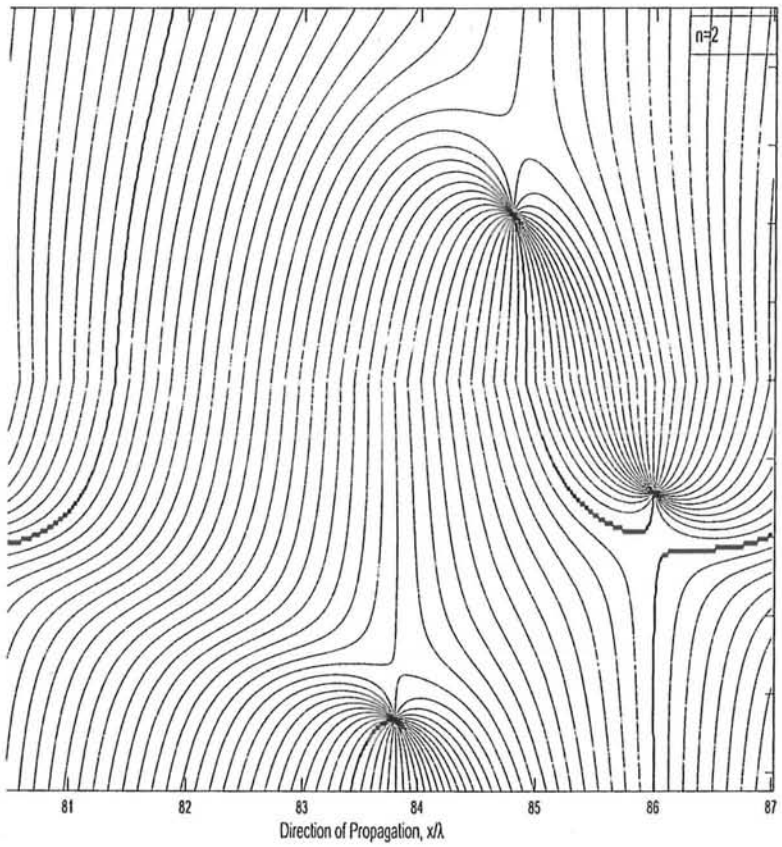

Figure 3.9: Critical points move away as refractive index decreases in lower half space

Chapter 4

Current Sheet Perpendicular to Plane Dielectric Interface

Behaviour of electric field phase velocity and phase map along the interface of two dielectric half spaces was investigated in Chapters 2 and 3. The sources of electromagnetic waves were finite in size. In Chapter 2 the source was an electric current line source placed at the interface of the two dielectric half spaces. Then in Chapter 3 the source was generalized to be an arbitrary z-directed source but finite in extent. The phase velocity plots of the electric field in both the chapters was in conformity with continuity of field across the interface.

The phase plots also showed interesting structures of phase map present along the interface. These structures of phase map were produced due to two types of critical points, the saddle type of critical point and the center type of critical point. The role of these critical points were explained as regards the phase velocity transition from one medium to the other. Now two points need further investigation. First point is that how would a wave generated due to a source of infinite dimensions behave near the interface? The second point is that if a plane wave propagates alongside the interface what would be the wave behaviour near the interface?

Chapter 4

Current Sheet Perpendicular to Plane Dielectric Interface

Behaviour of electric field phase velocity and phase map along the interface of two dielectric half spaces was investigated in Chapters 2 and 3. The sources of electromagnetic waves were finite in size. In Chapter 2 the source was an electric current line source placed at the interface of the two dielectric half spaces. Then in Chapter 3 the source was generalized to be an arbitrary z-directed source but finite in extent. The phase velocity plots of the electric field in both the chapters was in conformity with continuity of field across the interface.

The phase plots also showed interesting structures of phase map present along the interface. These structures of phase map were produced due to two types of critical points, the saddle type of critical point and the center type of critical point. The role of these critical points were explained as regards the phase velocity transition from one medium to the other. Now two points need further investigation. First point is that how would a wave generated due to a source of infinite dimensions behave near the interface? The second point is that if a plane wave propagates alongside the interface what would be the wave behaviour near the interface?

The source of an infinite extent can be a current sheet which generates plane electromagnetic waves. Consider Fig. 1.1 once again to determine if this simple text book problem can be modified so that propagation parallel to interface can be obtained? In this figure a source is placed at infinity in a medium having a finite dielectric interface. But it becomes a Fresnel transmission and reflection problem already solved by Fresnel in 1823. Another possibility is to extend the interface to infinity as shown in Fig. 1.1 but the source will cut the interface thereby presenting a complicated problem of transmission and reflection at the interface. Hence the convenient way to study the plane wave propagation problem near the interface is to place the sheet perpendicular to the interface. The resulting plane wave propagation will be parallel to the interface. Far away from the interface the plane wave will propagate according to the propagation constant of the respective dielectric half space. But near the interface the conditions will be different. The interest is to investigate how the fast wave in one medium changes over to a slower wave in the second medium across the interface and what type of phase map will be generated near the interface?

4.1 Problem Formulation

Consider two half current sheets of current densities $\vec{J_1}$ and $\vec{J_2}$ lying in $x = 0$ plane as shown in Fig. 4.1. The dielectric half space which exists for $y > 0$ has permittivity and permeability as ϵ_0 and μ_0 respectively. The second dielectric half space which occupies the $y < 0$ space has permittivity and permeability as ϵ_1' and μ_0 respectively. The flow of current in the sheets is parallel to the z-axis. The propagation constant of the plane wave in the upper half space is k_1 while for the lower half space it is k_2. The current

density may be written as,

$$\vec{J} = \begin{cases} \vec{J}_1 & y > 0; \\ \\ \vec{J}_2 & y < 0; \end{cases} = \begin{cases} I_1\delta(x)\hat{a}_z; \\ \\ I_2\delta(x)\hat{a}_z; \end{cases}$$

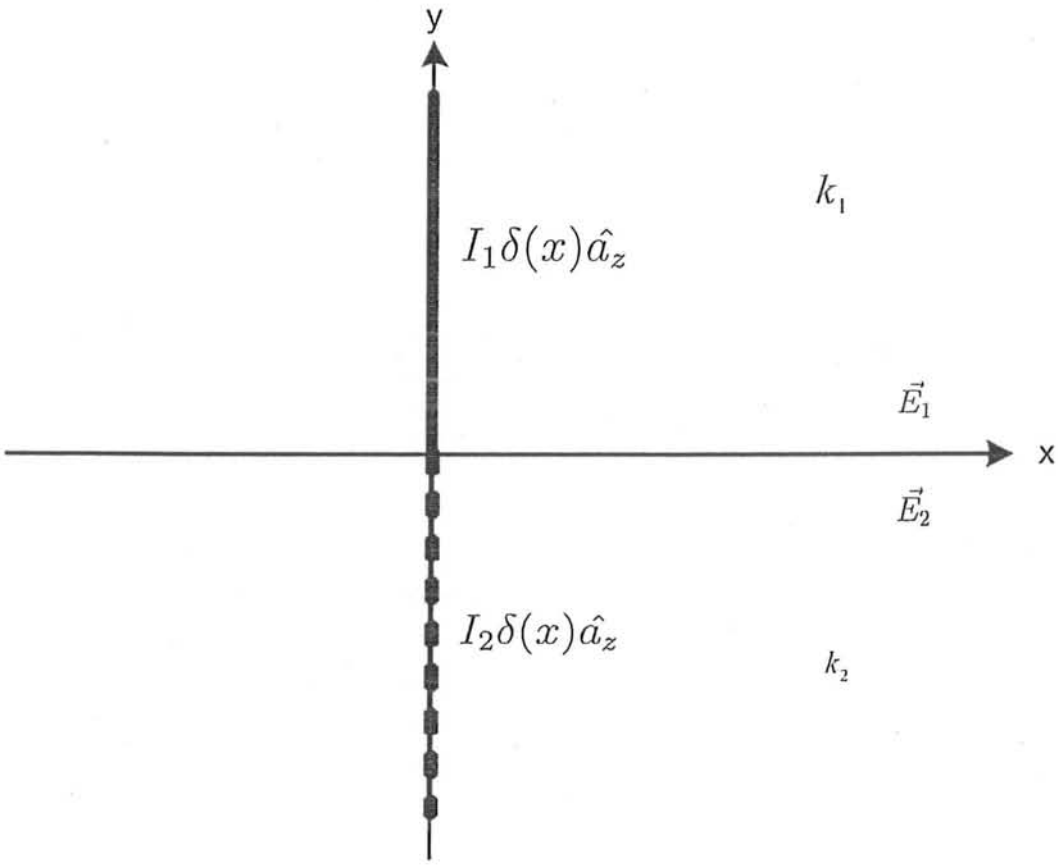

Figure 4.1: Two half current sheets present in the yz plane

I_1 and I_2 are the current magnitudes in the two sheets measured in amperes/meter. It is well known that the Helmohltz equation in a homogenous medium is,

$$\nabla^2\vec{E} + k^2\vec{E} = -i\omega\mu\vec{J}. \tag{4.1}$$

Since $\vec{J}$ is z directed and independent of z coordinate thus the electric field $\vec{E}$ is also z directed and independent of z coordinate. The electric field $\vec{E}$ in the two half spaces is defined as,

$$\vec{E} = \begin{cases} E_1 \hat{a_z} & y > 0; \\ \\ E_2 \hat{a_z} & y < 0; \end{cases}$$

Therefore (4.1) can be written as,

$$\nabla^2 E_1 + k_1^2 E_1 = -i\omega\mu I_1 \delta(x), \qquad y > 0. \tag{4.2}$$

$$\nabla^2 E_2 + k_2^2 E_2 = -i\omega\mu I_2 \delta(x), \qquad y < 0. \tag{4.3}$$

The solution of (4.2) will be considered first. This equation has a homogenous and a particular solution,

$$E_1 = E_{1\mathrm{h}} + E_{1\mathrm{p}},$$

where $E_{1\mathrm{h}}$ is the homogenous solution while $E_{1\mathrm{p}}$ represents the particular solution of (4.2).

An elementary solution to the homogenous form of this equation which satisfies the radiation conditions is,

$$E_{1\mathrm{h}} = e^{\pm ik_x x} e^{ik_{1y} y} \hat{a_z}.$$

where $+$ sign in the first exponential is for $x > 0$ while the $-$ sign is for $x < 0$ to satisfy the radiation conditions. Therefore a general solution to (4.2) can be written as,

$$E_{1\mathrm{h}} = \int_{-\infty}^{\infty} P(k_x) e^{\pm ik_x x} e^{ik_{1y} y} dk_x,$$

where,

$$k_{1y} = \sqrt{k_1^2 - k_x^2},$$

and $P(k_x)$ is an arbitrary complex amplitude function of the electric field. The particular solution which satisfies (4.2) is given as,

$$\vec{E}_{1\mathrm{p}} = Ae^{ik_1|x|}\hat{a}_z,$$

where A is the amplitude constant of the electric field. Since the current magnitude is constant over the sheet and its distribution is independent of y, the particular solution $E_{1\mathrm{p}}$ will not be a function of spatial coordinate y. The boundary condition at $x = 0$ which is Ampere's law results into the following relationship,

$$\left.\frac{\partial E_1}{\partial x}\right|_{x=0^+} - \left.\frac{\partial E_1}{\partial x}\right|_{x=0^-} = -i\omega\mu I_1, \qquad \forall y > 0 \tag{4.4}$$

Substitution of this proposed solution in (4.4) will help to find the value of A. This means,

$$ik_1A - (-ik_1)A = -i\omega\mu I_1,$$

or,

$$A = -\frac{\omega\mu I_1}{2k_1}.$$

Thus the total electric field in the region, $y > 0$ can be written as,

$$E_1 = \int_{-\infty}^{\infty} P(k_x)e^{i(k_x x + k_{1y} y)}dk_x - \frac{\omega\mu I_1}{2k_1}e^{ik_1|x|}. \tag{4.5}$$

In a similar manner the solution to (4.3) for the half space $y < 0$ that also satisfies radiation condition can be written as,

$$E_2 = \int_{-\infty}^{\infty} Q(k_x)e^{i(k_x x - k_{2y} y)}dk_x - \frac{\omega\mu I_2}{2k_2}e^{ik_2|x|}, \tag{4.6}$$

where,

$$k_{2y} = \sqrt{k_2^2 - k_x^2}.$$

and $Q(k_x)$ is an unknown complex amplitude function of the electric field in the lower half space.

The boundary conditions at $y = 0$ will now be applied to find the value of the unknown amplitude functions $P(k_x)$ and $Q(k_x)$ given in (4.5) and (4.6) respectively. There are two boundary conditions given as,

$$E_{t1} = E_{t2}, \tag{4.7}$$

and,

$$\hat{a_n} \times (\vec{H}_1 - \vec{H}_2) = \vec{J}. \tag{4.8}$$

According to the first boundary condition (4.7) the tangential components of the electric fields are continuous across the interface and the equations (4.5) and (4.6) give the following relationship,

$$\int_{-\infty}^{\infty} \Big\{P(k_x) - Q(k_x)\Big\} e^{ik_x x} dk_x \;=\; \frac{\omega\mu}{2}\left\{\frac{I_1}{k_1} e^{ik_1|x|} - \frac{I_2}{k_2} e^{ik_2|x|}\right\}. \tag{4.9}$$

The ratio $e^{ik_1|x|}/k_1$ in the above integral may be written as residue of a pole at $k_x = k_1$ of the integral $(i/\pi)\int_{-\infty}^{\infty} e^{ik_x x}/k_{1y}^2 dk_x$. Substitution of this fact in (4.9) gives the following relationship,

$$\int_{-\infty}^{\infty}\Big[\{P - Q\} - \frac{\omega\mu}{2\pi i}\Big\{\frac{I_2}{k_{2y}^2} - \frac{I_1}{k_{1y}^2}\Big\}\Big] e^{ik_x x} dk_x = 0. \tag{4.10}$$

Using orthogonality of the complex exponential function in the above expression the following relationship is obtained,

$$P(k_x) - Q(k_x) = \frac{\omega\mu}{2\pi i}\left\{\frac{I_2}{k_{2y}^2} - \frac{I_1}{k_{1y}^2}\right\}. \tag{4.11}$$

Similarly according to the second boundary condition (4.8) the difference of tangential component of magnetic field is equal to the current density on the interface. According to this condition no electric current exists at the interface except at origin. As the interface is dielectric in nature no surface currents exist or there is no $\delta(\cdot)$ function.

Hence according to Ampere's law,

$$\left.\frac{\partial E_1}{\partial y}\right|_{y=0^+} = \left.\frac{\partial E_2}{\partial y}\right|_{y=0^-} \qquad \forall x \neq 0. \tag{4.12}$$

Therefore,

$$\int_{-\infty}^{\infty} i\{k_{1y}P(k_x) + k_{2y}Q(k_x)\}e^{ik_x x}dk_x = 0. \tag{4.13}$$

Application of orthogonality property of complex exponential function to (4.13) gives,

$$k_{1y}P(k_x) + k_{2y}Q(k_x) = 0. \tag{4.14}$$

Solving (4.11) and (4.14) simultaneously, the following values of complex amplitude coefficients $P(k_x)$ and $Q(k_x)$ are obtained,

$$P(k_x) = \frac{\omega\mu k_{2y}}{2\pi i(k_{1y}+k_{2y})}\left\{\frac{I_2}{k_{2y}^2} - \frac{I_1}{k_{1y}^2}\right\}, \tag{4.15}$$

$$Q(k_x) = \frac{\omega\mu k_{1y}}{2\pi i(k_{1y}+k_{2y})}\left\{\frac{I_1}{k_{1y}^2} - \frac{I_2}{k_{2y}^2}\right\}. \tag{4.16}$$

Substitution of (4.15) and (4.16) in (4.5) and (4.6) gives,

$$E_1 = \int_{-\infty}^{\infty} \frac{k_{2y}}{(k_{1y}+k_{2y})}\left\{\frac{I_2}{k_{2y}^2} - \frac{I_1}{k_{1y}^2}\right\}e^{i(k_x x + k_{1y}y)}dk_x - \frac{\omega\mu I_1}{2k_1}e^{ik_1|x|}, \tag{4.17}$$

and,

$$E_2 = \int_{-\infty}^{\infty} \frac{k_{1y}}{(k_{1y}+k_{2y})}\left\{\frac{I_1}{k_{1y}^2} - \frac{I_2}{k_{2y}^2}\right\}e^{i(k_x x - k_{2y}y)}dk_x - \frac{\omega\mu I_2}{2k_2}e^{ik_2|x|}. \tag{4.18}$$

For simplification of problem consider Fig. 4.2. In this figure the two current sheets in the Fig. 4.1 has been replaced by a single sheet of current with the current density $I\delta(x)\hat{a}_z$ placed at $x = 0$. The electric field in the z-direction will now be represented by the following equations in the two half spaces,

$$E^{\mathrm{U}} = \frac{\omega\mu I}{2k_1}e^{ik_1|x|} + \frac{\omega\mu I}{2\pi i}\Big\{I_{1\mathrm{U}} - I_{2\mathrm{U}}\Big\}, \tag{4.19}$$

and,

$$E^{\mathrm{L}} = \frac{\omega\mu I}{2k_2}e^{ik_2|x|} + \frac{\omega\mu I}{2\pi i}\Big\{I_{1\mathrm{L}} - I_{2\mathrm{L}}\Big\}. \tag{4.20}$$

where,

$$I_{1U} = \int_{-\infty}^{\infty}\left\{\frac{e^{ik_x x + ik_{1y}y}}{k_{1y}k_{2y}}\right\}dk_x$$

$$I_{2U} = \int_{-\infty}^{\infty}\left\{\frac{e^{ik_x x + ik_{1y}y}}{k_{1y}^2}\right\}dk_x$$

$$I_{1L} = \int_{-\infty}^{\infty}\left\{\frac{e^{ik_x x - ik_{2y}y}}{k_{1y}k_{2y}}\right\}dk_x$$

and,

$$I_{2L} = \int_{-\infty}^{\infty}\left\{\frac{e^{ik_x x - ik_{2y}y}}{k_{2y}^2}\right\}dk_x$$

It has been decided to change the notations of electric field representations such that E_1 is replaced by E^U while E^L will replace E_2. This has been done in conformity with the notations used for electric fields in the previous chapters. The 'U' in the superscript denotes the Upper half space Electric field while 'L' in the superscript stands for Lower half space. Evaluation of the electric field expressions E^U and E^L will be carried out now.

4.2 Electric Field In Upper Half Space

The total field in the upper half space is sum of a plane wave propagating with wavenumber k_1 and two integrals I_{1U} and I_{2U} as given in (4.20). Consider $I_{1\mathrm{U}}$ in (4.19) first, which is given as,

$$I_{1\mathrm{U}} = \int_{-\infty}^{\infty}\frac{e^{ik_x x + ik_{1y}y}}{k_{1y}k_{2y}}\,dk_x, \tag{4.21}$$

where,

$$k_{2y} = \sqrt{k_2^2 - k_x^2}$$

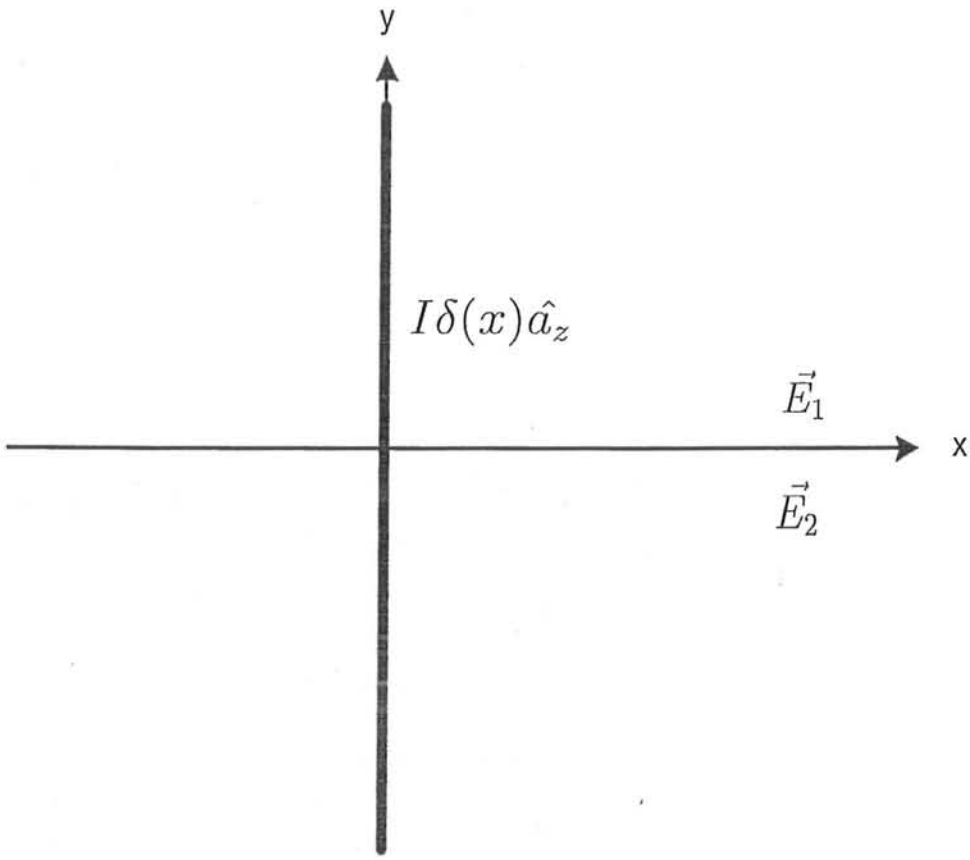

Figure 4.2: Current sheet present in the yz plane

$$k_{1y} = \sqrt{k_1^2 - k_x^2}$$

The path of integration in this integral runs along real axis of k_x plane. There are two pairs of branch points in I_{1U} at $k_x = \pm k_2$ and $k_x = \pm k_1$. The branch cuts originating from these branch points are shown in Fig. 2.2 in chapter 2. These cuts run in the first quadrant of the complex k_x plane because $\Im[e^{ik_{1y}}] > 0$ will satisfy the radiation conditions when the contour of integration is closed at $k_x = \infty$. A transformation from

k_x plane to α plane is carried out to simplify the evaluation process according to,

$$k_x = k_1 \cos\alpha.$$

A subsequent transformation of cartesian coordinates x and y to polar coordinate r and θ according to,

$$x = r\cos\theta, \qquad y = r\sin\theta$$

converts I_{1U} to the following form,

$$I_{1U} = -\int_Q F(\alpha) e^{k_1 r f(\alpha)}\, d\alpha, \tag{4.22}$$

where,

$$f(\alpha) = i\cos(\alpha - \theta),$$

and,

$$F(\alpha) = \frac{1}{k_1\sqrt{n^2 - \cos^2\alpha}}.$$

The path of integration Q which extends from $\pi - i\cosh\eta$ to $i\infty$ is shown in Fig. 4.3. It can be seen that the choice $k_x = k_1\cos\alpha$ results in the removal of the branch point at $k_x = k_1$. The second pair of branch points are located on the imaginary axis of α plane. Complex function $f(\alpha)$ is multiplied by large parameter $k_1 r$ has a saddle point at $\alpha = \theta$. The complex exponent with a large parameter in the integrand of (4.22) demands application of steepest descent method for evaluation of I_{1U}. The path of integration, Q will be deformed to run on a constant phase path and also pass through the saddle point. The deformed path is shown as Q' in the Fig. 4.3. The contribution from saddle point will be represented by $I_{1U\text{-sd}}$ while that from branch point will be represented by $I_{1U\text{-br}}$. The pair of branch points present in α plane corresponds to those at $k_x = \pm k_2$ in the original k_x plane. It may be remembered that as electric field for $x > 0$ is being investigated near the interface, the branch point at $\alpha = i\cosh\eta$ will contribute if the

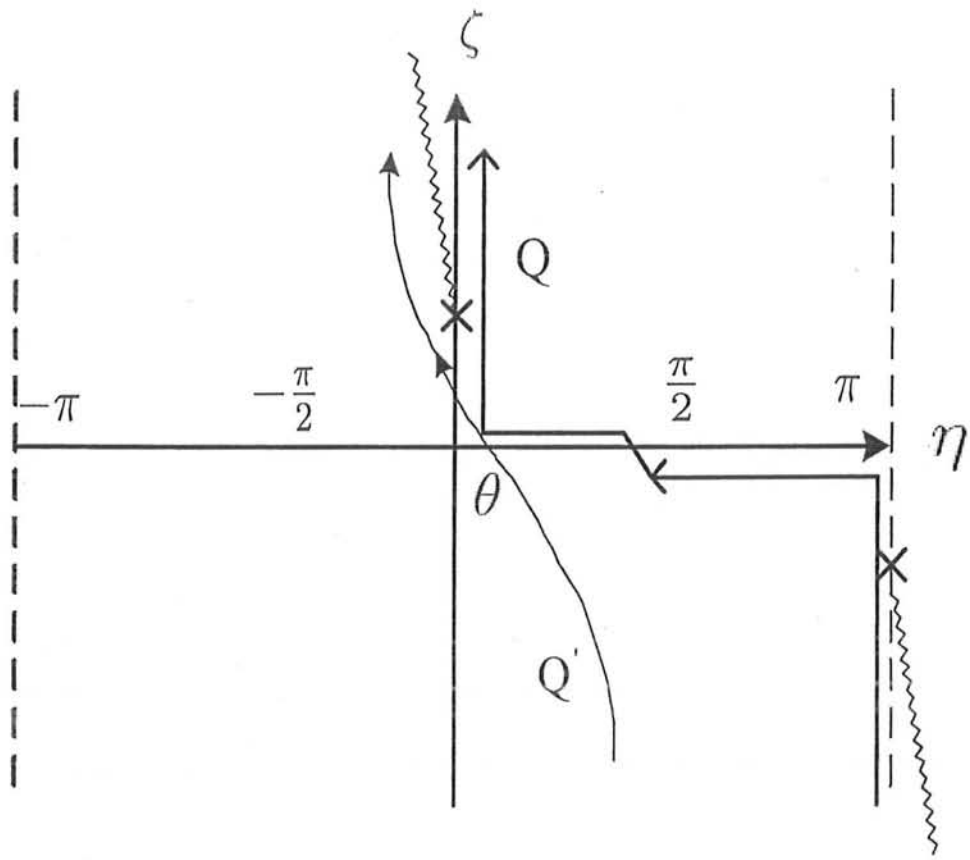

Figure 4.3: The corresponding path of integration in complex α plane of I_{1U}

point of observation θ is less than the critical angle. The branch cut will be made to run along a constant phase path to be able to apply method of steepest descent for asymptotic evaluation of branch point contribution. In case angle of observation is greater than the critical angle only the saddle point contribution will be taken to express electric field in the upper half space.

To evaluate the saddle point contribution a transformation to the s plane is carried out according to (2.13) for convenience in the evaluation of $I_{1\text{U-sd}}$. The path of integration will now run on real s-axis while the saddle point will be shifted to origin of the new

plane. The integral (4.22) transforms to,

$$I_{1\text{U-sd}} = \frac{e^{k_1 r f(\alpha_s)}}{k_1} \int_{-\infty}^{\infty} G(s) e^{-k_1 r s^2} ds, \tag{4.23}$$

where,

$$G(s) = F(\alpha) \frac{d\alpha}{ds},$$

while,

$$F(\alpha) = \frac{1}{\sqrt{n^2 - \cos^2 \alpha}}.$$

As the saddle point is located at $s = 0$ in (4.23) a power series expansion of $G(s)$ at $s = 0$ will be taken. The first term of expansion is taken only which does not come out to be zero at the interface. This results into the following relationship,

$$G(0) = F(\alpha_s) \left. \frac{d\alpha}{ds} \right|_{s=0}$$

where,

$$F(\alpha_s) = \frac{1}{\sqrt{n^2 - \cos^2 \theta}}.$$

Hence the saddle point contribution due to the first integral comes out to be,

$$I_{1\text{U-sd}} = \frac{\omega \mu I}{\sqrt{2\pi i}} \frac{e^{ik_1 r} e^{-i\pi/4}}{k_1 \sqrt{k_1 r} \sqrt{n^2 - \cos^2 \theta}} \tag{4.24}$$

The following transformation is made to find out the contribution of the branch point at $\alpha = \alpha_b$,

$$i \cos(\alpha - \theta) = i \cos(\alpha_b - \theta) - s^2.$$

The new form of integral I_1 for finding the branch point contribution is,

$$I_{1\text{U-br}} = \frac{e^{ik_1 r \{n \cos\theta + i\sqrt{n^2-1} \sin\theta\}}}{k_1} \int_{-\infty}^{\infty} G(s) e^{-k_1 r s^2} ds, \tag{4.25}$$

where,

$$G(s) = F(\alpha_b) \frac{d\alpha}{ds} = \frac{1}{\sqrt{n^2 - \cos^2 \alpha}} \frac{d\alpha}{ds}.$$

Power series expansion of $F(\alpha_b)$ will be taken around $\alpha = \alpha_b$ while retaining the first two terms only. The resultant expansion comprising of these first two terms will be,

$$F(\alpha_b) = \frac{1}{\sqrt{2n}(1-n^2)^{1/4}\sqrt{\alpha-\alpha_b}} + \frac{(1-2n^2)\sqrt{\alpha-\alpha_b}}{4\sqrt{2}n^{3/2}(1-n^2)^{3/4}}.$$

It is known from α to s plane transformation that,

$$\sqrt{\alpha-\alpha_b} = \frac{se^{-i5\pi/4}}{\sqrt{\sin(\alpha_b-\theta)}},$$

and,

$$\frac{d\alpha}{ds} = \frac{2se^{-i\pi/2}}{\sin(\alpha_b-\theta)}.$$

The substitutions of the above relationships into the relationship of $G(s)$ results into the following form of $G(s)$,

$$G(s) = \frac{\sqrt{2}e^{i3\pi/4}}{\sqrt{n}(1-n^2)^{1/4}\sqrt{\sin(\alpha_b-\theta)}} + \frac{(1-2n^2)s^2e^{-i7\pi/4}}{2\sqrt{2}n^{3/2}(1-n^2)^{3/4}(\sin(\alpha_b-\theta))^{3/2}}.$$

Retaining only the first term of the expansion,

$$I_{1\text{U-br}} = \frac{\sqrt{2\pi}e^{ik_1r(n\cos\theta+i\sqrt{n^2-1}\sin\theta)}e^{i3\pi/4}}{k_1\sqrt{n}(1-n^2)^{1/4}(\sqrt{1-n^2}\cos\theta-n\sin\theta)^{1/2}\sqrt{k_1r}}. \tag{4.26}$$

Combination of saddle and branch point contributions give the following expression,

$$\begin{aligned} I_{1\text{U}} &= \frac{\omega\mu I}{\sqrt{2\pi}i}\left\{\frac{e^{ik_1r}e^{-i\pi/4}}{k_1\sqrt{k_1r}\sqrt{n^2-\cos^2\theta}}\right. \\ &+ \left.\frac{\sqrt{2\pi}e^{ik_1r(n\cos\theta+i\sqrt{n^2-1}\sin\theta)}e^{i3\pi/4}}{k_1\sqrt{n}(1-n^2)^{1/4}(\sqrt{1-n^2}\cos\theta-n\sin\theta)^{1/2}\sqrt{k_1r}}\right\}. \end{aligned} \tag{4.27}$$

The second integral in (4.19) is given as,

$$I_{2\text{U}} = \int_{-\infty}^{\infty}\frac{e^{ik_xx}e^{ik_{1y}y}}{k_{1y}^2}\,dk_x. \tag{4.28}$$

The path of this integral runs also along real axis of complex k_x plane. This integral has a pair of branch points at $k_x = \pm k_1$ and a pair of poles at $k_x = \pm k_1$ as well, as shown in

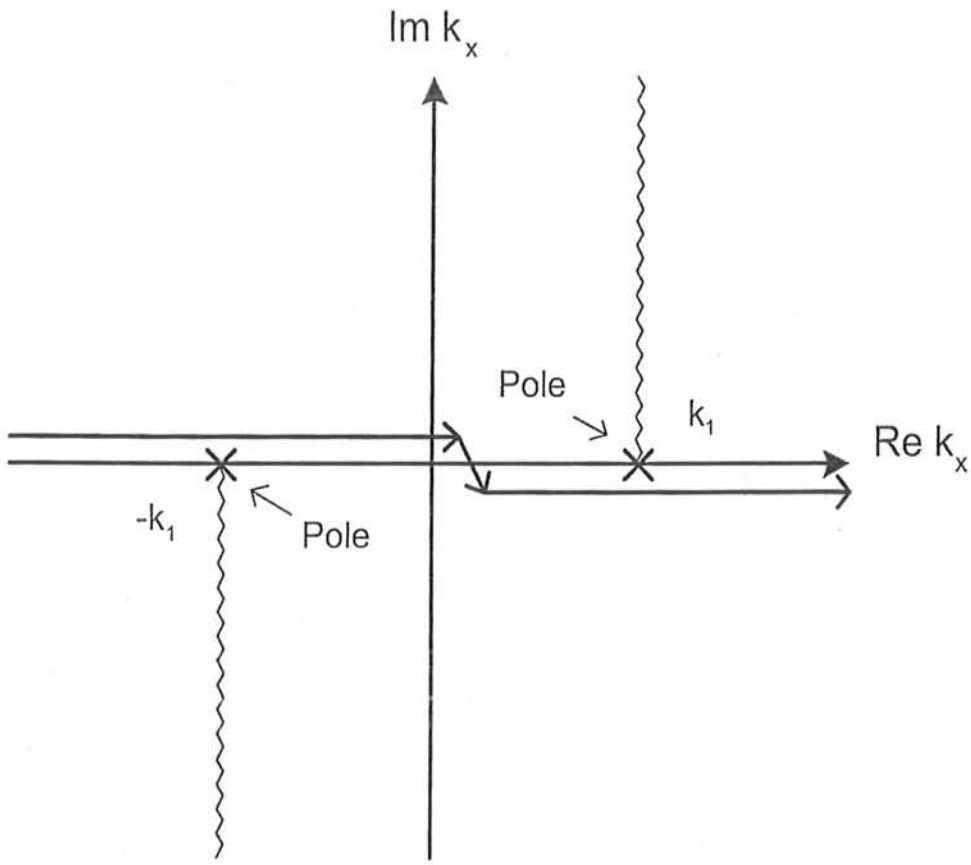

Figure 4.4: Integration path and two branch cuts with poles in the k_x plane of I_{2U}

Fig. 4.4. The k_x to α plane transformation as well as the cartesian to polar cordinate transformation is carried out as in the case of I_{1U}. The resulting form of the integral is,

$$I_{2U} = -\int_Q F(\alpha) e^{k_1 r f(\alpha)} d\alpha, \tag{4.29}$$

where,

$$f(\alpha) = i\{\cos(\alpha - \theta)\},$$

and,

$$F(\alpha) = \frac{1}{\sin\alpha}.$$

$F(\alpha)$ indicates that a pole exists at the origin of new complex α plane while $f(\alpha)$ shows that a saddle point exists at $\alpha = \theta$. The original path of integration, P runs as shown in Fig. 4.4.

To describe the saddle point arrangement in the simplest form at $\alpha = \theta$, the exponential function $f(\alpha)$ in equation (4.29) is replaced by a polynomial so as to convert the integral I_{2U} into a canonical form. The transformation is given as,

$$f(\alpha) = f(\alpha_s) - s^2 = i - s^2,$$

or,

$$\cos(\alpha - \theta) = 1 + is^2,$$

and,

$$\frac{d\alpha}{ds} = -\frac{2is}{\sin(\alpha - \theta)}.$$

This results into the following form of I_{2U}

$$I_{2u} = -e^{k_1 r f(\alpha_s)} \int_{-\infty}^{\infty} G(s) e^{-k_1 r s^2} ds, \tag{4.30}$$

where,

$$G(s) = \frac{1}{\sin\alpha}\frac{d\alpha}{ds} = -\frac{2i}{\sqrt{s^2 - 2i}\{s\sqrt{s^2 - 2i}\cos\theta + (1 + is^2)\sin\theta\}},$$

It can be seen from the above expression that a pair of poles exist at,

$$s_{1,2} = \pm\sqrt{2}e^{i\pi/4}\sin(\theta/2),$$

while first order branch point singularities are present at $s = \pm\sqrt{2}e^{i\pi/4}$. The integral has now been converted to a Laplace type integral. This allows to take the power series expansion of the function $G(s)$ at $s = 0$. The steepest descent path through the saddle point in the complex α plane, is defined by;

$$\Im[f(\alpha)] = \Im[f(\alpha_s)] = i$$

It is seen from Fig. 4.5 that the transformation of the integration variable α to s, results into SDP on real axis of s-plane while the pole shifts to, $s = -\sqrt{2}e^{i\pi/4}\sin(\theta/2)$. Region

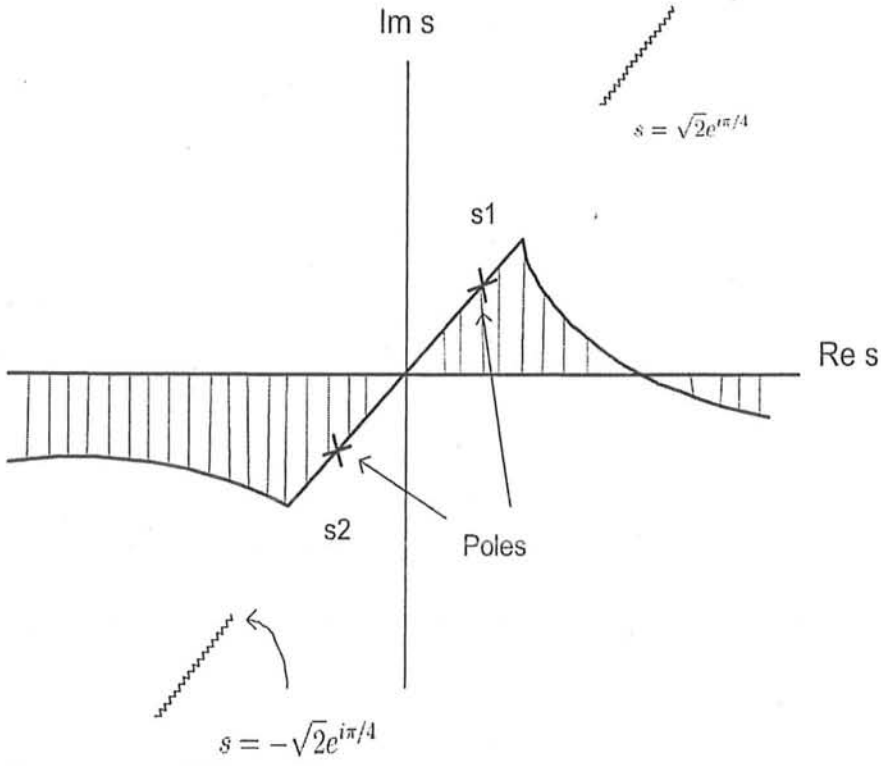

Figure 4.5: Integration path in the mapped s plane of I_{2U}

of convergence is defined by the area enclosed by the original contour in the s-plane and the SDP which runs on the real s-axis, as shown in the figure 4.5. The location of the poles at $s = \pm\sqrt{2}e^{i\pi/4}\sin(\theta/2)$ is at the boundary of the convergent region.

The contribution of this integral can be examined in two regions of observation. One region is very near to the interface i-e; $\theta \to 0$ while the second is away from the interface, $\theta \gg 0$. In the situation when the observation point is away from the interface or the pole is away from origin only the saddle point contributes in the electric field expression

and the pole being at the boundary of the convergent region does not contribute.

Under the conditions that $\theta \to 0$, the following relationship is used, [10],

$$I_{2U}(k_1 r) \sim e^{ik_1 r}\left\{ \pm i2a\sqrt{\pi}e^{-k_1 r b^2} Q(\mp ib\sqrt{k_1 r}) + \sqrt{\frac{\pi}{k_1 r}} T(0) \right\}, \tag{4.31}$$

where,

$$b = -\sqrt{2}e^{i\pi/4}\sin\left(\frac{\theta}{2}\right),$$

$$a = 1,$$

and,

$$T(0) = \frac{e^{-i\pi/4}}{\sqrt{2}\sin(\theta/2)}\{\cos(\theta/2) - 1\}.$$

Therefore the field comes out to be due to this integral having a pole giving dominant contribution at origin,

$$I_{2U}(k_1 r) \sim e^{ik_1 r}\left\{ \pm i2a\sqrt{\pi}e^{-k_1 r b^2} Q(\mp ib\sqrt{k_1 r}) + \sqrt{\frac{\pi}{k_1 r}} \frac{e^{-i\pi/4}}{\sqrt{2}\sin(\theta/2)}\{\cos(\theta/2) - 1\} \right\} \tag{4.32}$$

According to [10] when $|b| \to 0$ then $T(0)$ vanishes and $Q(\pm ib\sqrt{k_1 r}) \to \sqrt{\pi}/2$. This means that for the condition $|b|\sqrt{k_1 r} \gg 1$ to be satisfied so as to include the parabolic cylinder functions as the solution of I_{2U}. When this condition is not satisfied a plane wave is obtained from this integral, I_{2U} which cancels the plane wave contained in the solution of E^U. Hence the total expression for the electric field above the interface is

given as,

$$
\begin{aligned}
E^U &= \frac{\omega\mu I}{2k_1}e^{ik_1|x|} \\
&+\frac{\omega\mu I}{2\pi i}\left[\frac{\sqrt{2\pi}e^{ik_1 r}e^{-i\pi/4}}{k_1\sqrt{k_1 r}\sqrt{n^2-\cos^2\theta}}+\frac{\sqrt{2\pi}e^{ik_1 r(n\cos\theta+i\sqrt{n^2-1}\sin\theta)}e^{i3\pi/4}}{k_1\sqrt{n}(1-n^2)^{1/4}(\sqrt{1-n^2}\cos\theta-n\sin\theta)^{1/2}\sqrt{k_1 r}}\right] \\
&-\frac{\omega\mu I e^{ik_1 r}}{\sqrt{\pi}k_1}\left\{\frac{\sqrt{\pi}}{2}-\sqrt{\frac{\pi}{2}}e^{-i\pi/4}\left\{C(\sqrt{k_1 r}\sin(\frac{\theta}{2}))+iS(\sqrt{k_1 r}\sin(\frac{\theta}{2}))\right\}\right. \\
&\left.+\sqrt{\frac{\pi}{2}}\frac{e^{-i\pi/4}}{\sqrt{k_1 r}\sin(\theta/2)}\{\cos(\theta/2)-1\}\right\}, \quad |b|\sqrt{k_1 r}\gg 1
\end{aligned}
\tag{4.33}
$$

It should be noted that when $\theta \approx 0$ the argument of the Error function in the last term of the above equation becomes zero and the integral contributes only a plane wave. This wave is due to the pair of poles which have shifted to origin when angle of observation is reduced to zero. The asymptotic effects of this term become significant only when the argument has a large value or $|b|\sqrt{k_1 r} \gg 1$.

4.3 Electric Field In Lower Half Space

The solution for the equation (4.3) which is valid for $y < 0$ region is similar in form as the solution for equation (4.2) already obtained and given in (4.33).

$$
E^L = \frac{\omega\mu I}{2k_2}e^{ik_2|x|}+\frac{\omega\mu I}{2\pi i}\Big\{I_{1L}-I_{2L}\Big\}, \tag{4.34}
$$

where,

$$
I_{1L} = \int_{-\infty}^{\infty}\frac{e^{ik_x x-ik_{2y}y}}{k_{1y}k_{2y}}dk_x,
$$

and,

$$
I_{2L} = \int_{-\infty}^{\infty}\frac{e^{ik_x x-ik_{2y}y}}{k_{2y}^2}dk_x.
$$

Evaluation of I_{1L} will be carried out first. The path of integration in this integral runs along the real axis of the k_x plane. There are two pairs of branch points present in the integrand which are at $k_x = \pm k_1$ and $k_x = \pm k_2$. The path of integration and branch cuts shown in Fig. 2.2 are also valid for this integral. It can be seen that the exponential term, $e^{-ik_{2y}y}$ in the integrand satisfies the radiation conditions when the contour is closed at $k_x = \infty$. Transformation to the α plane is carried out using the relationship $k_x = k_2 \cos\alpha$. The resulting integral is,

$$I_{1L} = -\frac{1}{k_2}\int_Q \frac{e^{ik_2 r\cos(\alpha-\theta)}}{\sqrt{1/n^2 - \cos^2\alpha}}\, d\alpha. \tag{4.35}$$

The path of integration Q now runs from $\pi - i\cosh\eta$ to $i\cosh\eta$ as shown in the Fig. 4.3. The transformation from k_x to α plane has also removed the branch point at $k_x = k_2$ while the remaining pair shifted to the real axis of α plane at $\alpha_1 = \cos^{-1}(1/n)$ and $\alpha_2 = \pi - \cos^{-1}(1/n)$. The branch cut contribution which is present at $\alpha_1 = \cos^{-1}(1/n)$ will be included only when the observation angle is less than the critical angle. The path of integration and branch cut arrangement is the same as for E_S^U.

It is known that $\alpha = -\theta$ is the saddle point and θ is a negative number below the interface, therefore the saddle point lies in the $(0 < \alpha < \pi/2)$ in the α-plane for $x > 0$ region. The path of integration Q will be deformed to run through the saddle point at $\alpha = -\theta$ shown as Q' in the Fig. 4.3. The branch cut is also deformed to extend along a constant phase path so that when observation angle is less than the critical angle steepest descent method can be used while avoiding the branch cut. A transformation is carried out according to (2.13) to evaluate the integral asymptotically. This transformation will convert the integral into the following form,

$$I_{1L} = \frac{e^{k_2 r f(\alpha_s)}}{k_2}\int_{-\infty}^{\infty} G(s) e^{-k_2 r s^2}\, ds, \tag{4.36}$$

where,

$$G(s) = F(\alpha_s)\frac{d\alpha}{ds}.$$

As the path of integration now runs along real axis of new s plane therefore the power series expansion of $G(s)$ in (4.36) is taken at $s = 0$ due to the presence of the saddle point at the origin of s plane. In the relationship of $G(s)$ the function $F(\alpha_s)$ is given as,

$$F(\alpha_s) = \frac{1}{k_2\sqrt{1/n^2 - \cos^2\theta}}.$$

This leads to,

$$I_{1\text{Lsd}} = \frac{\sqrt{2\pi}e^{ik_2r}e^{-i\pi/4}}{k_2\sqrt{k_2r}\sqrt{1/n^2 - \cos^2\theta}}. \tag{4.37}$$

The contribution of the branch point will be evaluated now. The branch point is present at $\alpha = \alpha_b = \cos^{-1}(1/n)$ in the α plane. The following transformation,

$$i\cos(\alpha - \theta) = i\cos(\alpha_b - \theta) - s^2$$

shifts the branch point to the origin of the new complex s-plane. The new form of integral, I_{1L}, is,

$$I_{1L} = \frac{e^{ik_1r\{\cos\theta - \sqrt{n^2-1}\sin\theta\}}}{k_2}\int_{-\infty}^{\infty} G(s)e^{-k_2rs^2}ds, \tag{4.38}$$

where,

$$G(s) = F(\alpha_b)\frac{d\alpha}{ds},$$

and,

$$F(\alpha_b) = \frac{1}{\sqrt{1/n^2 - \cos^2\alpha_b}}.$$

The derivative $(d\alpha/ds)$ is expanded in a power series at $s = 0$. Only the first term of the expansion will be used in further calculations or,

$$\frac{d\alpha}{ds} \approx \frac{2se^{-i\pi/2}}{\sin(\alpha_b - \theta)} = \frac{2nse^{-i\pi/2}}{(\sqrt{n^2-1}\cos\theta - \sin\theta)}.$$

$F(\alpha_b)$ is expanded in a Power series about the branch point, $\alpha = \alpha_b$. The first two terms of the expansion are given as,

$$= \frac{n}{\sqrt{2}(n^2-1)^{1/4}\sqrt{\alpha-\alpha_b}} + \frac{n(n^2-2)\sqrt{\alpha-\alpha_b}}{4\sqrt{2}(n^2-1)^{3/4}},$$

where,

$$\sqrt{\alpha-\alpha_b} = \frac{se^{-i5\pi/4}}{\sqrt{\sin(\alpha_b-\theta)}}.$$

Substituting the value of $\sqrt{\alpha-\alpha_b}$ the first two terms of Power series expansion becomes,

$$F(\alpha_b) = n\Big\{\frac{\sqrt{\sin(\alpha_b-\theta)}e^{i5\pi/4}}{\sqrt{2}(n^2-1)^{1/4}s} + \frac{(n^2-2)se^{-i5\pi/4}}{4\sqrt{2}(n^2-1)^{3/4}\sqrt{\sin(\alpha_b-\theta)}}\Big\}.$$

The function $G(s)$ is given as,

$$G(s) = 2n\Big\{\frac{e^{i3\pi/4}}{\sqrt{2}(n^2-1)^{1/4}\sqrt{\sin(\alpha_b-\theta)}} + \frac{(n^2-2)s^2e^{-i7\pi/4}}{4\sqrt{2}(n^2-1)^{3/4}(\sin(\alpha_b-\theta))^{3/2}}\Big\}.$$

The integral is evaluated as,

$$I_{1\mathrm{Lbr}} = \frac{\sqrt{2\pi}e^{ik_1r(\cos\theta-\sqrt{n^2-1}\sin\theta)}e^{i3\pi/4}}{k_1(n^2-1)^{1/4}(\sqrt{n^2-1}\cos\theta-\sin\theta)^{1/2}\sqrt{k_1r}}. \tag{4.39}$$

The last integral to be evaluated in the lower half space is,

$$I_{2L} = \int_{-\infty}^{\infty}\frac{e^{ik_xx}e^{-ik_{2y}y}}{k_{2y}^2}dk_x. \tag{4.40}$$

Obviously the pole and the branch point lie at the same point i-e; $k_x = \pm k_2$. Transformation into the polar coordinate systems, introduces a saddle point on the real axis and a pole at the origin. The same approach is adapted in this evaluation as was done for evaluation of I_{2U}, in (4.29),

$$I_{2L}(k_2r) \sim \frac{\omega\mu Ie^{ik_2x}}{\sqrt{\pi}k_2}\Bigg[\frac{\sqrt{\pi}}{2} - \sqrt{\frac{\pi}{2}}e^{-i\pi/4}\Big\{C(\sqrt{k_2r}\sin(\frac{\theta}{2})) + iS(\sqrt{k_2r}\sin(\frac{\theta}{2}))\Big\}$$
$$+\sqrt{\frac{\pi}{k_2r}}\frac{e^{-i\pi/4}}{\sqrt{2}\sin(\theta/2)}\{\cos(\theta/2)-1\}\Bigg]. \tag{4.41}$$

It can be said now that the total electric field below the interface also has two regions for the nature of the electric field. One form of electric field is represented near the interface while another form of electric field is represented while the point of observation is away from the interface. So the total electric field below the interface becomes,

$$
\begin{aligned}
E_S^L \simeq\ & \frac{\omega\mu I}{2k_2} e^{ik_2|x|} \\
& + \frac{e^{\sqrt{2\pi} i k_2 r} e^{-i\pi/4}}{k_2\sqrt{k_2 r}\sqrt{1/n^2 - \cos^2\theta}} + \frac{\sqrt{2\pi} e^{ik_1 r(\cos\theta - \sqrt{n^2-1}\sin\theta)} e^{i3\pi/4}}{k_1(n^2-1)^{1/4}(\sqrt{n^2-1}\cos\theta - \sin\theta)^{1/2}\sqrt{k_1 r}} \\
& - \frac{\omega\mu I e^{ik_2 x}}{\sqrt{\pi} k_2} \left[\frac{\sqrt{\pi}}{2} - \sqrt{\frac{\pi}{2}} e^{-i\pi/4} \left\{ C(\sqrt{k_2 r}\sin(\frac{\theta}{2})) + iS(\sqrt{k_2 r}\sin(\frac{\theta}{2})) \right\} \right. \\
& \left. + \sqrt{\frac{\pi}{k_2 r}} \frac{e^{-i\pi/4}}{\sqrt{2}\sin(\theta/2)} \{\cos(\theta/2) - 1\} \right] \qquad (4.42)
\end{aligned}
$$

The above field expression which represents electric field below the interface has a plane wave term. This wave travels with wavenumber k_2 in the lower half space. Near the interface this wave term is canceled by a similar wave but of opposite polarity contributed by the pole present in I_{2L}. The contribution of the pole becomes dominant near the interface. The branch point contribution field decays as $(kr)^{-1/2}$.

Asymptotic solutions for electric fields have been obtained for two dielectric half spaces due to the current sheet placed perpendicular the interface. The results showed that diffraction terms appeared in the field expressions in the form of parabolic cylinder functions near the interface in both half space. These diffraction terms vanished as $|b|\sqrt{k_{1,2}r} \gg 1$ is satisfied. The asymptotic solutions for the two half spaces also contained plane wave terms with wavenumbers k_1 and k_2 for the half spaces which exist for $y > 0$ and $y < 0$ respectively. These plane wave term get canceled near the interface when $\theta \to 0$ while became dominant when $\theta \gg 0$ or the condition $|b|\sqrt{k_{1,2}r} \gg 1$ is satisfied. The saddle and branch point terms in both half spaces decay as $(kr)^{-1/2}$. The electric field expression for the region $y > 0$ contain evanescent wave near the interface

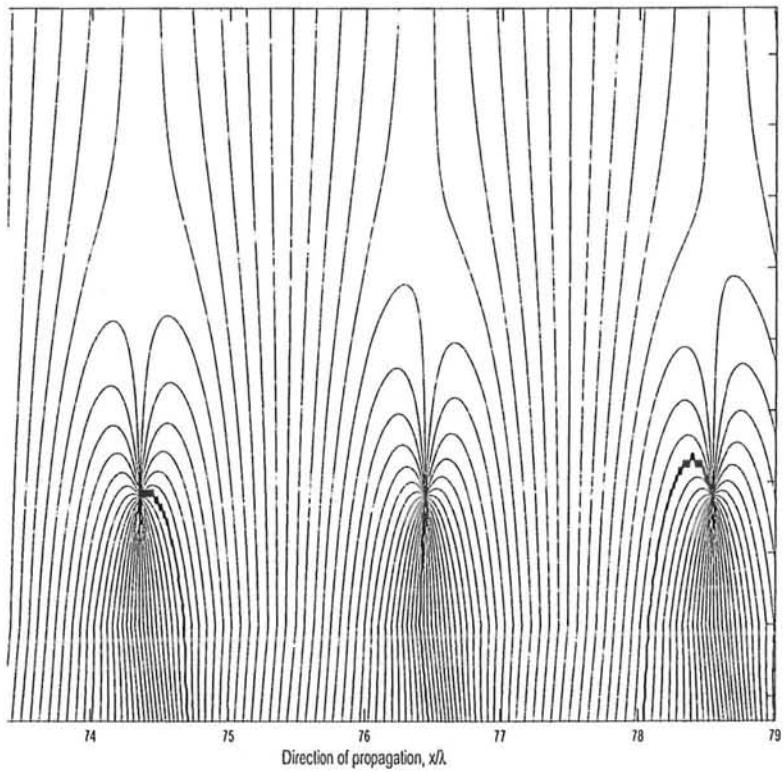

Figure 4.6: Critical points in the region, $y > 0$ due to a current sheet across the interface while no such points in $y < 0$

which decay exponentially perpendicular to the interface. The evanescent wave when interacts with the plane wave near the interface and as a result the critical points appear in the upper half space as shown in Fig. 4.6. The critical points for the region $y < 0$ are not observed while the continuity of the phase map is preserved across the interface. The frequency of occurrence of these points in the upper half space is proportional to the refractive index, n of the second medium for $y < 0$.

Chapter 5

Conclusion

This work was carried out to study the behavior of electromagnetic waves along the plane interface of dielectric media. The media considered throughout this work consisted of two dielectric half spaces such that their interface was located at $y = 0$ plane in the cartesian coordinate system. In order to simplify this investigation of electromagnetic wave behaviour near the interface, sources of finite and infinite extents were used. The finite sources included electric current line source as well as sources of arbitrary shape placed parallel to the interface. Electric current sheet placed perpendicular to the interface was used as a source of infinite extent. The electric field component of the electromagnetic waves, propagating parallel to the dielectric interface was investigated.

The leading terms of the asymptotic field expressions valid above and below the interface due to sources of finite or infinite extent show that the field is zero on the entire interfacial plane. This solution is good enough if one wants to observe the power propagating to infinity in a certain direction, because this is the only term which decays as $(k\rho)^{-1/2}$. Unfortunately this does not give the full picture of wave propagation near the interface when $ky \ll 1$. Moreover zero field condition on the interface represents a structural instability in the phase map of the electromagnetic waves. This structurally

unstable condition of the phase map is converted to structurally stable forms on perturbation by higher order terms in the asymptotic solution of the electric field. Perturbation by higher order terms results into creation of periodic structures of phase map near the interface. These structures are formed around isolated critical points. The critical points are of two types, the saddle type critical points and the center type critical points. The phase velocity and the Poynting vector field are zero at both the critical points. These two types of critical points always exist in pair when index of rotation of the Poynting vector field is zero [9].

A common behaviour of the equiphase lines is observed above the interface for both kinds of sources. The density of the equiphase lines in the rarer medium is lower than the density of the equiphase lines in the denser medium. The center type critical points produce additional phase lines periodically and saddle type critical points redirect the additional phase lines into the denser medium where they are required to support the slower wave. It is known that phase velocity is orthogonal to the equiphase contours. The phase velocity near center type of critical points forms closed curves and waves seem to circulate around these points. This circulation phenomenon results into slowing down of the wave in the rarer medium. Above each center type of critical point is a saddle type critical point. The lines of phase velocity near saddle type critical points form hyperbolic curves thus showing as if the wave is avoiding these points. The overall effect of this structure can be seen qualitatively in Fig. 5.1. There is one major difference in the phase maps of the finite extent source and infinite extent plane wave propagating parallel to the surface. In the case of finite extent sources the flow line through a saddle type critical point eventually ends up going below the structure and into the denser medium. The passing of flow lines below the structure into the denser medium can be seen in Fig. 5.2. It means that interconnection of saddle points by flow lines is avoided. This is perfectly

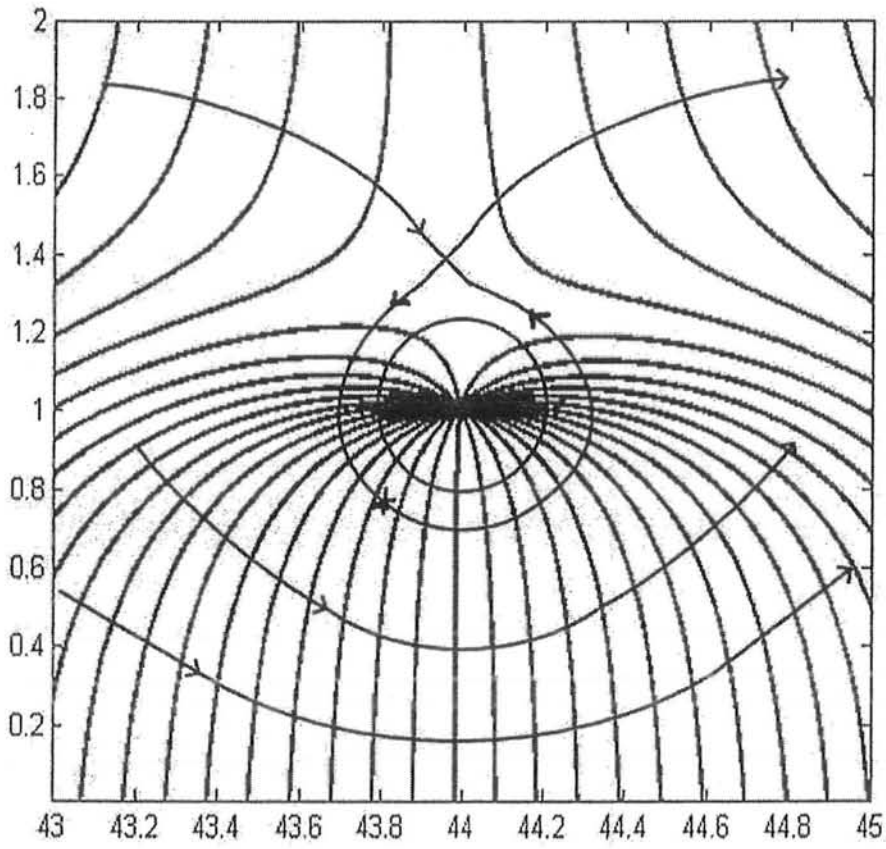

Figure 5.1: Poynting vector and the phase map in the rarer medium

reasonable because such an interconnection is inherently unstable [14]. In case of plane wave the flow lines through saddle type critical points are interconnected. Although this is structurally unstable but it is supported due to the inherent symmetry of the plane wave. Hence region above the interface is effectively divided in two parts. A flow line above the interconnecting line remains above and a flow line below the interconnecting remains below. It has been shown in The interconnecting flow line serves as a boundary between the two parts. The separation of the two parts has been shown in Fig. 5.3.

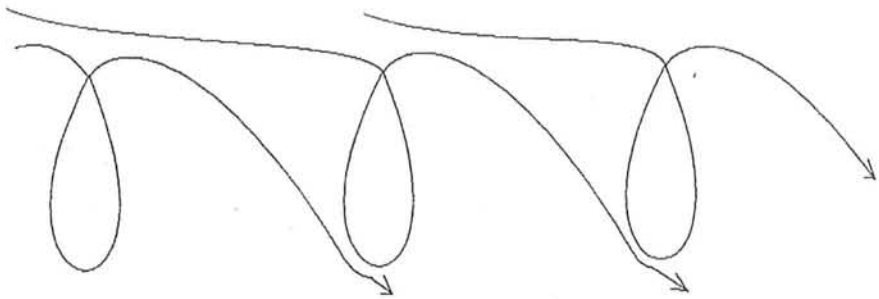

Figure 5.2: Flow lines due to finite extent sources in the rarer medium

There is another difference in the phase map of electromagnetic waves due to finite extent sources and infinite extent sources. For each pair of saddle type critical point and center type critical point in the rarer medium two such pairs of these points exist in the denser medium in case the sources are of finite extent. The arrangement of these points in the denser medium is such that the saddle type critical points of all the structures of phase map are almost on a line parallel to x–axis. Whereas the center of each pair of phase map structure is slightly displaced horizontally from its corresponding phase map structure in the rarer medium. This slight displacement can be seen in Fig. 5.4. The flow lines entering from the rarer medium are trapped in these structures for a few wavelengths before moving further down in the denser medium.

It is known that the phase velocity and Poynting vector field of a wave are proportional to each other. Therefore by looking at the phase map near the interface due to various source configurations it is possible to predict the behaviour of Poynting vector field qualitatively near and along the interface of dielectric media. It can be said that for any type of problem involving propagation near the interface the wave will behave in a manner discussed above.

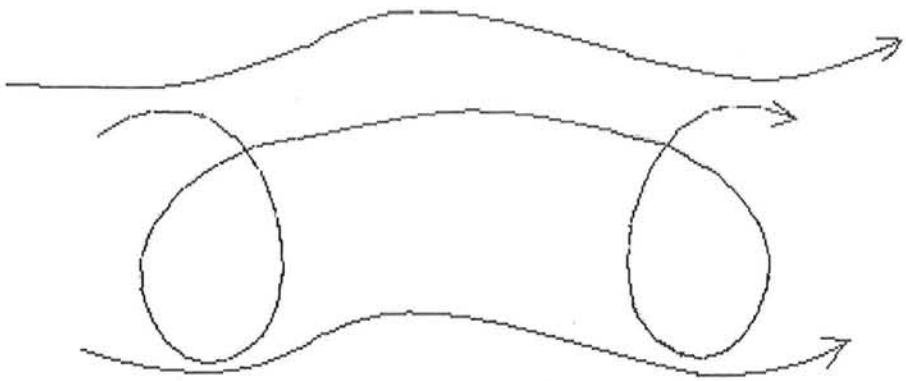

Figure 5.3: Flow lines due to current sheet in the rarer medium

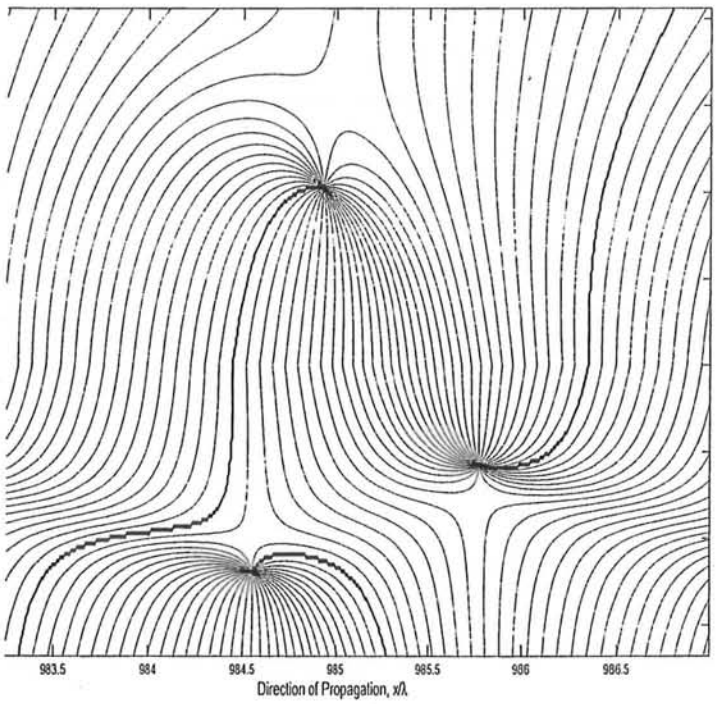

Figure 5.4: Close view of phase map structures with horizontal displacement of the lower pair

References

[1] R. Samii, P. Parhami and R. Mittra. "An efficient approach for evaluating sommerfeld integrals encountered in the problem of a current element radiating over lossy ground". *IEEE Trans. Antennas and Propagation*, 17:100–104, January 1980.

[2] P. Parhami and R. Mittra. "Wire antennas over a lossy half space". *IEEE Trans. Antennas and Propagation*, AP-28(3):397–403, May 1980.

[3] Kin-Lu Wong. "Effects of electromagnetic interference for electromagnetic pulses incident on microstrip circuits". *IEE Proceedings*, 137(1):75–77, February 1990.

[4] Engheta, N., C. H. Papas and C. Elachi, "Interface extinction and subsurface peaking of the radiation pattern of a line source,". *Applied Physics*,Vol. 26, No. 4, 231–238, December 1981.

[5] G. Volski, V. Vandenbosch. "Radiation pattern of an electric line source located in a semi-inifinite grounded dielectric slab calculated using expansion wave concept and geometrical theroy of diffraction". *Proc. IEE Trans. on Microw. Antennas Propag.*, 150 No.2:70–76, April 2003.

[6] G.D Maliuzhinets. "Exitation, reflection and emission of surface waves from a wedge with given face impedance". *Sov. Phys. Dokl.*, 3(4):752–755, 1958.

[7] E. A. Kraut and G. W. Lehman. "Diffraction of electromagnetic waves by a right angled dielectric wedge". *J. Math. Phys.*, 10(8):1340–1348, August 1969.